12-2011

Prevention of iron- and copper-mediated oxidative DNA damage by neurotransmmitters and related compounds: Evidence for metal binding as an antioxidant mechanism

Carla Garcia
Clemson University, seajellie@gmail.com

PREVENTION OF IRON- AND COPPER-MEDIATED OXIDATIVE DNA DAMAGE BY NEUROTRANSMITTERS AND RELATED COMPOUNDS: EVIDENCE FOR METAL BINDING AS AN ANTIOXIDANT MECHANISM

A Thesis
Presented to
the Graduate School of
Clemson University

In Partial Fulfillment
of the Requirements for the Degree
Master of Science
Inorganic Chemistry

---

by
Carla Renee García
December 2011

Accepted by:
Dr. Julia L. Brumaghim, Committee Chair
Dr. Shiou-Jyh Hwu
Dr. Joseph W. Kolis

ABSTRACT

An array of health concerns have been attributed to oxidative DNA damage from the hydroxyl radical ($^{\bullet}OH$), and the presence of the most biologically available redox-active metals, iron and copper, perpetuate the production of this radical through the Fenton and Fenton-like reactions, respectively. The concentrations at which flavonol and polyphenol antioxidants prevent 50% of DNA damage (IC_{50}) were measured using gel electrophoresis assays upon Fe(II)/H_2O_2- and Cu(I)/H_2O_2-mediated DNA damage (Chapter 2). Results show that catechol- and gallol-containing antioxidants differ greatly in preventing DNA damage by Cu(I)/H_2O_2, compared to Fe(II)/H_2O_2, behavior that was explained using electron paramagnetic resonance spectroscopy. Semiquinone and other radical formation indicated that some polyphenol compounds could promote copper redox cycling, leading to increased DNA damage and prooxidant activity. DNA damage assays also revealed that hydroxy-keto functional groups participate in preventing iron-mediated DNA damage prevention depending on the type of hydroxy-keto group present in the flavonolic compound (Chapter 2).

Concentrations of labile iron and copper are elevated in patients with neurological disorders, causing concern about metal-neurotransmitter interactions. Both catecholamine and amino acid neurotransmitters are known to bind these metals, and their antioxidant properties have been previously examined. To further investigate the extent to which metal-binding affects the antioxidant activity of both neurotransmitter types their iron-mediated DNA damage inhibition was quantified, UV-vis studies were used to detect iron and copper binding, and cyclic voltammetry was used the determine redox potentials for these

neurotransmitters with and without iron (Chapter 3). In contrast to the amino acid neurotransmitters, catecholamine neurotransmitters prevent iron-mediated DNA damage and are electrochemically active. When bound to iron, these catecholamines shift redox potentials outside the range for iron(II) generation of $^{\bullet}OH$. Curcumin, a novel preventative treatment for Alzheimer's symptoms, also demonstrated the ability to inhibit iron- and copper-mediated DNA damage (IC_{50} values of 28 and 55 μM, respectively) as well as versatile redox activity, indicating that metal binding can explain most of the antioxidant and prooxidant activity of this compound. These mechanistic insights into metal binding as an antioxidant mechanism will help in identifying antioxidants to treat and prevent neurodegenerative diseases.

DEDICATION

My blood, sweat, and tears are dedicated to my Lord and Savior, Jesus Christ, my mother and father for giving me every opportunity I could ask for, Richard Starr for giving me all of his support, my brother D. Rizzle, and to Cricket. This is also dedicated to my Grandpa Ruben and Aunt Becky.

In loving memory of Glenda M. Gallegos and T. Douglas Seale.

ACKNOWLEDGEMENTS

A lot of thanks are needed for this work. Firstly, I thank the Clemson University Chemistry Department for their help. Big thanks for Dr. Julia L. Brumaghim for being my guide and being there for all of my questions and, mostly, for believing in the project I proposed. The staff, stockroom, and faculty employees of the Clemson Chemistry Department were all contributors to my success. The Brumaghim group has also played role in my success, specifically Jenna Wilkes, Carlos Angéle-Martínez, Sabina Wang, and Ria Ramoutar for all of their inputs, efforts, and late nights. Next, I would like to thank Kimberly Poole for all of her help, suggestions, and patience; I absolutely *could not* have done this without her. The Redfern staff is amazing and care about the health of the students and they are deserving of appreciation. Finally, the following people also have my deepest gratitude: Amy Massingill, Cheryl Moore, Kristen, Barbara Lewis, and William Wannamaker.

TABLE OF CONTENTS

LIST OF TABLES

LIST OF FIGURES

CHAPTER ONE

INTRODUCTION

Antioxidants and the Fenton Reaction

Antioxidants are consumed daily worldwide, yet little is known about their mechanistic behaviors in biological systems. For example, flavonoids, one class of naturally occurring polyphenolic antioxidants, are found in chocolate, vegetables, fruits, and wines, and the average intake of flavonoids from all sources is 23 mg/day [1]. The estimated total polyphenol consumption for men and women is 296.9 and 260.0 mg/day, respectively, from edible portions of fruits and vegetables [2]. Tea, the second most consumed drink in the world (aside from water) [3, 4], is rich in antioxidants such as epigallocatechin gallate (EGCG), epigallocatechin (EGC), epicatechin gallate (ECG), and epicatechin (EC) [5] that have proven to be effective against cellular oxidative stress [6-8]. Antioxidants have stepped into the limelight and have become a selling point for juice and tea advertisements due to their health benefits, but many questions are still to be answered regarding how these compounds exert their antioxidant effects.

One definition of an antioxidant is a compound that prevents or delays oxidation of an oxidizable substrate when the antioxidant is in low concentrations compared to the oxidizable substrate [9]. Reactive oxygen species (ROS) are generated in many forms and cause cellular oxidative damage and oxidative stress that can be moderated by antioxidants. Consequences of this oxidative stress include DNA damage, enzyme inactivation, and the alteration of lipid-protein interactions leading to Parkinson's disease, cancer, heart disease and stroke, and Alzheimer's disease [10, 11]. ROS are often derived from molecular oxygen, O_2 [12], and created through many processes, including metal ion oxidation [13] and

irradiation [14]. One very common ROS is the hydroxyl radical ($^{\bullet}OH$), which is typically produced through Fenton (or Fenton-like) reactions by Fe(II) or Cu(I) [15] (Reaction 1). Hydroxyl radical generation by Fe(II) and Cu(I) occurs frequently in mitochondria, macrophages, and perosisomes [12].

$$\text{Fe(II) or Cu(I)} + H_2O_2 \rightarrow \text{Fe(III) or Cu(II)} + {}^{\bullet}OH + {}^{-}OH \qquad (1)$$

Both the DNA backbone [16, 17] and the nucleobases [18] can be oxidatively damaged by metal-generated $^{\bullet}OH$. Specifically, the 5'-G of a 5'-GG-3' doublet is the most susceptible nucleotide sequence to oxidative nucleobase damage, and guanine is the most susceptible to oxidative nucleobase damage, regardless of position [19]. In fact, iron-mediated DNA damage is the most common source of damage in prokaryotes and eukaryotes and is the primary cause of cell death under oxidative stress conditions for both types of cells [20].

Relevance of Metals in Disease

In the human brain, the concentration of both labile and bound iron is approximately 34 mM [21]. The concentration of labile iron in the human brain has not been reported, however, non-protein-bound iron in a lamb's brain was found to be 10.7 μM [22]. If a lamb's brain is similar to a human's, the implication is that labile iron is nearly 15 times more prevalent in the brain than labile copper, which is present in a concentration of 0.2 μM [23]. It is not currently known whether mis-regulated labile iron or copper plays a more significant role in cellular ROS damage. However, the imbalance of these biologically relevant metals observed in disease states indicates importance of studying the *in vitro*

consequences of metal-antioxidant interactions to gain insight into complex *in vivo* biological systems.

The closely regulated balance of metal ions in cells for both human and animals is fundamental to health. Many studies strongly suggest correlations between metal concentration imbalance and disease. Elevated total iron levels in serum have been associated with an increased risk of myocardial infarction [24] as well as restless leg syndrome [25]. In a recent review, Jomova and Valko discuss pro-mutagenic DNA base modifications that result from metal-mediated DNA damage and link cellular metal ions to cancer development [26]. This review also concludes that protection from metal-mediated damage can occur by chelating Fe(II) to prevent ROS-forming reactions, to keep it in a redox state, Fe(III), that is unable to reduce oxygenated species, or to trap free radicals [26]. Total iron concentrations are elevated in several areas of the brain in those who experience migraines [27]. Labile iron serum levels are about the same in depressed patients as with people who are not depressed (82 μM and 93 μM, respectively), but labile copper concentrations differ greatly (3.9 μM and 0.2 μM, respectively) [23]. This contrast between labile copper and iron concentrations may imply that copper produces a higher quantity of ROS compared to iron, due the fact that Cu(II) is more easily reduced than Fe(III) [28] to increase hydroxyl radical formation *in vivo*.

Recent research suggests that copper abundance also plays a direct role in Alzheimer's disease. Copper can bind to His13, His14, His6, and Tyr10 on the amyloid-β protein (Aβ) [29], causing oxidative damage that leads to neurotoxicity [30]. Elevated levels of both iron and copper have been detected by electron paramagnetic resonance (EPR) spectroscopy in patients with atherosclerosis compared to healthy patients (0.370 versus

0.022 nmol iron/mg tissue and 7.51 versus 2.01 pmol copper/mg tissue, respectively) [31]. Total copper concentration in the gray matter of the human brain is about 40 μM, with the largest concentration detected in the hippocampus [32]; the concentration of labile copper in these areas is 0.7 μM [33]. In patients with Alzheimer's disease, the average concentration of labile copper in the brain tissue was found to be 4.9 μM [33], which may be a contributing factor in development of this disease. Aggregates of Aβ protein have also been shown to increase H_2O_2 concentrations [34], which will further perpetuate hydroxyl radical production and may be yet another reason for disease development, especially in patients with elevated labile metal concentrations.

Polyphenols as Antioxidants/Prooxidants in Relation to Structure and Chemical Environment

Many polyphenol compounds prevent oxidative damage to plasmid DNA [20, 35-37] and to cells [38-40]. Among these polyphenols are flavonols [41, 42], flavanols [43], and anthocyanins [44] that often contain catechol, gallol, and keto-hydroxy functional groups [20, 35] (Figure 1.2). The potential for a compound to have prooxidant properties can be dependent on the presence of metal ions. Redox cycling is known to promote radical formation by electron transfer (NAD(P)H is a common biological source of electrons) that can generate $O^{\bullet}_{2}{}^{-}$ and then becomes damaging $^{\bullet}OH$ in reactions facilitated by metal ions [45]. In the presence of copper, the known antioxidants [46-48] resveratrol [49] and ascorbic acid [50] promote DNA damage, reinforcing how great a role chemical environment plays in antioxidant/prooxidant behavior.

Flavonoids can have metal-binding catechol, gallol, and keto-hydroxy functional groups within their structure. For example, if the basic flavonol structure (Figure 1.1) has a

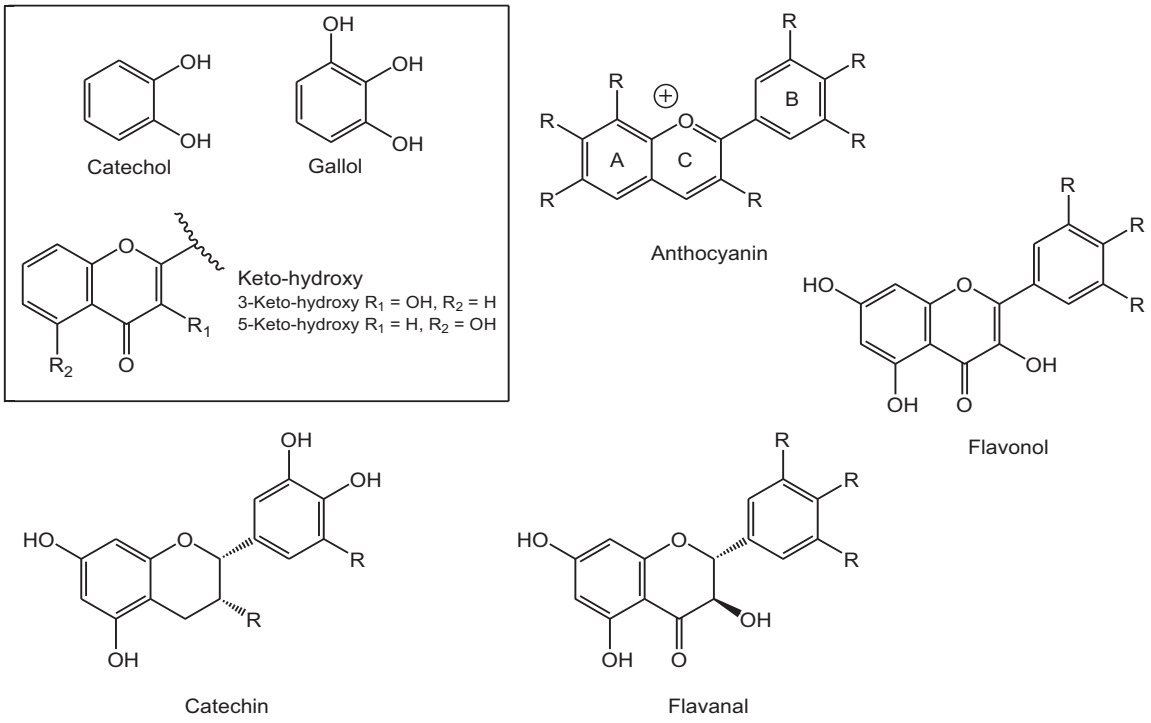

Figure 1.1. Structures of common polyphenolic classes and metal-binding functional groups (in box).

3'-OH and 5'-H, the structure is quercetin, which is a flavonol with a catechol group on the B-ring as well as keto-hydroxy groups on the A and C rings. Catechols and gallols have very different antioxidant behavior and differences in metal binding. Methyl-3,4,5-trihydroxyl-benzoate (MEGA) and methyl-3,4-dihydroxybenzoate (MEPCA) are examples of gallol and catechol compounds that differ only by one hydroxyl group, yet behave quite differently in preventing DNA damage. The concentration at which MEGA prevents 50% of iron-mediated DNA damage (IC_{50}) is over 4 times lower than that for MEPCA [20]. Quercetin and myricetin are also catechol and gallol analogs, respectively, and myricetin effectively prevents over 5 times more iron-mediated DNA damage than quercetin at the same concentration (IC_{50} values of 2.0 μM vs. 10.7 μM, respectively) [20]. Thus, simply by varying

one hydroxyl group, antioxidant behavior in the presence of a metal ion can differ greatly. Not only do synthetic and dietary compounds fall under the polyphenolic structural groups already mentioned, but also certain endogenous compounds in humans such as hormones and neurotransmitters.

Radical Scavenging Assays

The most common method for analyzing antioxidant potency is the use of radical scavenging assays. Flavonoid antioxidants have been studied thoroughly using methods such as 2,2-diphenyl-1-picrylhydrazyl (DPPH) radical scavenging and are potent radical scavengers [51]. Catecholamine neurotransmitters have also been studied for their antioxidant activity using such assays. A recent study analyzed the abilities of catecholamine neurotransmitters to scavenge radicals through either a hydrogen atom transfer mechanism or a metal-ion-coupled-electron transfer with Mg(II) [52]. Using ultraviolet-visible (UV-vis) spectroscopy and gel electrophoresis, it was determined that dopamine had the highest radical scavenging ability compared to other catecholamines, preventing radical-induced DNA damage most efficiently in the presence of Mg(II) [52].

Another study analyzed the bark extract of *Spondias pinnata* (a fruit plant from Thailand that is rich in flavonoids) using a variety of radical scavenging techniques, including nitric oxide, peroxynitrite, hydrogen peroxide, and singlet oxygen scavenging assays [53]. The total antioxidant activity of the extract was determined its ability to scavenge the 2,2'-azinobis-(3-ethylbenzothiazoline-6-sulfonic acid) cationic radical ($ATBS^{\bullet+}$) in comparison to the well-known antioxidant standard 6-hydroxy-2,5,7-tetramethylchroman-2-carboxylic acid (Trolox), a water-soluble vitamin E analog, to calculate the Trolox equivalent antioxidant

concentration (TEAC) value [53]. Although radical scavenging assays are useful, they do not address the role of metal ions that may generate ROS in biological systems.

Neurotransmitters

The anti- or prooxidant behavior of neurotransmitters is still an active area of research. Dopamine (DA), epinephrine (EP), and norepinephrine (NE) are catecholamine neurotransmitters (Figure 1.2), and all three are monoamine polyphenol compounds. An interspecies comparison shows that DA is found at higher concentrations than EP and NE in most animals, including humans (Table 1.1). The levels of these neurotransmitters in the brain (1-10 μM) are in quantities at or near IC_{50} values the Brumaghim group has measured for other catechol and carboxylic acid compounds for both iron- [10, 13] and copper-mediated DNA damage prevention [10, 35] (Table 1.1). Three additional monoamine neurotransmitters of interest are γ-aminobutyric acid (GABA), glutamate (Glu), and glycine (Gly) (Figure 1.2), all of which are monoamine carboxylic acid neurotransmitters. A

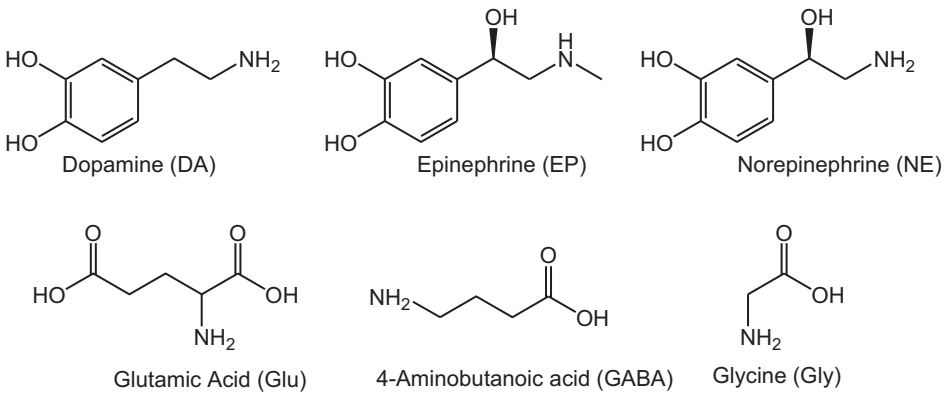

Figure 1.2. Structures of monoamine neurotransmitters.

Table 1.1. Concentrations of neurotransmitters in Figure 1.2. References are given in brackets.

Tissue	Concentration Range for Each Compound (μM)					
	Dopamine	**Norepinephrine**	**Epinephrine**	**GABA**	**Glycine**	**Glutamate**
Cat Brain	N/R	N/R	N/R	0.00158[a] [54]	0.489[a] [54]	0.901 [a] [54]
Swine Brain	N/R	N/R	N/R	N/R	N/R	9.65-7.57 [a] [55]
Rat Brain	1.0-2.7 [56]	0.914 - 7.76 [a] [57]	0.56 - 1.69 [a] [57]	N/R	N/R	0.285-21.9 [58, 59]
Mouse Brain	8.6 [a] [60]	2.3 [a] [60]	N/R	N/R	N/R	N/R
Human Plasma	N/R	0.00068-0.0011 [61]	0.000095-0.00017 [61]	N/R	0.12-0.32 [62]	0.5 [63]
Human Brain	0.42-8.9 [a] [64]	0.00025-0.014 [a] [65]	N/R	1840 [66]	N/R	N/R

N/R = not reported; [a] used wet brain density conversion from [67].

comparison between concentrations of these three neurotransmitters shows that GABA is by far the most concentrated in the human brain, and that Gly and Glu are similar in abundance to the catecholamines (Table 1.1).

The concentration of total copper in the *substantia nigra*, where dopamine is produced in the brain [68], can be as high as 0.4 mM [69], increasing the potential for interactions between catecholamine compounds and copper. Gene expression disruption has been proposed to occur in the presence of presence of both DA and 10-20 μM of either Fe(III) or Cu(II) [70], near the biological concentrations for both metal ions. Direct comparisons between DA, EP, and NE show that DA produces the most oxidative DNA damage

products, including 8-hydroxydeoxyguanosine (8-oxodG), especially in the presence of Cu(II) [70, 71]. These results that show the damaging effect DA and copper ions can have on DNA has also been proven and quantified by the Brumaghim group; biologically relevant concentrations for compounds have a range of 0.3-10.0 μM [72-74], yet at 10 μM, DA was found to damage plasmid DNA in the presence of Cu(I) [35]. Thus, established research has shown the presence of both dopamine and metal ions, specifically copper, to cause significant DNA damage.

GABA is an amino acid neurotransmitter responsible for mood regulation [75]. The average concentration of GABA in the occipital cortex of the brain for patients in the follicular stage of premenstrual dysphoric disorder (PMDD) is 850 μM compared to 1840 μM in control patients [66] (Table 1.1), suggesting a correlation between the changes in mood and GABA levels. It has also been suggested that glutamate levels in the brain also influence behavior in menstruating women [76]. Although glutamate and glycine levels are not as high in the human brain as GABA, they are in the micromolar range for cats (0.901 μM and 0.489 μM, respectively) [54] and swine (9.65 μM glutamate) [55] (Table 1.1).

GABA-rich extract obtained from fermented seaweed has been shown to have potent antioxidant properties [77]. However, tea enriched with GABA was found to promote oxidative DNA damage in the presence of Cu(II), whereas GABA alone did not [78]. Further investigation concluded that Cu(I) must be produced in the oxidative DNA damage process, suggesting a reductive property of GABA [78]. GABA has also been crystallized coordinated to Cu(II) [79], indicating that copper binding may affect GABA antioxidant properties.

The most structurally simple amino acid, glycine (Gly), is also a neurotransmitter and binds Fe(III) with the formation constant $K_{Fe(III)\text{-}Gly} = 2.0 \times 10^2$ L·mol^{-1} [80]. Iron-glycine supplementation increases superoxide dismutase and catalase antioxidant enzyme activity *in vivo* [81]. Both Cu(I)-glycine (binding through the amino nitrogen) [82] and Cu(II)-glycine (binding through the amine nitrogen and the carboxylate oxygen in a distorted square-pyramidal geometry) [83] complexes have been reported. Glycine was found to be an ineffective antioxidant in the presence of iron (preventing only 31.9% of DNA damage at 10,000 μM), but prevented oxidative damage in the presence of copper at a much lower concentration (50% of DNA damage was prevented at 20.2 μM) [84]. The significant differences in behavior of glycine by changing the metal ion responsible for $^{\bullet}$OH generation emphasizes the importance of the metal ion in oxidative damage and its prevention.

Glutamate is the major excitatory neurotransmitter for motor functions, but in the presence of increased labile copper levels, decreased cortical excitability in patients with depression has been documented. This effect suggests disruption in glutamatergic neurotransmission from oxidative stress [23]. Glutamate's role as an agent involved in the regulation of oxidative stress is still relatively vague, especially since many of the publications deal with glutamate-containing compounds or glutamate receptors, not glutamate itself. It is known, however, that glutamate inhibits lipid peroxidation damage to the heart *in vivo* [85]. A direct comparison of antioxidant (and prooxidant) effects with neurotransmitter structure with both iron and copper will help establish the biological functions of these compounds that will be invaluable to understanding and treating neurological diseases.

Implications and Completed Research for Selected Compounds

As previously mentioned, flavonols and other polyphenols are known antioxidants, but the specifics regarding how flavonol-metal binding affects antioxidant activity are unclear. To investigate the importance of metal binding for polyphenol prevention of metal-mediated DNA damage, derivatives of the compounds of interest lacking metal binding sites were tested to determine the importance of metal coordination on the antioxidant activity of these compounds. Chromones are derivatives of flavonols that do not have a B-ring (Figure 1.1) but do have keto-hydroxy binding groups. The ability of these compounds to prevent iron-mediated DNA damage was examined in A.M. Verdan, S.W. Hsiao, C.R. García, W.P. Henry, J.L. Brumaghim, J. Inorg. Biochem. 105 (2011) 1314-1322. We determined that 3-hydroxychromone more effectively prevents iron-mediated DNA damage compared to 5-hydroxychromone and also has much faster kinetics of Fe(II) oxidation [42]. Specifics of this work are described in Chapter 2.

Not only do flavonols show a wide difference in antioxidant behavior from structure variations, but also their antioxidant activity differs widely depending on the metal ion causing the oxidative damage. Using EPR spectroscopy, we discovered that the low IC_{50} for copper-mediated DNA damage prevention by MEPCA may be due to a suppression of radical formation in a redox cycling mechanism (N.R. Perron, C.R. García, J.R. Pinzón, M.N. Chaur, J.L. Brumaghim Inorg. Biochem. 105 (2011) 745-753). With the prooxidant compound EC, several different radicals are formed (not only $^{\bullet}OH$ adduct, but also $^{\bullet}H$ radical), in greater quantity compared to the antioxidant MEPCA [35]. These results are also discussed in Chapter 2.

Metal binding is, therefore, proposed to be the most active antioxidant mechanism of the selected neurotransmitters and the related compounds discussed in this thesis. If this is the case, understanding the interactions of neurotransmitters and metals is crucial to understanding neurodegenerative diseases and their treatments. Interactions between neurotransmitters and both iron and copper vary greatly; catecholamines (dopamine, epinephrine, and norepinephrine) show iron and copper binding vis UV-vis spectroscopy, and show significant electrochemical activity both unbound and bound to iron (Chapter 3). The observed metal-binding activities explain why the catecholamines effectively prevent DNA damage in the presence of iron. In contrast, amino acid neurotransmitters (glycine, glutamate, and γ-aminobutyric acid), are inactive electrochemically and do not show binding to iron or copper, conclusions which explain their inactivity in preventing DNA damage in the presence of iron. With the rising use of *antioxidant* as a buzzword for advertisements and no absolute cure for diseases tied to increased biological metal levels, understanding the specifics of antioxidant structure and how it ties to metal binding and behavior is imperative to furthering the science of healthy living.

References

[1] P. Pedrielli, L.H. Skibsted, J. Agric. Food Chem. 50 (2002) 7138-7144.

[2] P. Brat, S. George, A. Bellamy, L. Du Chaffaut, A. Scalbert, L. Mennen, N. Arnault, M.J. Amiot, J. Nutr. 136 (2006) 2368-2373.

[3] Y. Shishikura, S. Khokhar, J. Sci. Food Agric. 85 (2005) 2125-2133.

[4] N.P. Seeram, S.M. Henning, Y. Niu, R. Lee, H.S. Scheuller, D. Heber, J. Agric. Food Chem. 54 (2006) 1599-1603.

[5] N. AlGamdi, W. Mullen, A. Crozier, Phytochemistry 72 (2011) 248-254.

[6] S.I. Rizvi, M.A. Zaid, R. Anis, N. Mishra, Clin. Exp. Pharmacol. Physiol. 32 (2005) 70-75.

[7] P.K. Maurya, S.I. Rizvi, Nat. Prod. Res. 23 (2009) 1072-1079.

[8] L. Chen, X. Yang, H. Jiao, B. Zhao, Toxicol. Sci. 69 (2002) 149-156.

[9] B. Halliwell, Biochem. Soc. Symp. (1995) 73-101.

[10] R.R. Ramoutar, J.L. Brumaghim, Main Group Chem. 6 (2007) 143-153.

[11] X. Xiao, J. Liu, J. Hu, X. Zhu, H. Yang, C. Wang, Y. Zhang, Eur. J. Pharmacol. 591 (2008) 21-27.

[12] N. Barabutis, A.V. Schally, Proc. Natl. Acad. Sci. USA 105 (2008) 20470-20475.

[13] N.R. Perron, J.N. Hodges, M. Jenkins, J.L. Brumaghim, Inorg. Chem. 47 (2008) 6153-6161.

[14] J.K. Leach, G.V. Tuyle, P.S. SLin, R. Schmidt-Ullrich, R.B. Mikkelsen, Cancer Res. 61 (2001) 3894-3904.

[15] S.Y. Qian, G.R. Buettner, Free Radic. Biol. Med. 26 (1999) 1447-1456.

[16] B. Balasubramanian, W.K. Pogozelki, T.D. Tullius, P. Natl. A. Sci. USA 95 (1998) 9738-9743.

[17] M. Valko, M. Izakovic, M. Mazur, C.J. Rhodes, J. Telser, Mol. Cell. Biochem. 266 (2004) 37-56.

[18] C. Luxford, R.T. Dean, M.J. Davies, Chem. Res. Toxicol. 13 (2000) 665-672.

[19] D.T. Odom, E.A. Dill, J.K. Barton, Nucleic Acids Res. 29 (2001) 2026-2033.

[20] N.R. Perron, J.N. Hodges, M. Jenkins, J.L. Brumaghim, Inorg. Chem. 47 (2008) 6153-6161.

[21] G. McAuley, M. Schrag, S. Barnes, A. Obenaus, A. Dickson, B. Holshouser, W. Kirsch, Magn. Reson. Med. 65 (2011) 1592-1601.

[22] M. Shadid, G. Buonocore, F. Groenendaal, R. Moison, M. Ferrali, H.M. Berger, F. van Bel, Neurosci. Lett. 248 (1998) 5-8.

[23] C. Salustri, R. Squitti, F. Zappasodi, M. Ventriglia, M.G. Bevacqua, M. Fonatana, F. Tecchio, J. Affective Disord. 127 (2010) 321-325.

[24] J.T. Salonen, K. Nyyssonen, H. Korpela, J. Tuomilehto, R. Seppanen, R. Salonen, Circulation 86 (1992) 803-811.

[25] C.J. Earley, J.R. Connor, J.L. Beard, E.A. Malecki, D.K. Epstein, R.P. Allen, Neurology 54 (2000) 1698-1700.

[26] K. Jomova, M. Valko, Toxicology 283 (2011) 65-87.

[27] M.C. Kruit, M.A. van Buchem, L.J. Launer, G.M. Terwindt, M.D. Ferrari, Cephalagia 30 (2010) 129-136.

[28] D.R. Lide (Ed.), CRC Handbook of Chemistry and Physics, CRC Press, Boca Raton, 2007, 8.20-8.23.

[29] Y.H. Hung, A.I. Bush, R.A. Cherny, J. Biol. Inorg. Chem. 15 (2010) 61-76.

[30] D.A. Butterfield, Free Rad. Res. 36 (2002) 1307-1313.

[31] N. Stadler, R.A. Lindner, M.J. Davies, Arterioscler. Thromb. Vasc. Biol. 24 (2004) 949-954.

[32] J. Dobrowolska, M. Dehnhardt, A. Matusch, M. Zoriy, N. Palomero-Gallagher, P. Koscielniak, K. Zilles, J.S. Becker, TALANTA 74 (2008) 717-723.

[33] R. Squitti, C.C. Quattrocchi, G.D. Forno, P. Antuono, D.R. Wekstein, C.R. Capo, C. Salustri, P.M. Rossini, Biomarker Insights 1 (2006) 205-213.

[34] B.J. Tabner, O.M.A. El-Agnaf, M.J. German, N.J. Fullwood, D. Allsop, Biochem. Soc. Trans. 33 (2005) 1082-1086.

[35] N.R. Perron, C.R. García, J.R. Pinzón, M.N. Chaur, J.L. Brumaghim, J. Inorg. Biochem. 105 (2011) 745-753.

[36] S.C. Grace, M.G. Salgo, W.A. Pryor, FEBS Lett. 426 (1998) 24-28.

[37] L.C. Wilms, P.C.H. Hollman, A.W. Boots, J.C.S. Kleinjans, Mutat. Res. 582 (2005) 155-162.

[38] C.A. Barden, H.L. Chandler, P. Lu, J.A. Bomser, C.M. Colitz, Am. J. Vet. Res. 69 (2008) 94-100.

[39] G. Graziani, G. D'Argenio, C. Tuccillo, C. Loguercio, A. Ritieni, F. Morisco, C.D.V. Blanco, V. Fogliano, M. Romano, Gut 54 (2005) 193-200.

[40] S.K. Katiyar, H. Mukhtar, J. Leukoc. Biol. 69 (2001) 719-726.

[41] M.E. Inal, A. Kahraman, Toxicology 154 (2000) 21-29.

[42] A.M. Verdan, S.W. Hsiao, C.R. Garcia, W.P. Henry, J.L. Brumaghim, J. Inorg. Biochem. 105 (2011) 1314-1322.

[43] A.M. Gonzalez-Paramas, S. Esteban-Ruano, C. Santos-Buelga, S. de Pascual-Teresa, G. Rivas, J. C., J. Agric. Food Chem. 52 (2004) 234-238.

[44] T.O. Ajiboye, N.A. Salawu, M.T. Yakubu, A.T. Oladiji, M.A. Akanji, J.I. Okogun, Drug Chem. Toxicol. 34 (2011) 109-115.

[45] P.L. Gutierrez, Front. Biosci. (2000) 629-638.

[46] D.T. Magrane, D.J. Saxon, C.H. Garret, FASEB J. 15 (2001) A1131-A1131.

[47] H. Ghanim, C.L. Sia, K. Korzeniewski, T. Lohano, S. Abuaysheh, A. Marumganti, A. Chaudhuri, P. Dandona, J. Clin. Endocrinol. Metabolism 96 (2011) 1409-1414.

[48] N.O. Metreveli, K.K. Jariashvili, L.O. NamicheishviliB, D.V. Svintradze, E.N. Chikvaidze, A. Sionkowska, J. Skopinska, Ecotoxicol. Environ. Saf. 73 (2010) 448-455.

[49] A.S. Azmi, S.H. Bhat, S.M. Hadi, Febs Lett. 579 (2005) 3131-3135.

[50] S.M. Hadi, M.F. Ullah, U. Shamim, S.H. Bhatt, A.S. Azmi, Chemotherapy 56 (2010) 280-284.

[51] N.E. Es-Safi, S. Ghidouche, P.H. Ducrot, Molecules 12 (2007) 2228-2258.

[52] T. Kawashima, K. Ohkubo, S. Fukuzumi, J. Phys. Chem. B 114 (2010) 675-680.

[53] B. Hazra, S. Biswas, N. Mandal, BMC Complementary Altern. Med. 8 (2008) 63-72.

[54] D. Nitz, J.M. Siegel, Neuroscience 78 (1997) 795-801.

[55] J.L. Wu, Y. Lin, Z.W. Shen, Y.W. Miao, R.H. Wu, L.Z. J., BMEI 2 (2008) 348-352.

[56] M.K. Zachek, P. Takmkov, J. Park, M. Wightman, G.S. McCarthy, Biosensors Bioelec. 25 (2010) 1179-1185.

[57] R. Ramakrishnan, A. Namasivayam, Neurosci. Lett. 186 (1995) 200-202.

[58] C. Ballini, L.D. Corte, M. Pazzagli, M.A. Colivicchi, G. Pepeu, K.F. Tipton, M.G. Giovannini, J. Neurochem. 106 (2008) 1035-1043.

[59] Y.Z. Feng, T. Zhang, R.W. Rockhold, I.K. Ho, Neurochem. Res. 20 (1995) 745-751.

[60] T.S. Naka, M. Yaguchi, N. Okado, Brain Res. 924 (2002) 124-126.

[61] B. Rasch, C. Dodt, M. Molle, J. Born, Psychoneuroendochrinology 32 (2007) 884-891.

[62] D. Strzelecki, J. Rabe-Jablonska, Eur. Neuropsychoparmacol. 20 (2010) S470-S471.

[63] E.E. Castrillon, M. Ernberg, B.E. Cairns, K.L. Wang, B.J. Sessle, L. Arendt-Nielsen, P. Svensson, J. Orofacial Pain 24 (2010) 350-360.

[64] F. Musshoff, D.W. Lachenmeier, P. Schmidt, R. Dettmeyer, B. Madea, Alcohol. Clin. Exp. Res. 29 (2005) 46-52.

[65] J. Tong, O. Hornykiewicz, S. Kish, Arch. Neurol. 63 (2006) 1724-1728.

[66] C.N. Epperson, K. Haga, G.F. Mason, E. Sellars, R. Gueorguieva, W. Zhang, E. Weiss, D.L. Rothman, J.H. Krystal, Arch. Gen. Psychiatry 59 (2002) 851-858.

[67] R.A. Serway, C. Vuille, J.S. Faughn, Essentials of College Physics, Brooks Cole, Florence, 2006, 130-156.

[68] E.L. Que, D.W. Domailler, C.J. Chang, Chem. Rev. 1089 (2008) 1517-1549.

[69] J. Stöckel, J. Safar, A.C. Wallace, F.E. Cohen, S.B. Prusiner, Biochemistry 37 (1998) 7185-7193.

[70] Y. Nishino, M. Ando, R. Makino, K. Ueda, Y. Okamoto, N. Kojima, Neurotox. Res. 20 (2011) 84-92.

[71] W.A. Spencer, J. Jeyabalan, S. Kichambre, R.C. Gupta, Free Radic. Biol. Med. 50 (2011) 139-147.

[72] V.C. Reddy, G.V.V. Sagar, D. Sreeramulu, L. Venu, M. Raghunath, Ann. Nutr. Metab. 49 (2005) 189-195.

[73] A. Sugisawa, K. Umegaki, J. Nutr. 132 (2002) 1836-1839.

[74] K.H. van het Hof, G.A.A. Kivitis, J.A. Westrate, L.B.M. Tijburg, Eur. J. Clin. Nutr. 52 (1998) 356-359.

[75] F. Petty, M.H. Trivedi, M. Fulton, A.J. Rush, Biol. Psychiatry 38 (1995) 578-591.

[76] M.J. Smith, B.D. Greenberg, L.F. Adams, M. Nguyen, P.J. Schmidt, D.R. Rubinow, E.M. Wassermann, Biol. Psychiatry 47 (2000) 1S-173S.

[77] B.-J. Lee, J.-S. Kim, Y.M. Kang, J.-H. Lim, Y.-M. Kim, M.-S. Lee, M.-H. Jeong, C.-B. Ahn, J.-Y. Je, Food Chem. 122 (2010) 271-276.

[78] H.F. Wang, S.M. Chuang, C.C. Hsiao, S.H. Cherng, Food Chem. Toxicol. 49 (2011) 955-962.

[79] V.K. Sabirov, O.V. Shishkin, N.M. Kebets, M.A. Poraikoshits, Y.T. Struchkov, Koord. Khim. 20 (1994) 943-949.

[80] R. Prasad, S. Prasad, J. Chem. Ed. 86 (2009) 494-497.

[81] J. Feng, W.Q. Ma, Z.R. Xu, J. He, X., Y.Z. Wang, J.X. Liu, Animal Feed Sci. Tech. 150 (2009) 106-113.

[82] R. Osterber, Eur. J. Biochem. 13 (1970) 493-497.

[83] S.C. Zhang, X.G. Chun, Y. Chen, J.L. Zhou, Chin. J. Chem. 29 (2011) 65-71.

[84] E.E. Battin, The role of metal coordination in the inhibition of iron(II)- and copper(I)-mediated DNA damage by organoselenium and organosulfur compounds., Clemson University, Clemson, SC, 2008, 117-156.

[85] R. Sivakumar, P.V.A. Babu, C.S. Shyamaladevi, Exp. Toxicol. Pathol. 63 (2011) 137-142.

CHAPTER TWO

INVESTIGATING THE METAL BINDING PROPERTIES OF HYDROXYCHROMONES, CATECHOLS, GALLOLS, AND CURCUMIN ON ANTIOXIDANT AND PROOXIDANT ACTIVITES *IN VITRO* FOR DNA DAMAGE

Labile Iron and Copper Cause DNA Damage and Cell Death

Non-protein-bound (labile) copper and iron concentrations are tightly controlled in the body [1-3]. Superoxide reacts with H_2O_2 to produce hydroxyl radical ($^{\bullet}OH$) through a Haber-Weiss reaction (reaction 1) [4]; however, the Haber-Weiss reaction is thermodynamically unfavorable in biological systems, necessitating a catalyst [5]. When iron is the catalyst, the reaction is then considered the Fenton reaction (reduction and oxidation reactions 2 and 3, respectively) [5]. Since about 70% of iron (bound or unbound) in atherosclerotic plaque tissue is Fe(III) at any given time [6], the cycle will become catalytic.

$$O_2^{\bullet-} + H_2O_2 \rightarrow O_2 + {}^{-}OH + {}^{\bullet}OH \qquad (1)$$

$$Fe(III) + O_2^{\bullet-} \rightarrow Fe(II) + O_2 \qquad (2)$$

$$Fe(II) + H_2O_2 \rightarrow Fe(III) + {}^{-}OH + {}^{\bullet}OH \qquad (3)$$

$$Cu(II) + O_2^{\bullet-} \rightarrow Cu(I) + O_2 \qquad (4)$$

$$Cu(I) + H_2O_2 \rightarrow Cu(II) + {}^{-}OH + {}^{\bullet}OH \qquad (5)$$

When copper ions are the catalyst for the Haber-Weiss reaction, the reaction is then considered a Fenton-like reaction (reduction and oxidation reactions 4 and 5, respectively)

[7]. Understanding hydroxyl radical formation is important because it is one of the few ROS capable of directly damaging most biomolecules [7].

To determine the effects of labile metal-ion-generated oxidative damage to DNA and a compound's ability to act as either a pro- or antioxidant to enhance or prevent this damage, the reduced forms of the most bioavailable metals (Fe(II) and Cu(I)) can be combined with plasmid DNA in an environment that mimics biological conditions. Using gel electrophoresis for these plasmid DNA damage assays, DNA damage can be quantified from the bands of damaged and undamaged DNA bands on the gel.

In these experiments, Fe(II) concentrations are 2 μM, well within cellular labile iron levels (1×10^{-5} – 25 μM [8, 9], Table 2.1). The concentration of 6 μM Cu(I) used in this DNA damage assay is also within the range found in human cells (0.2 - 80 μM [8, 9], Table 2.1). Even though typical cytoplasmic concentrations for labile copper in *Escherichia coli* (*E. coli*), are below 1 copper ion per cell [10, 11], *E. coli* toxicity occurs at concentrations above 100,000 μM [12]. It is worth noting that some strains of *E. coli* are known to have copper toxicity resistance systems in which copper transferred from the DNA-rich cytoplasm to the DNA-poor periplasm, explaining why toxic levels for some strains of *E. coli* are so high in comparison to human cells [13]. Labile iron and copper are not the only source of damaging ROS; protein-bound copper ions can also participate in redox activity, resulting in ROS generation [14]. Therefore, both protein-bound and labile copper concentrations should be taken into consideration. Total metal ion concentrations for Fe and Cu ions are generally within the micromolar range for human and *E. coli* cells, a promising find for the biological relevance of *in vitro* DNA damage prevention studies.

The unavoidable combination of oxidative ROS as well as redox-active metals and reductive compounds in cells can result in DNA damage [21, 22] and cell death [23, 24]. A review by Kroemer, *et al.* discusses programmed cell death that may occur when ROS are formed in the mitochondria and generate oxidative damage [23]. *In vivo*, it is proposed that phagocytes would recognize this damage and remove the cell, but *in vitro*, degradation of the DNA can be observed, and cytolysis is the ultimate consequence [23]. Therefore, investigation of DNA damage using an *in vitro* assay provides a clear correlation between metal ions and the damaging effects of ROS since this *in vitro* DNA damage can be directly quantified.

Table 2.1. Levels of iron and copper ions in human and *E. coli* cells. References are provided in brackets.

Metal Ion	Labile/Bound	Human Cells (μM)	*E. coli* Cells (μM)
Fe(II)/(III)	Labile + bound	≥ 25 [15] [a], 20 [16] [b]	–
	Labile	9.2×10^{-5} [8] [b], 0.57 ± 0.27 [17] [c]	10, 70, 80, and 160 [18] [e]
Cu(I)/(II)	Labile + bound	50 [9] [d]	≥100,000-400,000 can be toxic [12] [f]
	Labile	0.2 [8] [b], 1.6 [19] [b]	1×10^{-15} [10] [g]

[a] Myelomonocytic cell line THP-1; [b] human serum; [c] human lymphocyte; [d] human liver, using the wet density conversion of 1.0 g/1.0 mL [20]; [e] for *E. coli* strains AB1157 (wild-type), KK204 (Fur^-), JI132 (SOD^-), and KK216 (SOD^- Fur^-), respectively; [f] W3110 (wild-type); [g] value calculated based on Cu binding affinity for metalloregulatory protein CueR; this value is well below 1 Cu ion/*E. coli* cell [11].

Polyphenol Behavior in the Presence of Copper(I)

DNA damage assays were performed under Fenton-like conditions (6 μM Cu(II), 7.5 μM ascorbate, and 50 μM H_2O_2) to investigate the potential of catechol- and gallol-containing compounds (MEPCA, EC and MEGA, EGCG, respectively, Figure 2.1) to either prevent or promote DNA damage. Results from DNA damage assays of these compounds were quantified and the concentration at which 50% of DNA damage is inhibited (IC_{50}) values were determined if possible (Table 2.2). Electron paramagnetic resonance (EPR) spectroscopy was then employed to investigate the differences in radical formation and in order to better explain the antioxidant behavior. From the results of the DNA damage

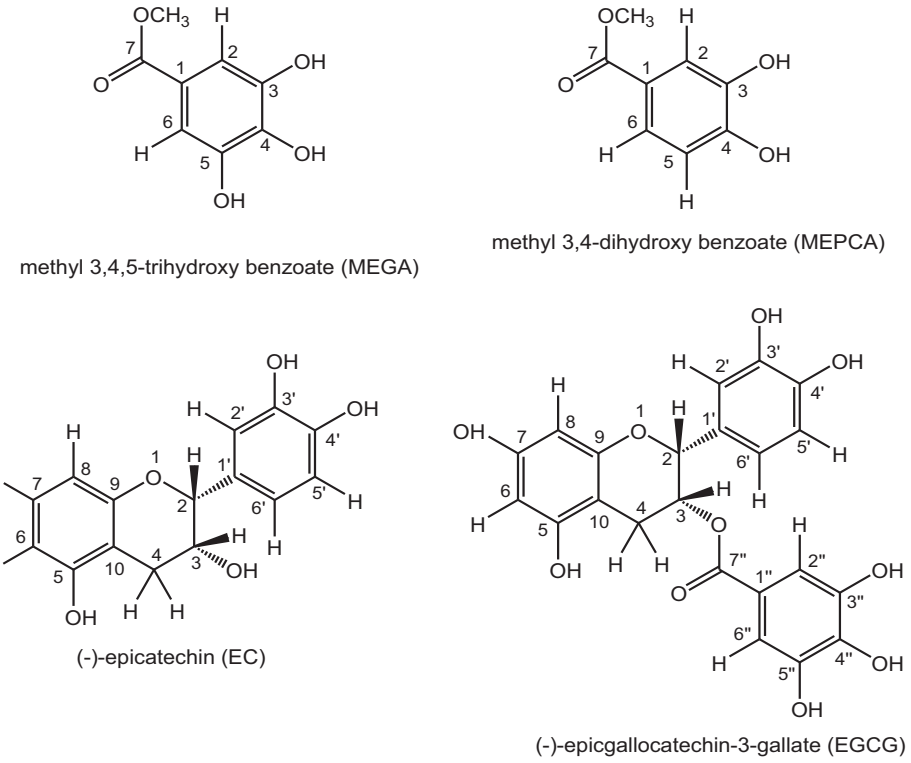

Figure 2.1. Molecular structures of MEGA, MEPCA, EC, and EGCG shown with structure numbering.

assays, an obvious difference can be seen in the activities of gallol- and catechol-containing polyphenols. For example, EC is a prooxidant at all the tested concentrations whereas EGCG prevents oxidative damage at all the tested concentrations [25]. Dopamine, a catecholamine neurotransmitter produced in the brain where labile copper pools are located [26], increases DNA damage by 2.5-fold at 10 μM, approximately the concentration of dopamine in the human brain [27].

The mixture of prooxidant and antioxidant behavior for the tested catechol and gallol compounds led us to use EPR spectroscopy to determine whether the semiquinone radical species are formed from the polyphenol/copper compounds under conditions similar to those used for the DNA damage assays, a result that would indicate polyphenol participation in copper redox-cycling. This information should correlate with the compound's observed ability to either prevent or promote DNA damage and provide insights into the biological behavior of these polyphenols.

Table 2.2. A summary of the prooxidant and antioxidant activity of polyphenols with Cu(I)-mediated DNA damage [25].[a]

Compound	Proox. Activity (Max %) [b]	Antiox. Activity (Max %)	IC_{50} (μM)
DA	0.2 - 2000 μM (-245.3% at 10 μM)	3000 μM (22.7% at 3000 μM)	–
EC	0.2-500 μM (-20.8% at 200 μM)	–	–
EGCG	–	10 - 3000 μM (100% at 3000 μM)	225
MEGA	0.2-10 μM (-55.1% at 4 μM)	50 - 3000 μM (100% at > 1000 μM)	102.3 ± 0.1
MEPCA	–	86.1 ± 0.1	8.24 ± 0.03

[a] All data are reported as the average of three trials with calculated standard deviations.
[b] Negative percentage values represent prooxidant activity of the compound.

Mg(II) is commonly used to stabilize semiquinone radicals of polyphenols, thereby enabling detection by EPR spectroscopy [28, 29]. EC + Mg(II) shows a three-line EPR spectrum in every case at pH 7.2, regardless of Cu(II) or H_2O_2 addition (Figure 2.2A). Similar spectra have been observed for Zn(II)-trapped EC semiquinone radical [30] and in both cases, the polyphenol undergoes a one-electron oxidation to semiquinone that is trapped by coordination and stabilization with Mg(II) or Zn(II). Analysis of the EC spectra indicates that the three-line pattern is not a true triplet, since a weak signal is observed to the

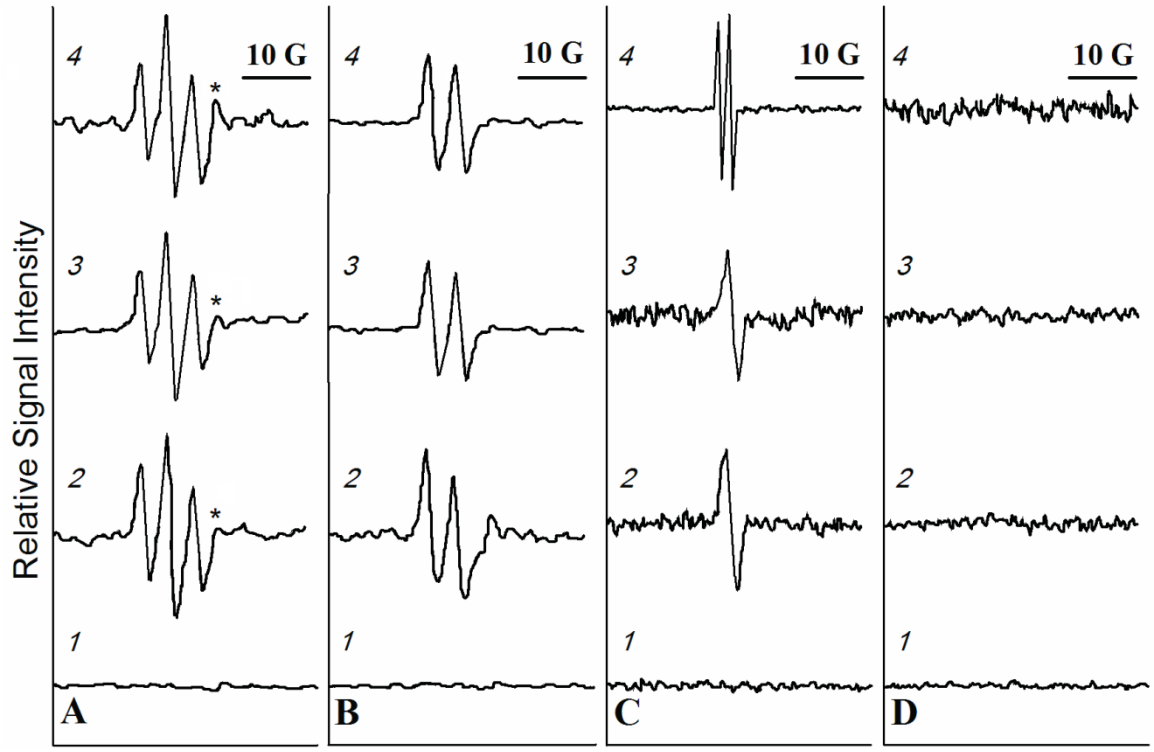

Figure 2.2. EPR spectra of A) EC, B) EGCG, C) MEGA, and D) MEPCA with Mg(II) at pH 6.0 (1), Mg(II) at pH 7.2 (2), same as 2 plus Cu(II) (3), and same as 2 plus Cu(II), ascorbate, and H_2O_2. From reference [25]; used with permission (Appendix A).

right of the three primary resonances (Figure 2.2A, marked with *). These resonances are assigned to splitting of the semiquinone radical by H2', H5', and H6' of the catechol rings (Figure 2.1).

The MEGA semiquinone is observed as a singlet (Figure 2.2C, panels 2 and 3) formed by the hydrogen extraction of the 4-OH group (Figure 2.1) [31]. The doublet observed for MEGA is the ascorbate radical [32], indicating that MEGA does not scavenge the ascorbate radical (Figure 2.2C). No radical was detected for MEPCA solutions, consistent with its significantly lower IC_{50} value for DNA damage prevention when compared to the other three compounds (Table 2.2). Interestingly, three of the tested polyphenol compounds appear to undergo significant autooxidation (excluding MEPCA), existing in substantial quantity as semiquinone radical even in the absence of copper or H_2O_2. At pH 6.0, semiquinone radicals were not detected for any of the tested compounds (Figure 2.2).

Another method used to detect semiquinone formation in the presence of copper was by using α-(4-pyridyl-1-oxide)-*N*-*t*-butylnitrone (POBN), a spin trap capable of detecting the $^{\bullet}OH$ radical in solution by forming a spin adduct with $^{\bullet}CH(OH)CH_3$, the α-hydroxyethyl radical, formed when $^{\bullet}OH$ abstracts a hydrogen from ethanol [33-36]. Cu(II) alone displayed no EPR signal in the presence of POBN; however, the addition of Cu(II) and ascorbate with and without H_2O_2 resulted in the $^{\bullet}CH(OH)CH_3$ adduct of POBN (Figure 2.3B and C). The EPR resonances for this adduct agree with reported values (a_N = 15.8 G, a_H = 2.6 G compared to the established values a_N = 15.6 G, a_H = 2.6 G [32, 37]; Table 2.5 in the

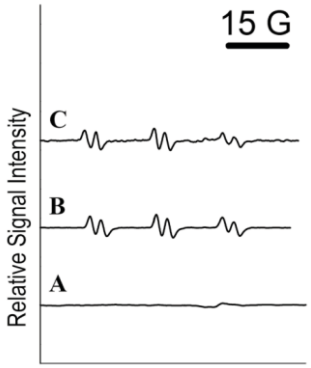

Figure 2.3. EPR spectra of A) Cu(II) with POBN, B) Cu(II) and ascorbate with POBN, and C) Cu(II), ascorbate, and H_2O_2 with POBN. All spectra were acquired in the presence of ethanol, MOPS buffer (pH 7.2), and NaCl. From reference [25]; used with permission (Appendix A).

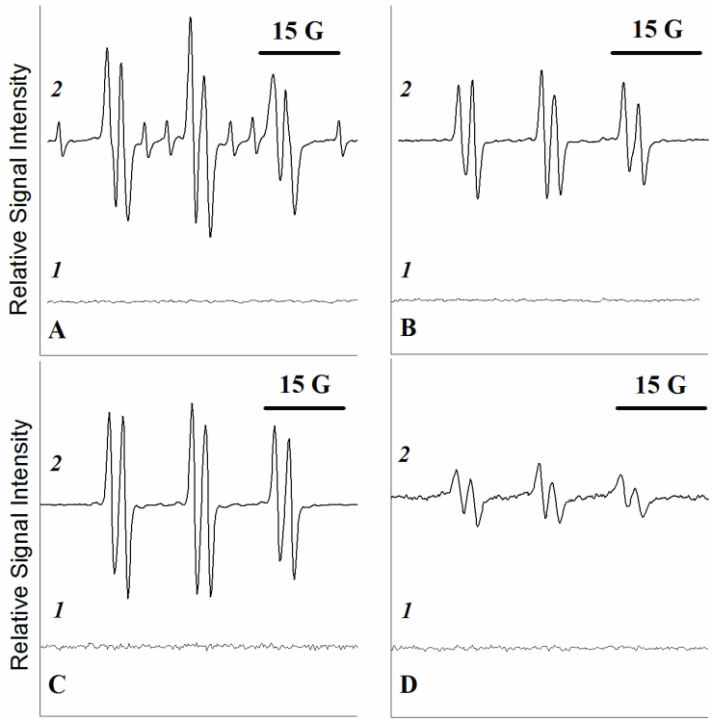

Figure 2.4. EPR spectra of A) EC, B) EGCG, C) MEGA, D) MEPCA with POBN (1), and Cu(II), ascorbate, H_2O_2, and POBN (2). From reference [25]; used with permission (Appendix A).

Experimental Section). EC also showed the α-hydroxyethyl-POBN adduct when Cu(II) was added, indicating that EC can reduce Cu(II) similarly to ascorbate. However, when Cu(II) is first reduced with ascorbate and then combined with EC and lastly H_2O_2, a much more intense α-hydroxyethyl-POBN adduct signal was obtained and multiple spin environments are present (Figure 2.4: a_{N1}= 15.8 G, a_{N2}= 16.2 G, a_{H1}= 2.6 G, a_{H2}~ 11.5 G; Table 2.5). The additional resonances are due to the hydrogen radical ($^{\bullet}$H) adduct of POBN reported by Gunther and coworkers [33].

The α-hydroxyethyl-POBN radical was the only radical detected in solutions of MEGA and MEPCA compounds when POBN was used as a spin trap (Figure 2.4). However, the intensity of the detected POBN adduct is significantly less intense when MEPCA is present than MEGA (Figure 2.5C and D), indicating less radical formation [38, 39] and is consistent with MEPCA's lower IC_{50} value (Table 2.2). Because EGCG, MEGA, and MEPCA did not prevent all radical formation but also did not display the six lower-intensity resonances for the $^{\bullet}$H adduct of POBN similar to EC, these results suggest that EGCG, MEGA, and MEPCA may be scavenging radical species. These results agree with those reported by Luo, *et al.* who reported that MEGA prevents hydroxyl radical formation *in vivo* [40]. Our EPR results also correlated to the measured IC_{50} values for the four compounds, since only the α-hydoxyethyl POBN adduct was formed when MEGA, MEPCA, and EGCG were present. For the prooxidant EC, however, the hydrogen radical was observed in addition to the α-hydoxyethyl radical adduct (Figure 2.4), which may explain the increase in DNA damage compared to that for the other three compounds.

The detection of both •OH and semiquinone radical adducts in solutions with EC and copper by EPR spectroscopy, as well as brown quinone species formed from EC in the presence of Cu(II), ascorbate, and H_2O_2, indicates redox-cycling is occurring within this system (Figure 2.5). This redox-cycling may account for the increase in DNA damage observed for EC from the gel electrophoresis studies. Because the hard polyphenol oxygen ligands have little affinity for the soft Cu(I) ion, Cu(I) is free to react with H_2O_2, generating DNA-damaging •OH. When Cu(II) is generated, the polyphenol subsequently binds Cu(II) and reduces it to Cu(I). This copper-polyphenol complex then may dissociate into semiquinone radical and Cu(I), recycling the metal ion to once again react with H_2O_2, ultimately restarting the redox cycle. Some compounds, such as EGCG and MEPCA, are not easily oxidized to the quinone product, causing a lack of participation in the redox-cycling pathway and accounting for their antioxidant rather than prooxidant behavior.

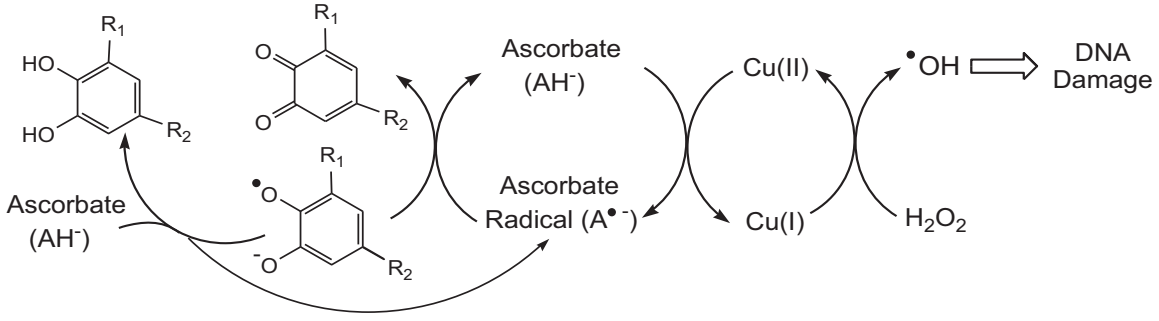

Figure 2.5. Proposed copper and polyphenol redox cycling mechanism leading to both prooxidant and antioxidant activity for polyphenol compounds. From reference [25]; used with permission (Appendix A).

Compounds such as ascorbic acid, assorted polyphenolic acids, and thiols have been shown to be strong reductants and can perpetuate the redox cycling of vitamin E [41], a

compound known for its radical-scavenging antioxidant abilities [42], demonstrating that pro- or antioxidant capacity can be greatly influenced by surrounding chemical environment. Accordingly, it is important to determine the compound's antioxidant ability in the presence and absence of reducing agents to further determine its potential behavior in the complex environment of a cell.

In the absence of the reductant ascorbic acid, any actively damaging radicals that result must come from the polyphenolic compound itself. Gel electrophoresis DNA damaging experiments were again conducted to determine whether or not MEGA, MEPCA, EC, or EGCG directly reduce Cu(II) to Cu(I). The results shown in Figure 2.6 indicate that EC does reduce Cu(II) to Cu(I) that then reacts with H_2O_2 to cause substantial DNA damage (-82.2 ± 0.8% at 500 μM EC), whereas the other compounds did not (Figure 2.6). EGCG, MEGA, and MEPCA did not reduce Cu(II), since no significant DNA damage was observed (4.6 ± 0.6% at 3000 μM, 5.4 ± 0.2 at 3000 μM, and 6.1 ± 0.7% at 3000 μM, respectively, Table 2.3). These EPR spectroscopy and DNA damage gel data suggest that redox cycling causes prooxidant behavior for polyphenols, since they have little affinity for Cu(I) binding to the hard oxygen atoms, allowing Cu(I) to dissociate from the polyphenol and to react with H_2O_2 to form $^{\bullet}OH$ that then damages DNA. Understanding the causes of polyphenol antioxidant or prooxidant activity and the effects of the chemical environment, specifically the presence of metal ions, has on the polyphenols' behavior using *in vitro* models is vital to understand results of cellular and animal studies as well as understanding and predicting therapeutic outcomes.

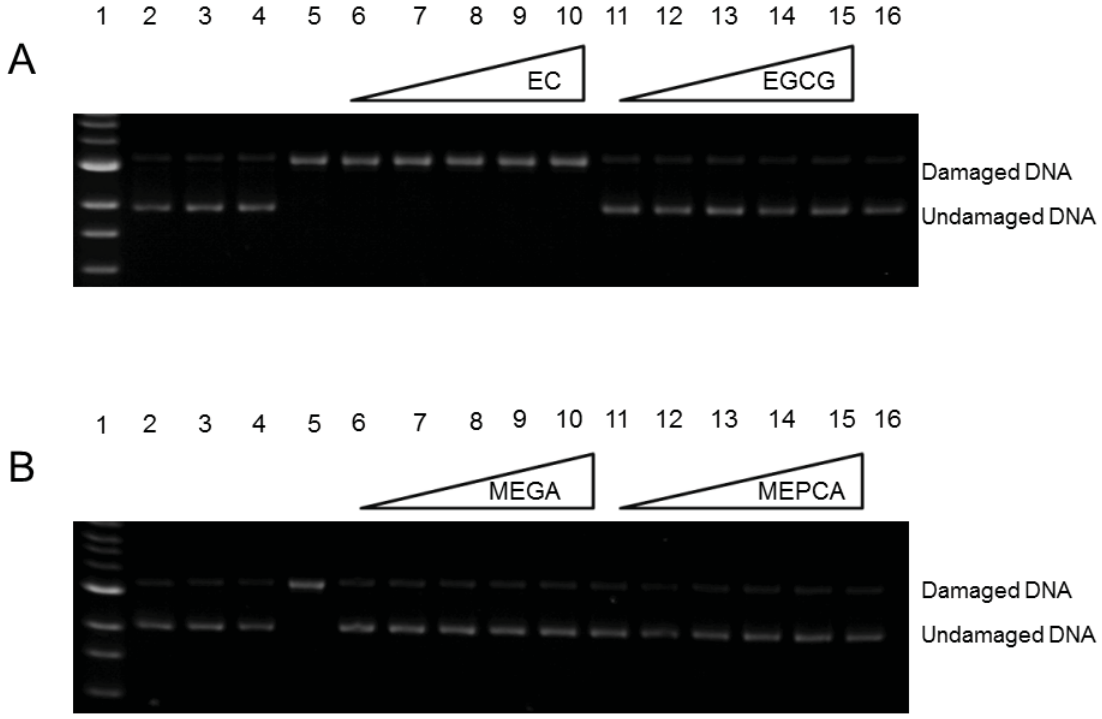

Figure 2.6. A) Gel electrophoresis image of EC and EGCG DNA damage assays with Cu(II) and H_2O_2 (50 μM). Lane 1: MW marker, 1 kb ladder; 2: plasmid (p); 3: p + H_2O_2 (50 μM); 4: p + 500 μM EC; 5: p + H_2O_2 + Cu(II) (6 μM) + ascorbate (7.5 μM); 6-10: H_2O_2 + Cu(II) + 500 μM EC; 11-15: H_2O_2 + Cu(II) + 3000 μM EGCG; 16: p + 500 μM EGCG. B) Gel electrophoresis image of MEGA and MEPCA with Cu(II) (6 μM) and H_2O_2 (50 μM). Lane 1: MW marker, 1 kb ladder; 2: plasmid (p); 3: p + H_2O_2 (50 μM); 4: p + 500 μM MEGA; 5: p + H_2O_2 + Cu(II) (6 μM) + ascorbate (7.5 μM); 6-10: H_2O_2 + Cu(II) + 500 μM MEGA; 11-15: H_2O_2 + Cu(II) + 3000 μM MEPCA; 16: p + 500 μM MEPCA.

Table 2.3. Tabulation of DNA gel electrophoresis results for EC, EGCG, MEGA, and MEPCA with 6 μM Cu(II) and 50 μM H_2O_2.[a]

Lane	Polyphenol, μM	% Supercoiled	% Nicked	% Damage Inhib.	*p* Values
plasmid	None	92.98	7.02	0	-
EC	500	0.6 ± 0.5	99.4 ± 0.5	-82.19 ± 0.81	3.24×10^{-5}
EGCG	3000	86.1 ± 0.2	13.9 ± 0.2	4.59 ± 0.60	5.65×10^{-3}
Plasmid	None	90.58	9.42	0	-
MEGA	3000	86.08 ± 0.1	13.9 ± 0.1	5.40 ± 0.15	2.57×10^{-4}
MEPCA	3000	86.6 ± 0.5	13.4 ± 0.5	6.08 ± 0.66	3.90×10^{-3}

[a] All data are an average of three trials; calculated standard deviations are shown.

Flavonol Derivatives and Their Implications for Flavonol Antioxidant Behavior with Iron

Flavonols are a subgroup of flavonoids that include quercetin, myricetin, and morin (Figure 2.7), that effectively prevent iron-mediated DNA damage. IC_{50} values for myricetin and quercetin DNA damage inhibition are of 2.0 μM and 10.7 μM, respectively [43]. Both myricetin and quercetin have keto-hydroxy metal binding sites in addition to catechol and gallol metal binding sites on the B ring (Figure 2.7). To determine the role of metal binding at the 5-keto-hydroxy and 3-keto-hydroxy sites, the abilities of 5-hydroxychromone, 3-hydroxychromone, and sulfonated morin to prevent DNA damage were determined.

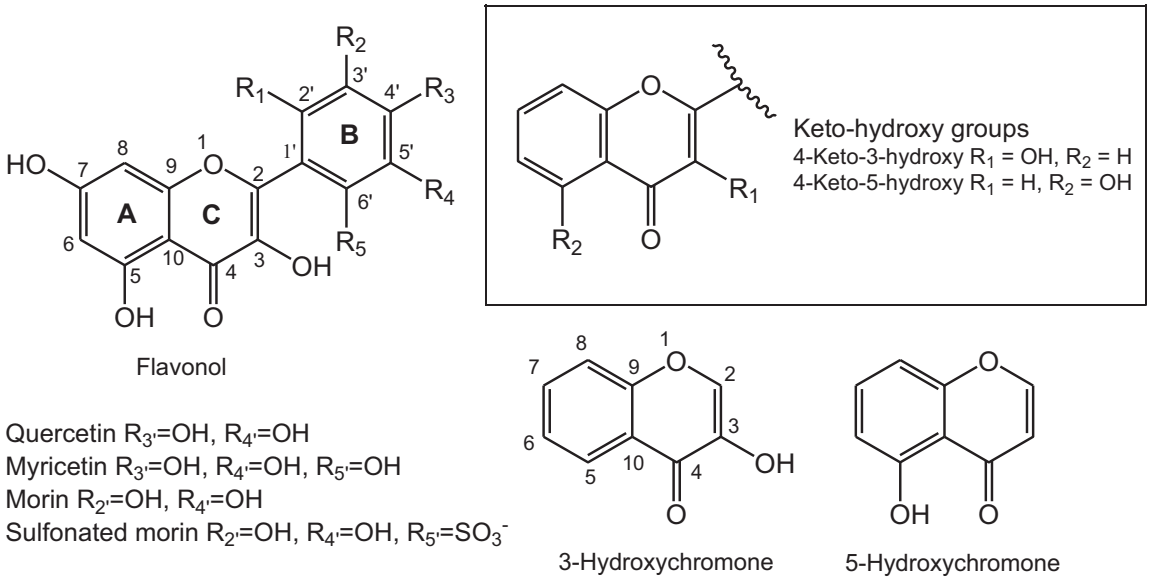

Figure 2.7. Chemical structures for the keto-hydroxy functional group flavonols, and 3- and 5-hydroxychromone showing atomic numbering.

The DNA damage assay results shown in Figure 2.8 indicate that 5-hydroxychromone prevents iron-mediated DNA damage with an IC_{50} value of 419 ± 1 μM. In the same assay, 3-hydroxychromone demonstrated more than twice the antioxidant potency of 5-hydroxychromone (IC_{50} = 193.4 ± 0.6 μM), indicating that the 3-hydroxy-4-keto functionality plays a greater role in preventing iron-mediated DNA damage than the 5-hydroxy-4-keto functionality. Though a direct comparison of the antioxidant activity of 3-hydroxychromone to morin cannot be made due to morin's very low water solubility, comparisons can be made with the antioxidant activity of the more water-soluble sulfonated morin. The IC_{50} values of 3-hydroxychromone (193.4 ± 0.6 μM) and sulfonated morin (91.8 ± 0.2 μM) are significantly different, demonstrating that the presence of the B ring and/or both 3- and 5-hydroxy-keto sites increase antioxidant activity.

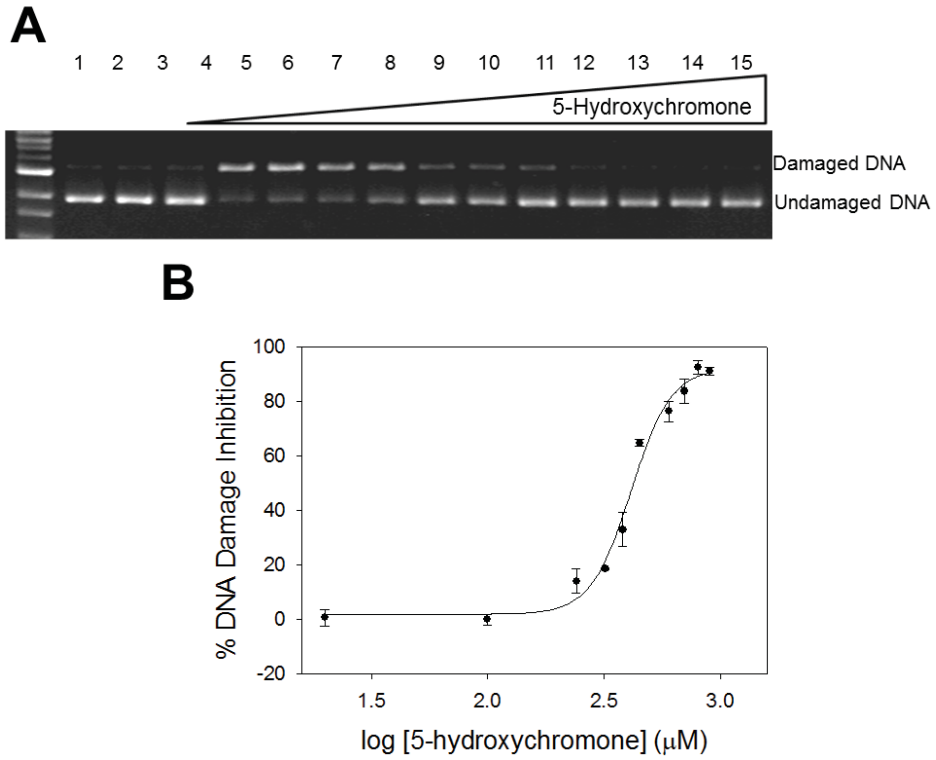

Figure 2.8. A) Gel electrophoresis image of 5-hydroxychromone DNA damage assays with Fe(II) (2 μM) and H_2O_2 (50 μM). Lanes: MW = 1 kb ladder; 1 = plasmid DNA (p); 2 = p + H_2O_2 ; 3 = p + 900 μM 5-hydroxychromone + H_2O_2; 4 = p + Fe(II) + H_2O_2; and lanes 5-14: p + 2 μM Fe(II) + 50 μM H_2O_2 + 20, 100, 240, 320, 380, 450, 600, 700, 800, and 900 μM 5-hydroxychromone, respectively. B) Dose-response curve for 5 hydroxychromone inhibition of iron-mediated DNA damage. Data are reported as the average of three trials with calculated standard deviations. From reference [44]; used with permission (Appendix A).

Combining $Fe(EDTA)^{2-}$ and H_2O_2 alone results in significant DNA damage (lane 4), and addition of increasing concentrations of sulfonated morin has no effect on DNA damage inhibition. In contrast, both 3- and 5- hydroxychromone inhibit DNA damage by $Fe(EDTA)^{2-}/H_2O_2$ at high concentrations. 3-Hydroxychromone inhibits a maximum of 70 ± 1% DNA damage at 1000 μM, whereas 5-hydroxychromone inhibits a maximum of 49 ± 4% DNA damage at 875 μM (Figure 2.9). Thus, 5-hydroxychromone has an IC_{50} value for

prevention of $Fe(EDTA)^{2-}/H_2O_2$-mediated DNA damage greater than the maximum concentration that can be achieved in these gel studies. The IC_{50} value for 3-hydroxychromone inhibition of DNA damage by $Fe(EDTA)^{2-}/H_2O_2$ is 293 ± 2 μM, significantly higher than for prevention of iron-mediated DNA damage (IC_{50} = 193 μM). Comparing the DNA damage results from Fe(II) and $Fe(EDTA)^{2-}$, it is clear that iron binding is the only mechanism for iron-mediated DNA damage prevention by sulfonated morin and is the primary antioxidant mechanism for both 3- and 5-hydroxychromone, since the IC_{50} values for DNA damage prevention are considerably lower when iron is unchelated. For the hydroxychromones, a second mechanism (possibly ROS scavenging) also contributes to antioxidant behavior at high concentrations.

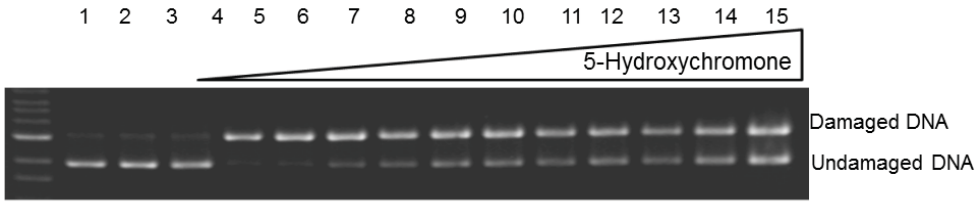

Figure 2.9. Gel electrophoresis image of 5-hydroxychromone DNA damage assays with $Fe(EDTA)^{2-}$ (400 μM) and H_2O_2 (50 μM). Lanes: MW = 1 kb ladder; 1 = plasmid DNA (p); 2 = p + H_2O_2; 3 = p + 875 μM 5-hydroxychromone + H_2O_2; and 4 = p + $Fe(EDTA)^{2-}$ + H_2O_2. Lanes 5-15: p + $Fe(EDTA)^{2-}$ + H_2O_2. + 20, 100, 240, 320, 380, 450, 600, 700, 800, and 875 μM 5-hydroxychromone, respectively. From reference [44]; used with permission (Appendix A).

Curcumin: An Answer to Radical Damage?

Curcumin (diferuloymethane) is the active compound in the herbal remedy and spice turmeric (*Curcuma longa*) [45] and has a wide range of potential uses, including oral

chemopreventative properties [46], anti-inflammatory properties both *in vitro* [47] and *in vivo* [48], and is a potential Alzheimer's treatment due to the suppression of Aβ-protein formation in animal studies [49]. Curcumin concentrations as low as 1 μM have been shown not only to prevent aggregation of monomeric Aβ, but also to promote its disaggregation *in vitro* [50]. The poor water solubility of curcumin has been an issue, so efforts have been made to create water-soluble curcumin analogs with similar biological properties to increase therapeutic applications [51]. Increasing the bioavailability of curcumin is also an active area of research, through developing analogs or alternate absorption methods. In a mouse brain, curcumin concentrations have reached around 3.2 μM [52, 53] and tetrahydrocurcumin, a bioavailable curcumin analog, can reach concentrations of up to 6.0 μM [53]. The preparation of curcumin is also a factor in to the bioavailability. For instance, when rats orally ingest curcumin, samples that are prepared as nanoparticles are much more bioavailable compared to curcumin samples paired with an absorption enhancer (0.71 μM curcumin in blood compared to 0.33 μM) [54].

Curcumin has two protonation states that exist in the pH range 2-8, containing either a keto-hydroxy or a β-diketo functional group [55] (Figure 2.10). The keto-hydroxy functional group was previously discussed in this chapter (Figure 2.7) and is capable

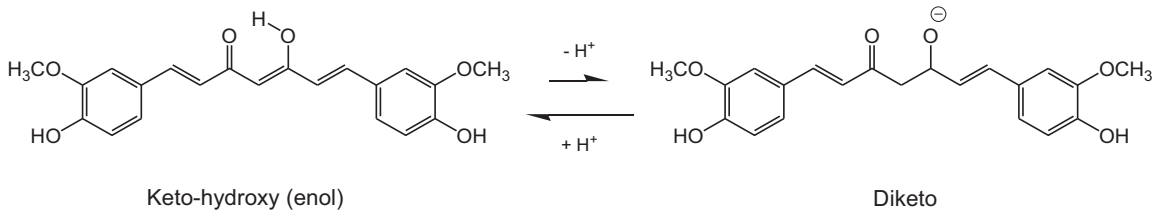

Figure 2.10. Curcumin protonation states at pH 2-8 [55].

of binding metal ions as well as contributing to antioxidant activity in polyphenolic compounds. The β-diketo moiety (Figure 2.10) is known to bind metals [56] and curcumin derivatives have shown strong β-diketonate-Fe(III) binding with a proposed 3:1 stoichiometry [57]. The β-diketo functional group is assumed to be involved in curcumin's antioxidant activity [58]; however, examination of the antioxidant activity for analogs that contain fewer than two phenol groups show that not only is the β-diketo necessary for antioxidant activity, the two phenol groups are as well [58].

In DNA damage assays, the IC_{50} for curcumin prevention of iron-mediated DNA damage is 28 ± 1 μM (Figure 2.11). With $Fe(EDTA)^{2-}$, curcumin prevented only 38 ± 6% damage at 75 μM (the maximum concentration attainable; Figure 2.12, Table 2.9) compared to 98 ± 6% at 75 μM with $Fe(II)/H_2O_2$. The somewhat high error for DNA the damage assay results at high curcumin concentrations are due to the limited solubility of curcumin, with ~75 μM being the most consistently attainable concentration for a prolonged period of time. These results establish that the primary mechanism for antioxidant activity is metal binding rather than ROS scavenging in the presence of Fe(II), similar to the results observed for catechol- and gallol- containing polyphenols [43].

In the presence of Cu(I), curcumin behaves as a slight prooxidant at low concentrations, with a maximum percentage of DNA damage (11.1 ± 0.5%) at 10 μM. At all higher concentrations, curcumin acts as an antioxidant, with a maximum DNA damage prevention of 81 ± 4% at 70 μM (Table 2.10, Figure 2.13), yielding an IC_{50} of 54.95 ± 0.05 μM for copper-mediated DNA damage (Figure 2.13B). The Fenton-like reaction does not occur when the copper ion is chelated prior to peroxide addition (with no statistically

significant change in DNA damage, Figure 2.14), indicating that metal-binding is the only antioxidant mechanism for curcumin in the presence of Cu(I).

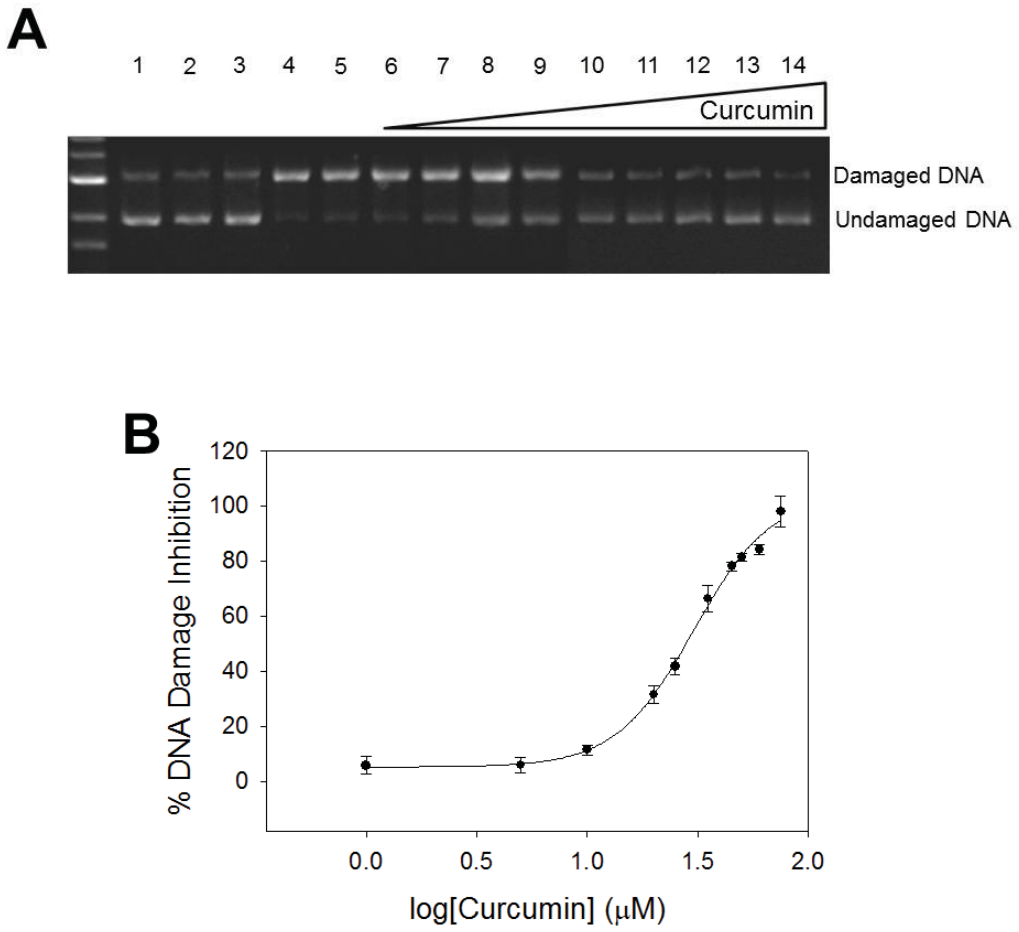

Figure 2.11. A) Gel electrophoresis image of curcumin DNA damage assays with Fe(II) (2 μM) and H_2O_2 (50 μM); lanes: MW = 1 kb ladder; 1: plasmid (p); 2: p + H_2O_2; 3: p + 75 μM curcumin; 4: p + H_2O_2 + Fe(II); 5-14: lane 5 + 1, 5, 10, 20, 25, 35, 45, 50, 60, and 75 μM, respectively. B) Dose-response curve for curcumin inhibition of iron-mediated DNA damage. Data are reported as the average of three trials with calculated standard deviations.

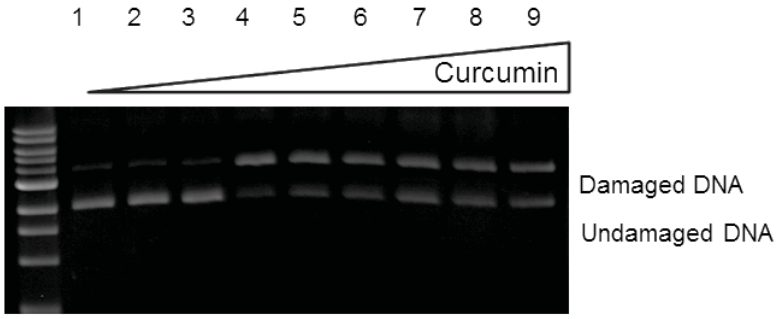

Figure 2.12. Gel electrophoresis image of curcumin DNA damage assays with $Fe(EDTA)^{2-}$ (400 μM) and H_2O_2 (50 μM); lanes: MW = 1 kb ladder; 1 = plasmid DNA (p); 2 = p + H_2O_2; 3 = p + 75 μM curcumin + H_2O_2; and 4 = p + $Fe(EDTA)^{2-}$ + H_2O_2. Lanes 5-9: p + $Fe(EDTA)^{2-}$ + H_2O_2. + 1, 10, 25, 45, and 75 μM curcumin, respectively.

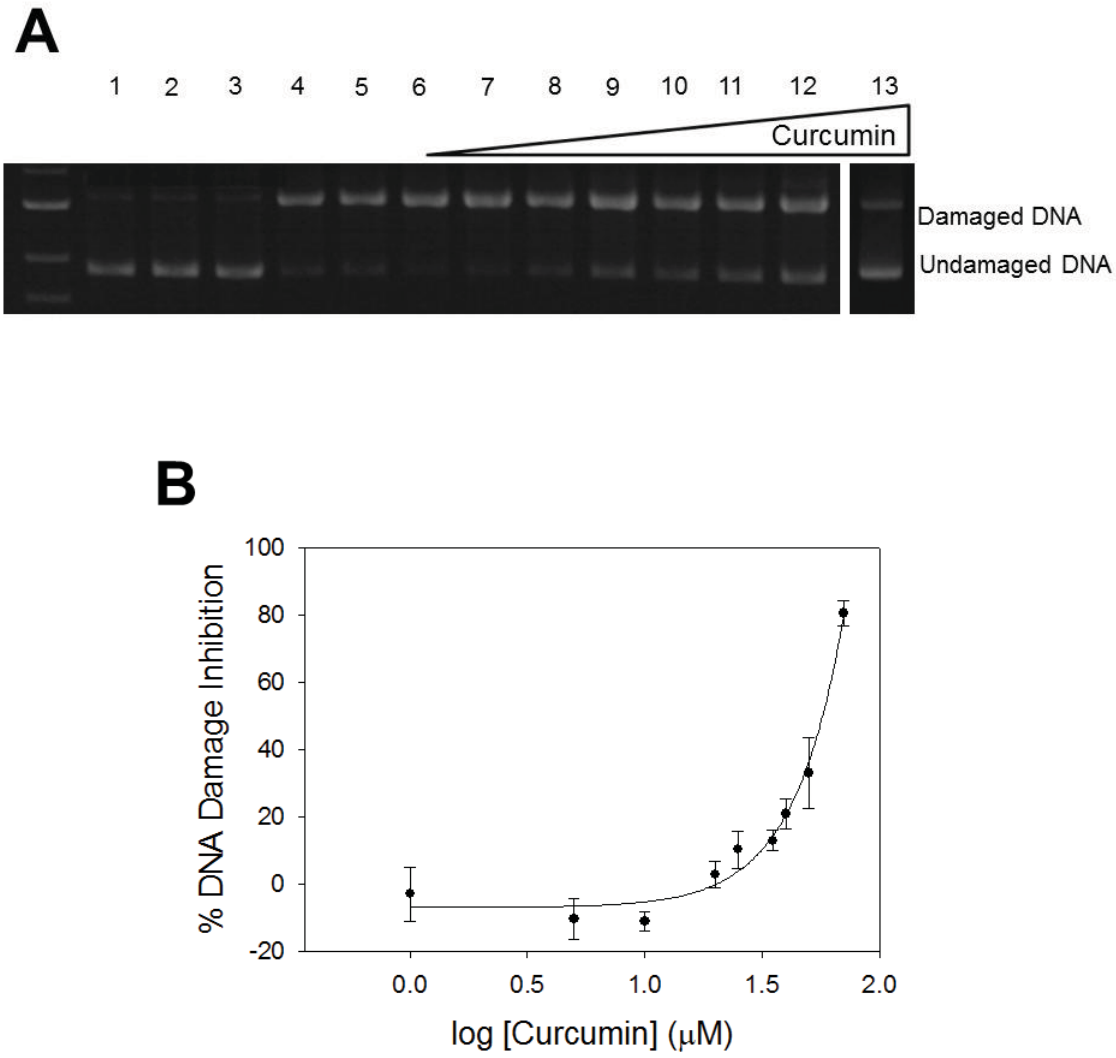

Figure 2.13. A) Gel electrophoresis image of curcumin DNA damage assays Cu(I) (6 μM) and H_2O_2 (50 μM); lanes: MW = 1 kb ladder; 1: plasmid (p); 2: p + H_2O_2; 3: p + 70 μM curcumin; 4: p + H_2O_2 + Cu(I); 5-13: lane 5 + 1, 5, 10, 20, 25, 35, 40, 50, and 70 μM, respectively. B) Dose-response curve for curcumin inhibition of copper-mediated DNA damage. Data are reported as the average of three trials with calculated standard deviations.

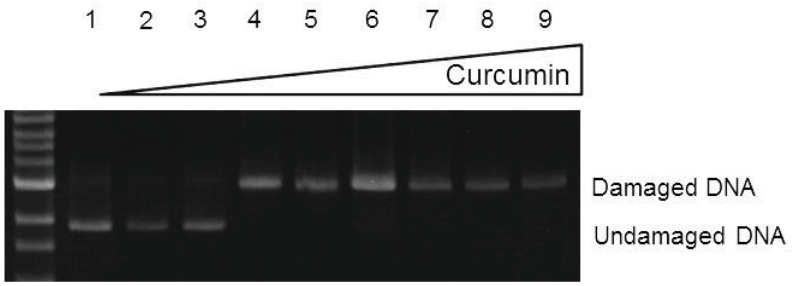

Figure 2.14. Gel electrophoresis image of curcumin DNA damage assays with $Cu(bpy)_2^+$ (50 μM) and H_2O_2 (50 μM). Lanes: MW = 1 kb ladder; 1: plasmid (p); 2: p + H_2O_2; 3: p + 70 μM curcumin; 4: p + H_2O_2 + $Cu(bpy)_2^+$; 5-9: lane 5 + 1, 10, 25, 40, and 70 μM, respectively.

Since metal-binding is a key mechanism for the antioxidant activity of curcumin based on the gel DNA damage assays results, further examination of iron and copper binding to curcumin could provide insight into iron and copper coordination modes and oxidation states. Upon addition of Fe(II), curcumin shows an absorbance band at 524 nm in the ultraviolet-visible (UV-vis) spectrum for both 1:1 and 1:3 curcumin-to-iron ratios after 10 min reaction time, indicative of Fe(III) binding, not Fe(II) binding (Figure 2.15A). This band represents a p(π) orbital of the phenolate ion interacting with the half-filled $d_{x-y}/d_{z2}(\pi)$ orbital of Fe(III) [59], confirming that the oxidized Fe(III)-curcumin complex has formed.

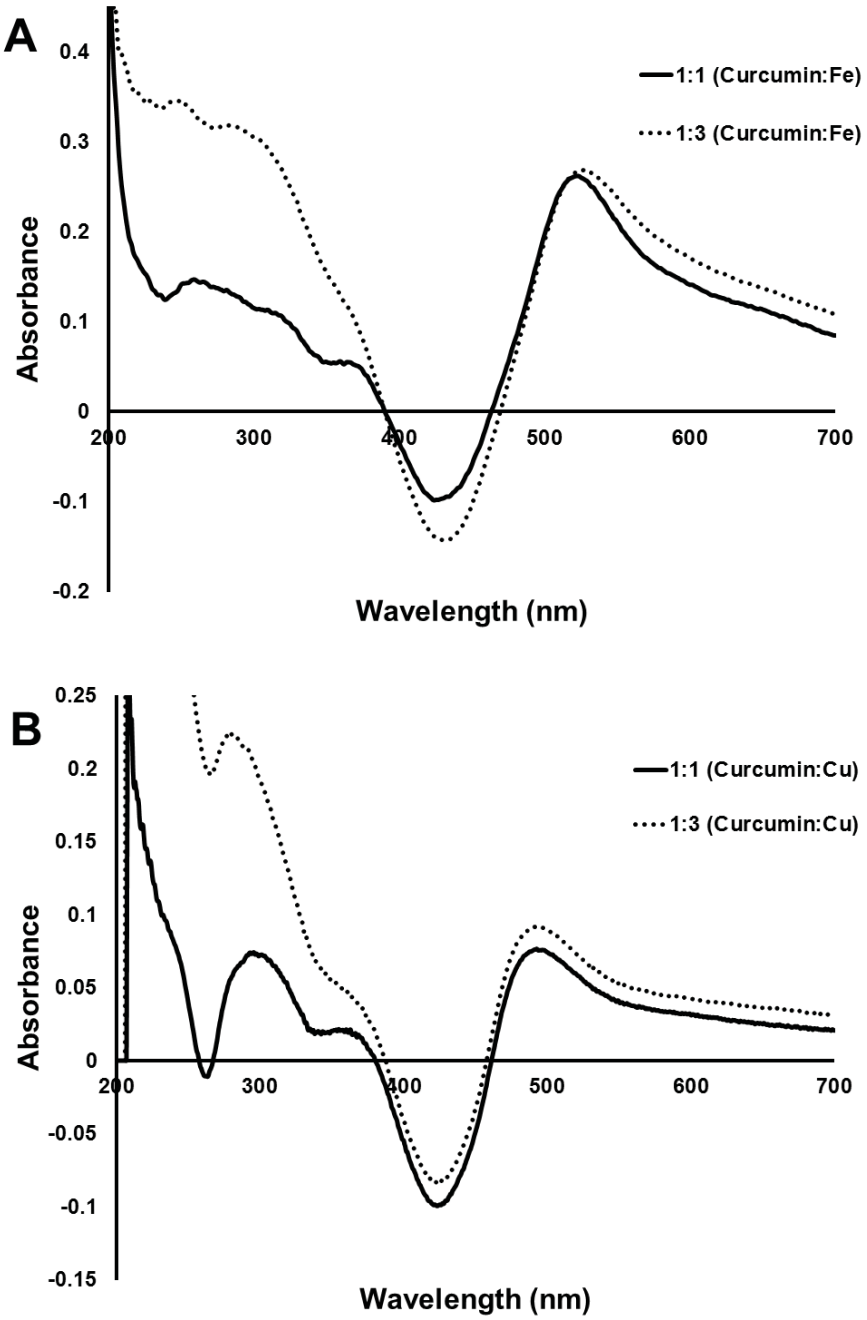

Figure 2.15. UV-vis difference spectra for curcumin (145 μM) in the presence of A) Fe(II) in MES buffer (10 mM, pH 6.0) and B) Cu(I) in MOPS buffer (10 mM, pH 7.2).

Similarly, 10 min after addition of Cu(I) to curcumin, the UV-vis spectra also showed phenolate binding to Cu(II), not Cu(I), at 295 nm [60] (Figure 2.15B). This oxidation behavior upon Cu(I)-O binding has been reported previously. Cvetkovic, and coworkers attempted to examine Cu(I)-phenolate complexes in an oxygenated system using UV-vis spectroscopy, yet the spectroscopic results were suggestive of Cu(II) complexes [61]. Since curcumin binding promotes the oxidation of Fe(II) and Cu(I), iron- and copper-curcumin complexation *in vivo* may aid in its observed antioxidant activity by stabilizing the oxidized form of the bound metal ion and preventing metal redox cycling.

In the presence of copper and iron, curcumin shows metal binding and prevents DNA damage mediated by Fe(II). However, the potential for curcumin as a radical scavenger is also worthy of investigation. Cyclic voltammetry (CV) experiments were conducted to determine whether its redox potentials could correlate with the antioxidant behavior of curcumin. Curcumin is electrochemically active when tested ± 1 V in aqueous solution and has one reversible redox couple that is electrochemically similar to the catechol oxidation [62] (Figure 2.16, indicated with I and I') and one irreversible oxidation reaction (Figure 2.16, indicated with II), attributed to a phenol redox potential [62] (Table 2.4). The irreversible reduction observed at pH 6.0 and 7.2 may be a reason why curcumin is an effective radical scavenger[64, 65]. In the body, the redox range for the metal-mediated

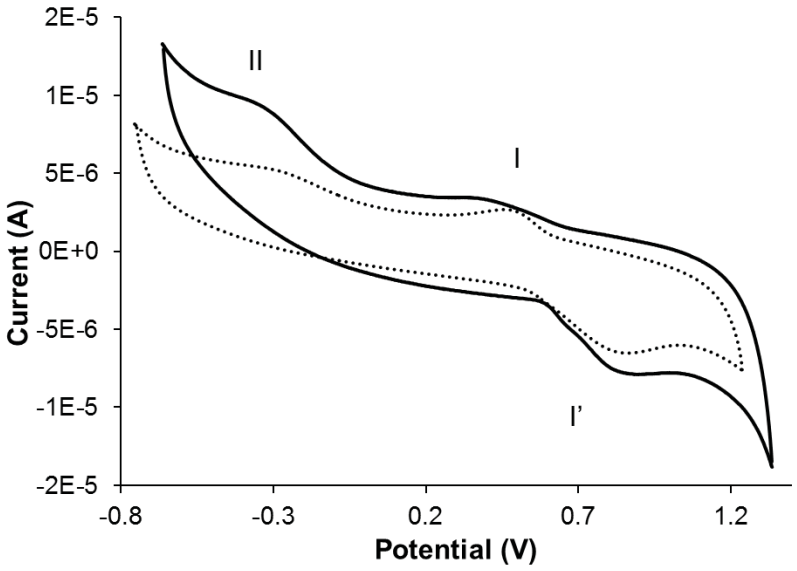

Figure 2.16. Cyclic voltammograms of curcumin (380 μM) vs. NHE in MES buffer (64 mM, pH 6.0, dotted line) and MOPS buffer (64 mM, pH 7.2, solid line) with KNO_3 (64 mM) as the supporting electrolyte.

Table 2.4. Electrochemical potentials vs. NHE of curcumin at various pH values.

pH	Ep_a (V)	Ep_c (V)	ΔE (V)	$E_{1/2}$ (V)	Source
5.0 [a]	-1.1, -0.8	-0.9, -1.1, -1.4	0.2, 0.3	-1.0, -0.95	[63]
6.0 [b]	0.456, -0.312	0.861	0.404	0.659	This work
7.2 [c]	0.337, -0.377	0.894	0.557	0.616	This work
8.5 [d]	0.5, 0.8	0.5	0.0	0.5	[63]

[a] In 0.2 M $NaCH_3COO$ buffer with 20 mM NaCl as a supporting electrolyte, [b] 64 mM MES buffer with 64 mM KNO_3 as a supporting electrolyte, [c] 64 mM MOPS buffer with 64 mM KNO_3 as a supporting electrolyte, and [d] 50 mM Na_3PO_4 buffer with 0.3 M NaCl for a supporting electrolyte.

catalytic generation of hydroxyl radical from hydrogen peroxide is 0.460 V to -0.324 V [66]. Using this range to gauge biologically spontaneous redox reactions, both oxidations and the reduction of curcumin are within this range, indicating that its redox behavior may also play a role in curcumin's biological antioxidant activity.

Stanić, *et al.* performed cyclic voltammetry on curcumin at pHs 5.0 and 8.5 and the results correlate with the redox behavior observed at pHs 6.0 and 7.2 [63]. It is difficult to compare the results obtained by Stanić, *et al.* with the data reported in this work, since the curcumin samples used by Stanić and coworkers were dissolved in pure ethanol before diluting to the required concentrations with aqueous buffer (resulting in 0.40 M and 0.34 M ethanol, final concentrations, for pH 5.0 and pH 8.5 samples, respectively), whereas the curcumin samples in this work were dissolved in significantly less ethanol (0.057 M ethanol final concentration). The redox values ($E_{1/2}$) at pHs 6.0, 7.2, and 8.5 shift to a more negative potential, exhibiting a pH dependence reported for other polyphenolic compounds [67-69]. The observed electrochemical activity coincides with reported non-polar cyclic voltammetry [63], and also lends credibility to the secondary DNA damage prevention mechanism of radical scavenging.

The electrochemical investigation shows that curcumin may act as a radical scavenger at high concentrations in addition to acting as a metal-binding antioxidant. Curcumin prevents a maximum of 98% of damage at 75 μM through iron chelation, but if curcumin the iron is chelated, only 38% of DNA damage is prevented at the same concentration. Thus, some small amount of antioxidant activity may be due to a non-iron-binding mechanism, such as radical scavenging. The fact that curcumin is electrochemically active supports this secondary antioxidant mechanism of radical scavenging. In contrast, copper-

binding is the only observed mechanism of antioxidant activity for curcumin in the presence of copper.

Conclusions

EPR spectroscopy results suggest that the prooxidant activity observed for some polyphenol compounds is the result of a redox-cycling pathway wherein the polyphenols initially share little affinity for Cu(I), allowing it to react with H_2O_2 to generate $^{\bullet}OH$ (detected as the α-hydroxyethyl radical adduct of POBN). Polyphenol compounds can then reduce Cu(II), generating Cu(I) and semiquinone radicals (detected through Mg(II) stabilization); the latter can reduce oxygen to superoxide and ultimately regenerate H_2O_2, or react with excess ascorbate to regenerate the parent polyphenol compound, to restart the copper redox cycle. These EPR results suggest a redox-cycling mechanism for polyphenol prooxidant effects on DNA damage by Cu(I)/H_2O_2 that is consistent with our observed gel electrophoresis results. MEPCA, with the greatest ability to prevent copper-mediated DNA damage, also formed the lowest concentration of $^{\bullet}OH$ radical as determined in EPR studies. Hence, EPR spectroscopy has proven to be an invaluable tool in predicting both the pro- and antioxidant activities of polyphenols in the presence of Cu(I).

Previous studies have investigated the antioxidant activities of 3-hydroxychromone, 5-hydroxychromone, and sulfonated morin primarily in acidic (pH = 2) or organic solvent systems. In contrast, this work focuses on the *in vitro* antioxidant properties of these three compounds in aqueous solution at physiologically relevant pH 6. The results from DNA damage prevention and other experiments prove that antioxidant activity of flavonols with competing 3- and 5-hydroxy-keto groups is controlled by iron binding at the 3-hydroxy-keto

site. In comparison, the antioxidant activities of quercetin and myricetin are controlled primarily by iron binding at the catechol and gallol groups, respectively, not at their hydroxy-keto sites. Only at high concentrations, alternative mechanisms (such as ROS scavenging) come into play for 3- and 5-hydroxychromone. Although the majority of research on flavonoid antioxidant activity primarily focuses on the ROS scavenging abilities of these compounds, this study reflects the importance of iron binding and oxidation on flavonoid antioxidant activity, specifically at the hydroxy-keto sites.

Curcumin demonstrates versatile chemical behavior that can account for its observed antioxidant activity. Curcumin binds Fe(III) and Cu(II) as measured by UV-vis spectroscopy, has demonstrated both reversible and irreversible redox potentials within a biologically relevant range, has a low IC_{50} for prevention of iron-mediated DNA damage, and prevents substantial copper-mediated DNA damage at concentrations above 35 μM. When Cu(I) or Fe(II) is chelated prior to curcumin addition, curcumin prevents little to no DNA damage, suggesting that metal chelation is the primary mechanism in antioxidant activity. These metal chelation antioxidant effects may be a reason why curcumin is such a promising treatment for diseases that are often associated with an abundance of labile iron and copper ions, such as Alzheimer's and Parkinson's disease.

Experimental Section

General. Water was purified using a Barnstead NANOpure DIamond Life Science (UV/UF) water deionization system (Barnstead International). (−)-Epicatechin (Aldrich), (−)-epigallocatechin-3 gallate (Cayman Chemical Company), methyl 3,4,5-trihydroxybenzoate, methyl 3,4 dihydroxybenzoate, curcumin (MP Biomedical),

$FeSO_4 \cdot 7H_2O$ (Acros Organics), $NaOH \cdot H_2O$ (99.996%), and NaCl (99.999%) (Alpha Aesar) were all used as received. High purity NaOH and NaCl were essential in order to avoid metal contamination. H_2O_2 (Fisher) was a 30% solution in water; absolute ethanol (Acros), Ultrol® grade 2-(N-morpholino)ethanesulfonic acid (MES) (Calibiochem) and 3-(N-morpholino)propanesulfonic acid (MOPS) buffers (Alfa Aesar), TRIS base, Na_2EDTA (J.T. Baker), ethidium bromide (Lancaster), and agarose (VWR) were also used as received. Because of the necessity for all experiments involving DNA damage to be as free from redox-active metals as possible, all microcentrifuge tubes were washed in 1 M HCl for at least 30 min, triply rinsed with deionized water, and dried.

To avoid use of radical scavenging solvents such as DMSO or ethanol that are typically used to dissolve polyphenol compounds, [70, 71] addition of a small amount of NaOH (20–100 μL of 1 M NaOH per 10 mL polyphenol stock solution in buffer) was sufficient to quickly and completely dissolve EC and EGCG. These stock solutions were then readjusted to either pH 6.0 in MES buffer or pH 7.2 in MOPS buffer as required, resulting in no precipitation of the polyphenol compound. To dissolve curcumin, a small measured amount of MES or MOPS buffer (2.0 mL, 10 mM, pH 6.0 or 7.2, respectively) was added to curcumin and then a small amount of pure ethanol was added (0.05 M EtOH in final stock solution, about 58 μL per 20 mL stock solution). The buffer/ethanol solution was then adjusted to a basic pH (~10) by use of less than 50 μL 1 M NaOH / 50 mL sample (identifiable by a dark red color) and then adjusted back to pH 6.0 or 7.2 by slowly adding buffer at low concentrations (10 - 45 mM), ramping up buffer concentrations slowly. The solution should be brilliant yellow with no precipitation. Precipitation indicates that the solution was prepared with MES or MOPS buffer at too high a concentration. Ethanol

concentrations in the curcumin solutions were accounted for in the gel electrophoresis experiments.

Transfection and amplification of *E. coli*, and purification of plasmid DNA. Plasmid DNA pBSSK was purified from *E. coli* strain DH1 using a PerfectPrep Spin kit (5-Prime). The plasmid DNA was dialyzed at 4 °C against EDTA (1 mM) and NaCl (50 mM) for 24 h and then against NaCl (130 mM) for 24 h to remove metal ions from the DNA. For all experiments, DNA absorbance ratios $A_{250}/A_{260} \leq 0.95$ and $A_{260}/A_{280} \geq 1.8$ were ensured for the dialyzed DNA sample.

Gel electrophoresis experiments under Fenton reaction conditions. MES buffer at pH = 6.0 (10 mM final concentration) was used to ensure the solubility of Fe(II) in all of these experiments [72], and iron solutions were immediately prepared from solid $FeSO_4 \cdot 7H_2O$ prior to each experiment. For each reaction, reagents were added in the following order to achieve the given final concentrations in a final volume of 10 μL: deionized H_2O, MES buffer (10 mM, pH 6.0), NaCl (130 mM), 100% ethanol (10 mM), the desired concentration of compound (0.01-1500 μM), and Fe(II) (2 μM). This mixture then was allowed to stand at room temperature for 5 min, followed by addition of pBSSK DNA (0.1 pmol in 130 mM NaCl). After again standing for another 5 min of standing, H_2O_2 (50 μM) was added and the Fenton reaction was allowed to occur for 30 min. EDTA (50 μM) was used to quench the reaction, and loading dye (2 μL) was added to achieve a final volume of 12 μL. Gel electrophoresis was run in TAE buffer for 30 min at 140 V to separate the nicked and supercoiled forms of the plasmid DNA. Gels were stained for 5 min using

ethidium bromide and then washed for an additional 10 min in deionized H_2O. The gels were imaged under UV light and the amount of damaged and undamaged DNA was quantified using UVIproMW software (Jencons Scientific Inc., 2003). Ethidium stains supercoiled DNA less efficiently than nicked DNA, so supercoiled DNA band intensities were multiplied by 1.24 prior to comparison [73, 74]. Intensities of the nicked and supercoiled bands were normalized for each lane so that % nicked + % supercoiled = 100 %. Gel results for these experiments are given in Tables 2.6 and 2.8.

Gel electrophoresis experiments with $Fe(EDTA)^{2-}$. To determine the role of iron binding in the antioxidant activities of the compounds, $Fe(EDTA)^{2-}$ was used as the iron source. Experiments were performed as described above, with 400 μM $Fe(EDTA)^{2-}$ replacing 2 μM $FeSO_4$. Gel results for these experiments are given in Tables 2.7 and 2.9.

Gel electrophoresis with Cu(I) and H_2O_2. Conditions were similar to the gel electrophoresis experiments with Fe(II) and H_2O_2 except that $CuSO_4 \cdot 5H_2O$ (6 μM, final concentration) and ascorbic acid (7.5 μM, final concentration) were combined prior to each gel experiment in place of Fe(II). Ascorbic acid concentration was 1.25× the Cu(II) concentration to ensure complete reduction of Cu(II) to Cu(I). For gel studies conducted without ascorbic acid, ascorbic acid solutions were replaced with water, keeping all final concentrations in the samples the same. Gel results for these experiments are given in Table 2.10.

Gel electrophoresis with $Cu(bpy)_2^+$ and H_2O_2. Conditions were similar to the gel electrophoresis experiments under Fenton reaction condition protocol except that $CuSO_4 \cdot H_2O$ (50 μM) and bipyridine (200 μM) prior to experimentation to ensure copper chelation and ascorbic acid (62.5 μM) was added prior to experimentation to ensure complete reduction of Cu(II) to Cu(I). Gel results for these experiments are given in Table 2.11.

EPR spectroscopy. EPR spectra were measured on a Bruker EMX spectrometer using a quartz flat cell at room temperature. For all experiments, modulation amplitude varied from 0.5 G to 1.0 G, depending on the sample, modulation frequency was 100 kHz, microwave power was 20 mW, microwave frequency was approximately 9.778 GHz, the time constant was 81.92 ms, conversion time was 81.92 ms, and a sweep width of 100 G centered at 3490 G was used for all samples. Each sample was referenced to the g-factor of 2,2-diphenyl-1- picrylhydrazyl (DPPH; g = 2.0036 [75]). Thirty to ninety seconds were required from the start of the reaction until the flat cell could be loaded into the spectrometer and tuned. These parameters are optimized to observe polyphenol radicals; to observe the Cu(II) complex radical signal, different parameters must be used (microwave frequency = 9.800 GHz, time constant and conversion time = 163.84 ms, modulation amplitude = 6 G, and a sweep width of 1000 G centered at 3386 G). Conditions for EPR experiments were identical to the gel electrophoresis experiments except that the concentrations of Cu(II), H_2O_2, and ascorbate were increased 50-fold to obtain a clear EPR signal, and DNA was excluded. Samples were prepared by adding aqueous solutions of $CuSO_4 \cdot 5H_2O$ (300 μM) to a solution of polyphenol compound (600 μM) along with NaCl

(130 mM), ethanol (10 mM), either MOPS buffer (10 mM, pH 7.2) or MES buffer (10 mM, pH 6.0), ascorbate (375 μM), H_2O_2 (22.5 mM), and either $MgSO_4 \cdot 7H_2O$ (0.53 M) or α-(4-pyridyl-1-oxide)-N-t-butylnitrone (POBN, 30 mM). In each case, copper was added last to initiate the reaction. All concentrations listed are final concentrations in a 1 mL sample volume; for samples without one or more of the listed reaction components, the volume was replaced by adding an equal portion of deionized H_2O so that the final volume of the solution was maintained at 1 mL. Mg(II) is commonly used to stabilize semiquinone radicals of polyphenols for detection by EPR [28, 29], and POBN is a preferred spin trap to use in systems with ethanol where $^{\bullet}OH$ is formed, since POBN traps the ethanol radical adduct of $^{\bullet}OH$ [76-79].

Metal binding analysis via UV-vis spectroscopy. All cuvettes were washed in 6 M HCl for at least 30 min, thoroughly rinsed 3 times with deionized water, and dried to avoid metal contamination. At room temperature, curcumin (145 μM) and MES or MOPS buffered solutions (10 mM, pH 6.0 and 7.2, respectively) were prepared and fresh $FeSO_4 \cdot 7H_2O$ or $CuSO_4 \cdot 5H_2O$ at the indicated concentration ratios were added for a total reaction time of 10 min prior to data collection with a Shimadzu UV-3101PC spectrophotometer (Shimadzu Corp.). Difference spectra were obtained by subtracting a spectrum of curcumin (145 μM) from the curcumin/Fe(II) or curcumin/Cu(I) spectra.

Electrochemical studies. Cyclic voltammetry and differential pulse voltammetry measurements for curcumin (380 μM) were measured using a CH Electrochemical Analyzer (CH Instruments, Inc.) in phosphate buffer (64 mM final concentration of KH_2PO_4, pH 6.0)

with KNO_3 as a supporting electrolyte (64 mM final concentration). Prior to analysis, the solutions were deoxygenated with argon for 45 min; during analysis, the sample was blanketed with N_2 to avoid oxidation. For cyclic voltammetry, the samples were cycled between -1.0 V and 1.0 V vs. Ag/AgCl/3 M KCl (+210 mV vs. NHE [80, 81]) using a glassy carbon working electrode and a platinum counter electrode at a scan rate of 100 mV/s. Differential pulse voltammetry was performed from -1.0 V to 1.0 V in increments of 0.004 V at amplitude 0.05 V, pulse width of 0.05 s, sample width 0.0167 s, and pulse period 0.2 s; sensitivity ranged from 1×10^{-5} to 1×10^{-6} A/V.

Table 2.5. EPR spectroscopy data for EC, EGCG, MEGA, and MEPCA samples under Fenton-like reaction conditions with copper, ascorbate (AA), and H_2O_2. From reference [25]; used with permission (Appendix A).

Sample Component	g	a_{H1}, G	a_{H2} , G	a_{N1} , G	a_{N2} , G	Color
Cu(II) + POBN	—	—	—	—	—	Colorless
(Cu(II), AA) + POBN	2.00434	2.6	—	15.8	—	Colorless
(Cu(II), AA, H_2O_2) + POBN	2.00453	2.6	—	15.8	—	Colorless
EC + Mg(II) (pH 6.0)	—	—	—	—	—	Colorless
EC + Mg(II)	2.00271	4.1 (2H)	—	—	—	Colorless
(Cu(II), EC) + Mg(II)	2.00271	4.1 (2H)	—	—	—	Colorless
(Cu(II), AA, EC, H_2O_2) + Mg(II)	2.00270	4.1 (2H)	—	—	—	Brown
(Cu(II), EC) + POBN	—	—	—	—	—	Colorless
(Cu(II), AA, EC, H_2O_2) + POBN	2.00470	2.6	11.5[e]	15.8	16.2	Brown
EGCG + Mg(II) (pH 6.0)	—	—	—	—	—	Colorless
EGCG + Mg(II)	2.00255	4.4	—	—	—	Colorless, White Ppt
(Cu(II), EGCG) + Mg(II)	2.00287	4.3	—	—	—	Colorless, White Ppt
(Cu(II), AA, EGCG, H_2O_2) + Mg(II)	2.00270	4.3	—	—	—	Faint Yellow, White Ppt
EGCG + POBN	—	—	—	—	—	Colorless
(Cu(II), EGCG) + POBN	—	—	—	—	—	Colorless
(Cu(II), AA, EGCG, H_2O_2) + POBN	2.00467	2.6	—	15.6	—	Faint Yellow
MEGA + Mg(II) (pH 6.0)	—	—	—	—	—	Colorless
MEGA + Mg(II)	2.00370	—	—	—	—	Colorless
(Cu(II), MEGA) + Mg(II)	2.00381	—	—	—	—	Faint Yellow
(Cu(II), AA, MEGA, H_2O_2) + Mg(II)	2.00372	1.8	—	—	—	Faint Yellow
MEGA + POBN	—	—	—	—	—	Colorless
(Cu(II), MEGA) + POBN	—	—	—	—	—	Faint Yellow
(Cu(II), AA, MEGA, H_2O_2) + POBN	2.00243	2.6	—	15.8	—	Faint Yellow
(Cu(II), AA, MEGA, H_2O_2) + POBN	2.00302	2.6	—	15.8	—	Faint Yellow
MEPCA + Mg(II) (pH 6.0)	—	—	—	—	—	Colorless
MEPCA + Mg(II)	—	—	—	—	—	Colorless
(Cu(II), MEPCA) + Mg(II)	—	—	—	—	—	Faint Yellow
(Cu(II), AA, MEPCA, H_2O_2) + Mg(II)	—	—	—	—	—	Faint Yellow
MEPCA + POBN	—	—	—	—	—	Colorless
(Cu(II), MEPCA) + POBN	—	—	—	—	—	Faint Yellow
(Cu(II), AA, MEPCA, H_2O_2) + POBN	2.00211	2.7	—	15.6	—	Faint Yellow
(Cu(II), AA, MEPCA, H_2O_2) + POBN	2.00241	2.5	—	15.6	—	Faint Yellow

Table 2.6. Tabulation of gel electrophoresis results for 5-hydroxychromone DNA damage assays with 2 μM Fe(II) and 50 μM H_2O_2. From reference [44]; used with permission (Appendix A).

Gel lane	5-HC, μM	% Supercoiled	% Nicked	% Damage Inhib.	*p* Values
4: Fe(II) + H_2O_2	0	6.47 ± 6.62	93.53 ± 6.62	0	-
5	20	7.67 ± 9.58	92.33 ± 9.58	0.61 ± 3.13	0.339
6	100	13.27 ± 19.47	86.73 ± 19.47	-0.05 ± 1.89	0.966
7	240	15.03 ± 3.19	84.97 ± 3.19	14.03 ± 4.44	3.17×10^{-2}
8	320	30.73 ± 18.94	69.27 ± 18.94	18.62 ± 0.47	2.12×10^{-4}
9	380	39.98 ± 13.83	61.02 ± 13.83	32.92 ± 6.22	1.17×10^{-2}
10	450	72.43 ± 2.05	27.57 ± 2.05	64.71 ± 1.22	1.18×10^{-4}
11	600	81.37 ± 2.00	18.63 ± 2.00	76.26 ± 3.73	7.96×10^{-4}
12	700	86.90 ± 3.24	13.10 ± 3.24	83.69 ± 4.58	9.97×10^{-4}
13	800	93.46 ± 1.83	6.54 ± 1.83	92.33 ± 2.46	2.37×10^{-4}
14	900	92.58 ± 1.15	7.42 ± 1.15	91.09 ± 1.52	9.28×10^{-5}

Table 2.7. Tabulation of gel electrophoresis results for 5-hydroxychromone DNA damage assays with 400 μM $Fe(EDTA)^{2-}$ and 50 μM H_2O_2. From reference [44]; used with permission (Appendix A).

Gel lane	5-HC, μM	% Supercoiled	% Nicked	% Damage Inhib.	*p* Values
4: $Fe(EDTA)^{2-}$ + H_2O_2	None	9.06 ± 6.41	90.94 ± 6.41	0	-
5	20	10.36 ± 7.84	89.64 ± 7.84	1.53 ± 1.77	0.273
6	100	17.35 ± 5.69	82.65 ± 5.69	9.52 ± 3.56	4.36×10^{-2}
7	240	28.99 ± 6.57	71.01 ± 6.57	22.92 ± 1.79	2.03×10^{-3}
8	320	33.25 ± 3.77	66.75 ± 3.77	27.72 ± 4.57	8.94×10^{-3}
9	380	38.00 ± 8.33	62.00 ± 8.33	33.34 ± 4.07	4.93×10^{-3}
10	450	40.43 ± 4.10	59.57 ± 4.10	35.99 ± 1.48	5.63×10^{-4}
11	600	47.77 ± 5.33	52.23 ± 5.33	41.03 ± 1.72	5.85×10^{-4}
12	700	47.21 ± 3.48	52.79 ± 3.48	43.73 ± 2.55	1.13×10^{-3}
13	800	50.81 ± 6.50	49.19 ± 6.50	48.01 ± 2.49	8.95×10^{-4}
14	875	51.93 ± 3.60	48.07 ± 3.60	49.20 ± 3.60	1.78×10^{-3}

Table 2.8. Tabulation of gel electrophoresis results for curcumin DNA damage assays with 2 μM Fe(II) and 50 μM H_2O_2.

Gel lane	Curcumin, μM	% Supercoiled	% Nicked	% Damage Inhib.	*p* Values
1: plasmid (p)	-	94.67 ± 4.22	5.33 ± 4.22	-	-
2: p + H_2O_2	-	90.79 ± 8.45	9.21 ± 8.45	-	-
3: p + H_2O_2 + CurQ	75	96.88 ± 2.55	3.12 ± 2.55	-	-
4: Fe(II) + H_2O_2	0	7.20 ± 2.73	92.80 ± 2.73	0	-
5	1	12.23 ± 1.41	87.77 ± 1.41	5.82 ± 3.22	0.0887
6	5	12.37 ± 0.40	87.63 ± 0.40	5.98 ± 2.79	0.0655
7	10	16.91 ± 2.47	83.09 ± 2.47	11.54 ± 1.81	8.10×10^{-3}
8	20	33.91 ± 2.37	66.09 ± 2.37	31.61 ± 3.10	3.19×10^{-3}
9	25	42.41 ± 2.28	57.59 ± 2.28	41.89 ± 3.10	1.82×10^{-3}
10	35	69.57 ± 8.97	30.43 ± 8.97	66.42 ± 4.87	1.79×10^{-3}
11	45	78.38 ± 5.53	21.62 ± 5.53	78.21 ± 1.61	1.41×10^{-4}
12	50	81.48 ± 2.43	18.52 ± 2.43	81.49 ± 1.53	1.17×10^{-4}
13	60	82.99 ± 2.56	18.52 ± 2.56	84.28 ± 1.83	1.57×10^{-4}
14	75	93.11 ± 1.92	6.89 ± 1.92	97.97 ± 5.58	1.08×10^{-3}

Table 2.9. Tabulation of gel electrophoresis results for curcumin DNA damage assays with 400 μM $Fe(EDTA)^{2-}$ and 50 μM H_2O_2.

Gel lane	Curcumin, μM	% Supercoiled	% Nicked	% Damage Inhib.	*p* Values
1: plasmid (p)	-	93.49 ± 1.48	6.51 ± 1.48	-	-
2: p + H_2O_2	-	92.99 ± 3.02	7.01 ± 3.02	-	-
3: p + H_2O_2 + CurQ	75	94.26 ± 1.43	5.74 ± 1.43	-	-
4: $Fe(EDTA)^{2-}$ + H_2O_2	0	14.50 ± 4.94	84.35 ± 4.94	0	-
5	1	29.96 ± 4.95	70.04 ± 4.95	19.41 ± 0.88	6.84×10^{-4}
6	10	35.70 ± 8.24	64.30 ± 8.24	26.73 ± 5.63	0.0145
7	25	43.61 ± 6.31	56.39 ± 6.31	36.59 ± 3.40	2.87×10^{-3}
8	45	47.35 ± 7.45	52.65 ± 7.45	41.15 ± 5.31	5.50×10^{-3}
9	75	44.79 ± 8.46	55.21 ± 8.46	38.12 ± 6.47	9.47×10^{-3}

Table 2.10. Tabulation of gel electrophoresis results for curcumin DNA damage assays with 6 μM Cu(I) and 50 μM H_2O_2.

Gel lane	Curcumin, μM	% Supercoiled	% Nicked	% Damage Inhib.	*p* Values
1: plasmid (p)	-	99.36 ± 0.55	0.64 ± 0.55	-	-
2: p + H_2O_2	-	99.16 ± 0.73	0.81 ± 0.73	-	-
3: p + H_2O_2 + CurQ	70	98.63 ± 1.13	1.37 ± 1.13	-	-
4: Cu(I) + H_2O_2	0	16.98 ± 2.46	83.02 ± 2.46	0	-
5	1	14.81 ± 4.83	85.19 ± 4.83	-2.85 ± 3.11	0.0253
6	5	9.22 ± 4.09	90.78 ± 4.09	-10.34 ± 6.54	0.0111
7	10	8.60 ± 2.86	91.40 ± 2.86	-11.08 ± 0.52	7.33×10^{-4}
8	20	13.44 ± 8.40	86.56 ± 8.40	2.76 ± 3.98	0.353
9	25	21.53 ± 15.36	78.47 ± 15.36	10.21 ± 5.48	0.0841
10	35	28.06 ± 2.62	71.94 ± 2.62	12.98 ± 3.11	0.0186
11	40	29.36 ± 11.18	70.64 ± 11.18	20.92 ± 4.53	0.0153
12	50	42.99 ± 10.35	57.01 ± 10.35	33.02 ± 1.72	9.03×10^{-4}
13	70	80.07 ± 3.50	19.93 ± 3.50	80.49 ± 3.67	6.92×10^{-4}

Table 2.11. Tabulation of gel electrophoresis results for curcumin DNA damage assays with 50 μM $Cu(bipy)_2^+$ and 50 μM H_2O_2.

Gel lane	Curcumin, μM	% Supercoiled	% Nicked	% Damage Inhib.	*p* Values
1: plasmid (p)	-	95.81 ± 3.25	4.19 ± 3.25	-	-
2: p + H_2O_2	-	97.89 ± 1.67	2.11 ± 1.67	-	-
3: p + H_2O_2 + CurQ	70	97.02 ± 0.45	2.98 ± 0.45	-	-
4: $Cu(bpy)^+$ + H_2O_2	0	94.81 ± 2.28	5.19 ± 2.28	0	-
5	1	98.32 ± 2.61	1.67 ± 2.61	-5.18 ± 3.53	0.126
6	10	98.00 ± 2.74	2.00 ± 2.74	-4.85 ± 3.93	0.166
7	25	98.32 ± 1.40	1.68 ± 1.40	-4.86 ± 2.25	0.0646
8	40	98.81 ± 1.94	1.82 ± 1.94	-4.77 ± 2.49	0.0801
9	70	98.14 ± 0.26	1.86 ± 0.26	-4.56 ± 3.06	0.123

References

[1] T.D. Rae, P.J. Schmidt, R.A. Pufahl, V.C. Culotta, T.V. O'Halloran, Science 284 (1999) 805-808.

[2] O.I. Aruoma, JAOCS 75 (1998) 199-212.

[3] Y. Yamamoto, K. Fukui, N. Koujin, H. Ohya, K. Kimura, Y. Kamio, J. Bacteriol. 186 (2004) 5997-6002.

[4] J. Emerit, C. Beaumont, F. Trivin, Biomed. Pharmacother. 55 (2001) 333-339.

[5] J.P. Kehrer, Toxicology 149 (2000) 43-50.

[6] N. Stadler, R.A. Lindner, M.J. Davies, Arterioscler. Thromb. Vasc. Biol. 24 (2004) 949-954.

[7] J.A. Imlay, Annu. Rev. Microbiol. 57 (2003) 395-418.

[8] C. Salustri, R. Squitti, F. Zappasodi, M. Ventriglia, M.G. Bevacqua, M. Fonatana, F. Tecchio, J. Affective Disord. 127 (2010) 321-325.

[9] S. Takacs, A. Tatar, Environ. Res. 42 (1987) 312-320.

[10] A. Changela, K. Chen, Y. Xue, J. Holschen, C.E. Outten, T.V. O'Halloran, A. Mondragon, Science 301 (2003) 1393-1387.

[11] C.E. Outten, T.V. O'Halloran, Science 292 (2001) 2488-2492.

[12] T.J. Tetaz, R.K.J. Luck, J. Bacteriol. 154 (1983) 1263-1268.

[13] L. Macomber, C. Rensing, J.A. Imlay, J. Bacteriol. 189 (2007) 1616-1626.

[14] M.D. Argirova, B.J. Ortwerth, Arch. Biochem. Biophys. 420 (2003) 176-184.

[15] G. Weiss, D. Fuchs, A. Hausen, G. Reibnegger, E.R. Werner, G. Werner-Felmayer, H. Wachter, Exp. Hematol. 20 (1992) 605-610.

[16] E. Kemna, P. Pickkers, E. Nemeth, H. van der Hoeven, D. Swinkels, Blood 106 (2005) 1864-1866.

[17] Y. Ma, Z. Liu, R.C. Hider, F. Petrat, Anal. Chem. Insights 2 (2007) 61-67.

[18] K. Keyer, J.A. Imlay, Proc. Natl. Acad. Sci. USA 93 (1996) 13635-13640.

[19] J.M. Walshe, Ann. Clin. Biochem. 40 (2003) 115-121.

[20] R.B. Perni, S.J. Amlmquist, R.A. Byrn, G. Chandorkar, P.R. Chaturvedi, L.F. Courtney, C.J. Decker, K. Dinehart, C.A. Gates, S.L. Harbeson, A. Heiser, G. Kalkeri, E. Kolaczkowski, K. Lin, Y.-P. Luong, B.G. Rao, W.P. Taylor, J.A. Thomson, T.R. D., Y. Wei, A.D. Kwong, C. Lin, Antimicrob. Agents Chemother. 50 (2006) 899-909.

[21] W.A. Spencer, J. Jeyabalan, S. Kichambre, R.C. Gupta, Free Radic. Biol. Med. 50 (2011) 139-147.

[22] W. Szczepanik, M. Kucharczyk-Klaminska, P. Stefanowicz, A. Staszewska, Z. Szewczuk, J. Skala, A. Mysiak, M. Jezowska-Bojczuk, Bioinorg. Chem. Appl. 2009 (2009) 906836.

[23] G. Kroemer, P. Petit, N. Zamzami, J.L. Vayssiere, B. Mignotte, FASEB J. 9 (1995) 1277-1287.

[24] J. Baurle, J. Kucera, S. Frischmuth, M. Lambertz, K. Kranda, Brain Pathol. 19 (2009) 586-595.

[25] N.R. Perron, C.R. García, J.R. Pinzón, M.N. Chaur, J.L. Brumaghim, J. Inorg. Biochem. 105 (2011) 745-753.

[26] J. Stöckel, J. Safar, A.C. Wallace, F.E. Cohen, S.B. Prusiner, Biochemistry 37 (1998) 7185-7193.

[27] F. Musshoff, D.W. Lachenmeier, P. Schmidt, R. Dettmeyer, B. Madea, Alcohol. Clin. Exp. Res. 29 (2005) 46-52.

[28] B. Kalyanaraman, R.C. Sealy, J. Biol. Chem. 259 (1984) 14018-14022.

[29] A.M. Seacat, P. Kuppusamy, J.L. Zweier, J.D. Yager, Arch. Biochem. Biophys. Acta 347 (1997) 45-52.

[30] W. Bors, C. Michel, K. Stettmaier, Arch. Biochem. Biophys. 374 (2000) 215-219.

[31] J.A. Pedersen (Ed.), Handbook of ESR Spectra from Quinones and Quinols, CRC Press, Inc., Boca Raton, 1985, 8.20-8.23.

[32] G.R. Buettner, P.L. Moseley, Free Rad. Res. Commun. 19 (1993) S89-S93.

[33] M.R. Gunther, P.M. Hanna, R.P. Mason, M.S. Cohen, Arch. Biochem. Biophys. 316 (1995) 515-522.

[34] D. Hoehler, R.R. Marquardt, A.R. McIntosh, G.M. Hatch, Biochim. Biophys. Acta 1357 (1997) 225-233.

[35] H.J. Halpern, C. Yu, E. Barth, M. Peric, G.M. Rosen, Proc. Natl. Acad. Sci. USA 92 (1995) 796-800.

[36] S. Pou, T. Ramos, E. Gladwell, E. Renks, M. Centra, D. Young, M.S. Cohen, G.M. Rosen, Anal. Biochem. 217 (1994) 76-83.

[37] C.F. Chignell, S.K. Han, A. Mouithys-Mickalad, R.H. Sik, K. Stadler, M.B. Kadiiska, Toxicol. Appl. Pharacol. 230 (2008) 17-22.

[38] B.A. Goodman, S.M. Glidewell, C.M. Arbuckle, S. Bernardin, T.R. Cook, J.R. Hillman, J. Sci. Food Agric. 82 (2002) 1208-1215.

[39] M.V. Martinez, J.R. Witaker, Trends Food Sci. Technol. 6 (2009) 195-200.

[40] Y. Luo, X.R. Wang, L.L. Ji, Y. Su, J. Hazard. Mater. 171 (2009) 1096-1102.

[41] V.E. Kagan, Y.Y. Tyurina, Ann. N. Y. Acad. Sci. 854 (1998) 435-434.

[42] M.G. Traber, J. Atkinson, Free Rad. Biol. Med. 43 (2007) 4-15.

[43] N.R. Perron, J.N. Hodges, M. Jenkins, J.L. Brumaghim, Inorg. Chem. 47 (2008) 6153-6161.

[44] A.M. Verdan, S.W. Hsiao, C.R. Garcia, W.P. Henry, J.L. Brumaghim, J. Inorg. Biochem. 105 (2011) 1314-1322.

[45] H. Hatcher, R. Palanalp, J. Cho, F.M. Torti, S.V. Torti, Cell. Mol. Life Sci. 65 (2008) 1631-1652.

[46] X. Rong, C.L. Smelley, G.C. Caldito, F.W. Abreo, C.O. Nathan, Cancer Prev. Res. 3 (2010) 1586-1595.

[47] K. Bisht, K.H. Wagner, A.C. Bulmer, Toxicology 278 (2010) 88-100.

[48] V.Y.L. Ung, R.R. Foshaug, S.M. MacFarlane, T.A. Churchill, J.S.G. Doyle, B.C. Sydora, R.N. Fedorak, Dig. Dis. Sci. 55 (2009) 1272-1277.

[49] T. Hamaguchi, K. Ono, M. Yamada, CNS Neurosci. Therap. 16 (2010) 285-297.

[50] F. Yang, G.P. Lim, A.N. Begum, O.J. Ubeda, M.R. Simmons, S.S. Ambegaokar, P. Chen, R. Kayed, C.G. Glabe, S.A. Frautschy, G.M. Cole, J. Biol. Chem. 280 (2005) 5892-5901.

[51] M.C. Wagner, M.V. Sursesh, K.A. Stringer, K.A. Min, J. Parkkinen, G.R. Rosania, R.C. Reddy, Am. J. Respir. Crit. Care Med. 183 (2011) 1092-1100.

[52] P. Anand, A.B. Kunnumakkara, R.A. Newman, B.B. Aggarwal, Mol. Pharmac. 4 (2007) 807-818.

[53] A.N. Begum, M.R. Jones, G.P. Lim, T. Morihara, P. Kim, D.D. Heath, C.L. Rock, M.A. Pruitt, F. Yang, B. Hudspeth, S. Hu, K.F. Faull, B. Teter, G.M. Cole, S.A. Frautschy, J. Pharm. Exp. Ther. 326 (2008) 196-208.

[54] J. Shaikh, D.D. Ankola, V. Beniwal, D. Singh, R.M.N.V. Kumar, Eur. J. Pharmaceut. Sci. 37 (2009) 223-230.

[55] D.W. Dyrssen, Y.P. Novikov, L.R. Uppstrom, Anal. Chim. Acta 60 (1972) 139-151.

[56] S. Daniel, J.L. Limson, A. Dairam, G.M. Watkins, S. Daya, J. Inorg. Biochem. 98 (2004) 266-278.

[57] R. Benassi, E. Ferrari, R. Grandi, S. Lazzari, M. Saladini, J. Inorg. Biochem. 101 (2007) 203-213.

[58] S.V. Janovic, C.W. Boone, S. Steenken, M. Trinoga, R.B. Kaskey, J. Am. Chem. Soc. 123 (2001) 3064-3068.

[59] M. Velusamy, M. Palaniandavar, Inorg. Chem. 42 (2003) 8283-8293.

[60] V. Rajendiran, R. Karthik, M. Palaniandavar, H. Stoekli-Evans, V.S. Periasmy, M.A. Akbarsha, B.S. Sringa, H. Srishnamurthy, Inorg. Chem. 46 (2007) 8208-8221.

[61] M. Cvetkovic, S.R. Batten, B. Moubaraki, K.S. Murray, L. Spiccia, Inorg. Chim. Acta 324 (2001) 131-140.

[62] M. Born, P.A. Carrupt, R. Zini, F. Bree, J.P. Tillement, K. Hostettmann, B. Testa, Helv. Chim. Acta 79 (1996) 1147-1150.

[63] Z. Stanić, A. Voulgaropoulos, S. Girousi, Electroanalysis 11 (2008) 1263-1266.

[64] T. Ak, I. Gulcin, Chemico-Biol. Interact. 174 (2008) 27-37.

[65] S.M. Khopde, K.I. Priyadarsini, P. Venkatesan, M.N.A. Rao, Biophy. Chem. 80 (1999) 85-91.

[66] J.L. Pierre, M. Fontecave, BioMetals 12 (1999) 195-199.

[67] C. Bian, Q. Zeng, H. Xiong, X. Zhang, S. Wang, Bioelectrochemistry 79 (2010) 1-5.

[68] S.M. Chen, K.T. Peng, J. Electroanal. Chem. 547 (2003) 179-189.

[69] M.M. Walczak, D.A. Dryer, D.D. Jacobson, M.G. Foss, N.T. Flynn, J. Chem. Ed. 74 (1997) 1195-1197.

[70] B. Halliwell, J.M.C. Gutteridge, O.I. Aruoma, Anal. Biochem. 165 (1987) 215-219.

[71] S.A. van Acker, G.P. van Balen, D.J. van den Berg, A. Bast, W.J.F. van der Vijgh, Biochem. Pharmacol. 56 (1998) 935-943.

[72] N.R. Perron, J.N. Hodges, M. Jenkins, J.L. Brumaghim, Inorg. Chem. 47 (2008) 6153-6161.

[73] P. Ryan, M.J. Hynes, J. Coord. Chem. 61 (2008) 3711-3726.

[74] R.T. Borchardt, J.A. Huber, J. Med. Chem. 18 (1975) 120-122.

[75] R.G. Mani, J.H. Smet, K. von, K., V. Narayanamurti, W.B. Johnson, V. Umansky, Phys. Rev. Lett. 92 (2004) 146801-146805.

[76] M.R. Gunther, P.M. Hanna, R.P. Mason, M.S. Cohen, Arch. Biochem. Biophys. 316 (1995) 515-522.

[77] D. Hoehler, R.R. Marquardt, A.R. McIntosh, G.M. Hatch, Biochim. Biophys. Acta 1357 (1997) 225-233.

[78] H.J. Halpern, C. Yu, E. Barth, M. Peric, G.M. Rosen, Proc. Natl. Acad. Sci. U.S.A. 92 (1995) 796-800.

[79] S. Pou, T. Ramos, E. Gladwell, E. Renks, M. Centra, D. Young, M.S. Cohen, G.M. Rosen, Anal. Biochem. 217 (1994) 76-83.

[80] E.P. Friis, J.E.T. Andersen, L.L. Madsen, N. Bonander, P. Moller, J. Ulstrup, Electrochim. Acta 43 (1998) 1114-1122.

[81] D.T. Sawyer, A. Sobkowiak, J.L. Roberts Electrochemistry for Chemists, Wiley-Interscience, New York, 1995, 184-204.

CHAPTER THREE

PREVENTION OF IRON-MEDIATED OXIDATIVE DNA DAMAGE BY CATECHOLAMINE AND AMINO ACID NEUROTRANSTMITTERS: METAL BINDING AS AN ANTIOXIDANT MECHANISM

Introduction

With the rising popularity of prescription medications that alter neurotransmitter levels in the brain and no cure for many neurodegenerative diseases, understanding the chemical behavior of neurotransmitters (NT) is becoming more essential. The two categories of monoamine neurotransmitters that will be examined in this chapter are the catecholamines, dopamine (DA), epinephrine (EP), and norepinephrine (NE), and the amino acids, glycine (Gly), glutamate (Glu), and γ-aminobutyric acid (GABA) (Figure 3.1).

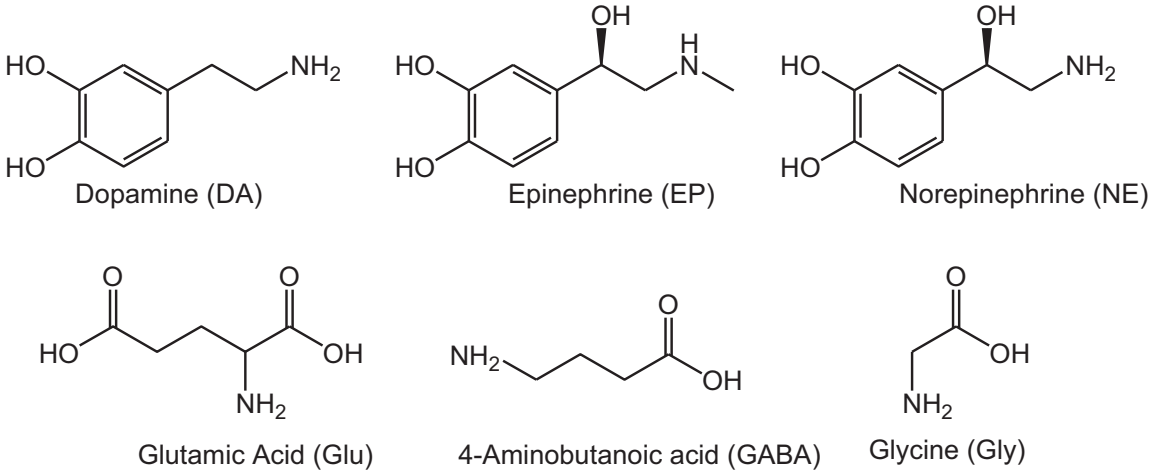

Figure 3.1. Structures of monoamine neurotransmitters.

Catecholamines are a class of polyphenol neurotransmitters that play a primary role in the way humans and other mammals think and behave. Each catecholamine discussed in this thesis, DA, EP, and NE, have an array of functions in the healthy brain. Dopamine plays a primary role in motor function [1], binge eating tendencies [2], and is proposed to play a role in depression [3]. Epinephrine (also known as L-adrenaline) plays a role in motor behavior and regulating emotional stress [4, 5]. Norepinephrine (also known as noradrenaline) regulates both anxiety and depressive mood disorders [6]. Dopamine is the most biologically abundant catecholamine, with concentrations in the human and mouse brain around 8 μM [7, 8]. Epinephrine and norepinephrine are typically found in the rat brain in low micromolar ranges (1 – 2 μM and 1 – 8 μM, respectively) [9], whereas human plasma concentrations of catecholamines are in the nanomolar ranges (approximately 1 nM each) [10].

Monoamine carboxylic acids include glycine, glutamate, and γ-aminobutyric acid. Poor regulation of glycine and GABA transmission can decrease rapid eye movement sleep [11] and cause epilepsy [12]. Elevated levels of glutamate are observed in patients with mania and diminished levels of this neurotransmitter are observed in patients with depression [13]. Glutamate levels in the mammalian brains of cats, swine, and rats range from 1 to 20 μM [14-17] and glycine levels in the human plasma are around 0.2 μM [18]. GABA, however, typically has human brain levels in the millimolar concentrations (1.8 mM) [19].

Both brain function and overall health have been linked to labile (non-protein bound) metal ion concentrations. Labile copper levels in human serum have an inverse relationship to cognitive state, but levels of protein-bound copper showed no effect,

emphasizing the influence of labile metals [20]. A positive correlation has been established between labile copper concentrations and Alzheimer's disease (about 7 times more abundant [21]). It has been proposed that labile iron pools in the brain could be the key player in the neurodegeneration that leads to Parkinson's disease [22]. The mounting evidence for mis-regulation of labile metal concentrations in patients with impaired brain function stresses the importance of understanding of metal-neurotransmitter interactions on a chemical level.

Catecholamines and amino acid neurotransmitters have also been investigated for their antioxidant properties. All three catecholamines are considered potent radical scavengers: DA is the most potent superoxide scavenger, followed by NE and EP as determined by electron paramagnetic resonance (EPR) spectroscopy [23]. However, catecholamines can also *increase* DNA damage in the presence of copper and iron [24, 25]. In the presence of Cu(II), DA and EP both promote DNA damage due to their ability to participate in copper redox cycling, with DA producing substantially more damage in the presence of copper [26]. Gly has also been established to be a potent radical scavenger [27] and glycine-iron supplementation has shown to increase superoxide dismutase and catalase antioxidant enzyme production *in vivo* [28], which may be due to radical scavenging properties, iron binding, or both. Most of the research on glutamate is on Glu-containing compounds or Glu receptors, but it has been shown that Glu itself inhibits lipid oxidation production *in vivo* [29]. Alone, GABA does not promote DNA damage, but in the presence of Cu(II), DNA damage has been reported [30].

The experiments described in this thesis will delve further into the metal-binding mechanisms for neurotransmitters antioxidant behavior, not just the effects of metal presence on biological damage and quantifying the ability of neurotransmitters to prevent

iron-mediated DNA damage. Both iron and copper binding to neurotransmitters will be directly examined and a comparison between neurotransmitters that do and do not bind iron and copper will also be made. To investigate the interactions between metal ions and neurotransmitters, plasmid DNA damage assays, ultraviolet-visible (UV-vis) spectroscopy, and cyclic voltammetry (CV) are all be used to provide comprehensive insight into metal binding as an essential antioxidant mechanism for these neurotransmitters. This work contains contributions from Jenna Wilkes, who aided in the CV data collection and completed some of the UV-vis spectroscopy as well as Carlos Angéle-Martínez for completing the Fe(II) and $Fe(EDTA)^{2-}$ DNA damage gels for two of the neurotransmitters.

Neurotransmitter Prevention of Iron-Mediated DNA Damage

Iron-mediated oxidative DNA damage has been linked to many health problems including Alzheimer's disease [31], heart disease [32], and cancer [33] and can lead to apoptosis [34, 35]. To quantify iron-mediated DNA damage prevention by neurotransmitters, a plasmid DNA damage assay was used; this method has been used previously to determine polyphenol DNA damage inhibition by Fe(II) and H_2O_2 [36-38]. The gel image in Figure 3.2A shows that dopamine prevents DNA damage by Fe(II)/H_2O_2 with a maximum DNA damage prevention of 98 ± 1% at 1600 μM, the highest concentration tested (Figure 3.2A). By graphing DNA damage inhibition vs. DA concentration, a dose-response curve was obtained to determine the concentration at which 50% of DNA damage prevention was observed (IC_{50}). For dopamine, this IC_{50} value is 111 ± 5 μM (Figure 3.2B). Epinephrine also behaves as an antioxidant to prevent iron-mediated DNA damage, with a maximum percent damage inhibition of 63 ± 3% at 50 μM and an IC_{50}

value of 15 ± 1 μM. Norepinephrine, like the other catecholamines, shows does-dependent behavior and has an IC_{50} value of 35 ± 1 μM, preventing 98.3% of DNA damage at 200 μM. Gel images and data tables for these DNA nicking assays are provided in Figures 3.2, 3.13, and 3.17 and Tables 3.4, 3.6, and 3.8. Of the catecholamines, epinephrine most effectively prevents iron-mediated oxidative DNA damage and is more than 2 times more effective than norepinephrine and about 8 times more effective than dopamine. In fact, epinephrine antioxidant activity falls within biological concentrations, preventing 14.0% DNA damage at 10 μM.

GABA was inactive as either a pro- or antioxidant in the presence of iron ions (Table 3.1). Glycine is a weak antioxidant, preventing only 31.9% of iron-mediated DNA damage at 10,000 μM [39]. Glutamate behaves much like GABA, acting as neither a pro- nor antioxidant at all tested concentrations (up to 200 μM). The catecholamines prevent significantly more DNA damage under these conditions than the amino acid neurotransmitters, which showed little or no activity.

To establish whether iron chelation is required for DNA damage prevention, similar DNA damage assays were conducted, but instead of using FeSO4 as the iron source, the Fe(II) was fully chelated with ethylenediaminetetracetate ($EDTA^{4-}$) prior to adding the neurotransmitter. The resulting $Fe(EDTA)^{2-}$ complex damages DNA upon H_2O_2 addition

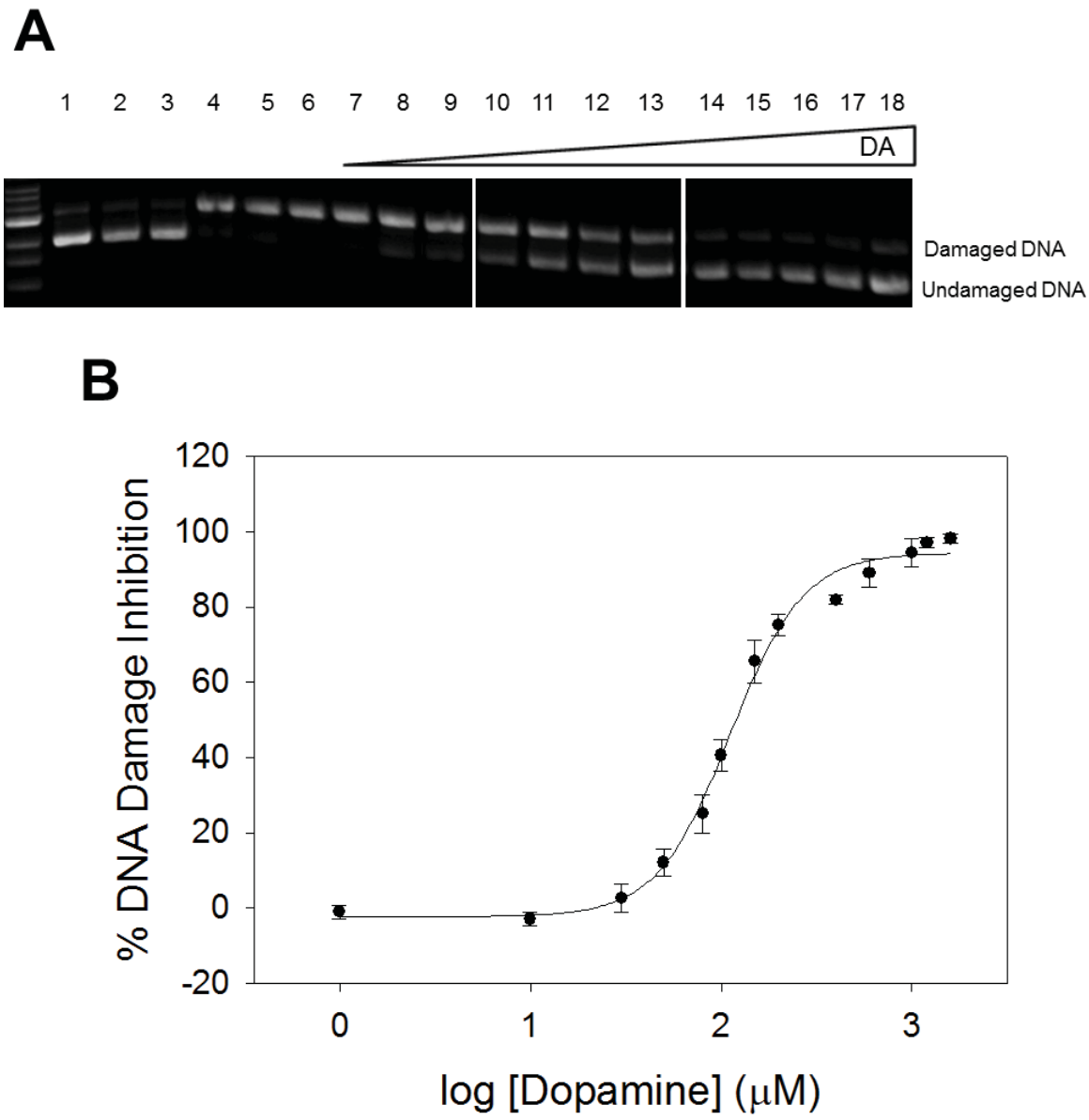

Figure 3.2. A) Gel electrophoresis image of dopamine DNA damage prevention with Fe(II) (2 μM) and H_2O_2 (50 μM). Lanes: MW = 1 kb ladder; 1: plasmid (p); 2: p + H_2O_2; 3: p + 75 μM; 4: p + H_2O_2 + Fe(II); 5-18: lane 5 + 1, 5, 10, 30, 50, 80, 100, 150, 200, 400, 600, 1000, 1200, and 1600 μM, respectively. B) Dose-response curve for dopamine inhibition of iron-mediated DNA damage. Data are reported as the average of three trials with calculated standard deviations.

Table 3.1. Gel electrophoresis data for neurotransmitter (NT) prevention of Fe(II)-mediated DNA damage and Fe(II)- and Cu(I) UV-vis spectra in the presence of neurotransmitters.

Compound	Antioxidant Activity (max %)	IC_{50} (μM)[a]	NT-Fe λ_{max} (nm)	NT-Cu λ_{max} (nm)
Dopamine (DA)	1 – 1600 μM (98.2% at 1600 μM)	111 ± 5	290, 583	288, 297
Epinephrine (EP)	1 – 50 μM (76.3% at 50 μM)	15 ± 1	281	282, 485
Norepinephrine (NE)	5 – 200 μM (98.3% at 200 μM)	35 ± 1	283, 579	286, 297
Glycine (Gly)	1-10000 μM (31.9% at 10000 μM)[b]	–	–	231
Glutamate (Glu)	–	–	–	234
γ-aminobutyric acid (GABA)	–	–	–	–

[a]IC_{50} values are an average of three trials and errors are calculated standard deviations. [b]From source [39].

(Figure 3.3, Lane 4) but does not permit neurotransmitter-iron binding. With $Fe(EDTA)^{2-}$ as the iron source, DA prevents significantly less DNA damage compared to unchelated Fe(II), with a maximum of 22 ± 1% damage inhibition compared to 91 ± 2% at 1200 μM (Figure 3.3 and 3.2A, respectively). EP also prevents substantially less damage under these conditions; 28 ± 6% compared to 76 ± 4% DNA damage inhibition at 50 μM for

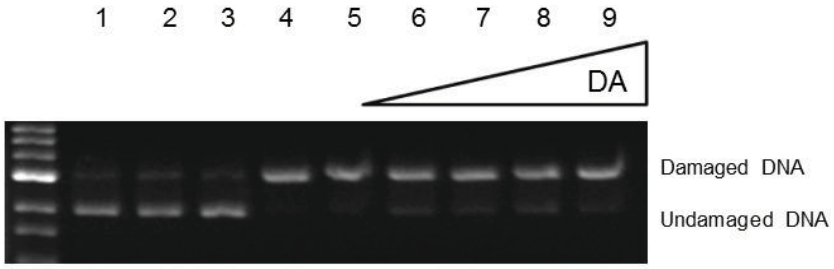

Figure 3.3. Gel electrophoresis image of dopamine with $Fe(EDTA)^{2-}$ (400 μM) and H_2O_2 (50 μM). Lanes: MW = 1 kb ladder; 1 = plasmid DNA (p); 2 = p + H_2O_2; 3 = p + 1200 μM dopamine + H_2O_2; and 4 = p + $Fe(EDTA)^{2-}$ + H_2O_2; lanes 5-9: p + $Fe(EDTA)^{2-}$ + H_2O_2 + 10, 80, 150, 600, and 1200 μM dopamine, respectively.

$Fe(EDTA)^{2-}$ and Fe(II), respectively. NE is virtually inactive in preventing $Fe(EDTA)^{2-}$ meditated DNA damage. For the tested catecholamines, using $Fe(EDTA)^{2-}$ as the iron source resulted in less than 50% DNA damage even at the highest neurotransmitter concentration, suggesting that iron-biding is the primary mechanism of DNA damage prevention. Similarly, curcumin shows a decreased ability to prevent DNA damage in the presence of chelated iron or copper when compared to the unchelated metal ions (Chapter 2). The small amount of DNA damage prevention observed for these neurotransmitters in the presence of $Fe(EDTA)^{2-}/H_2O_2$ is likely due to an alternate antioxidant mechanism, such as ROS scavenging, at high concentrations [39-42].

Iron and Copper Binding to Neurotransmitters

UV-vis spectroscopy experiments were conducted to confirm iron biding and establish neurotransmitter:metal stoichiometry. Upon addition of Fe(II) to all six

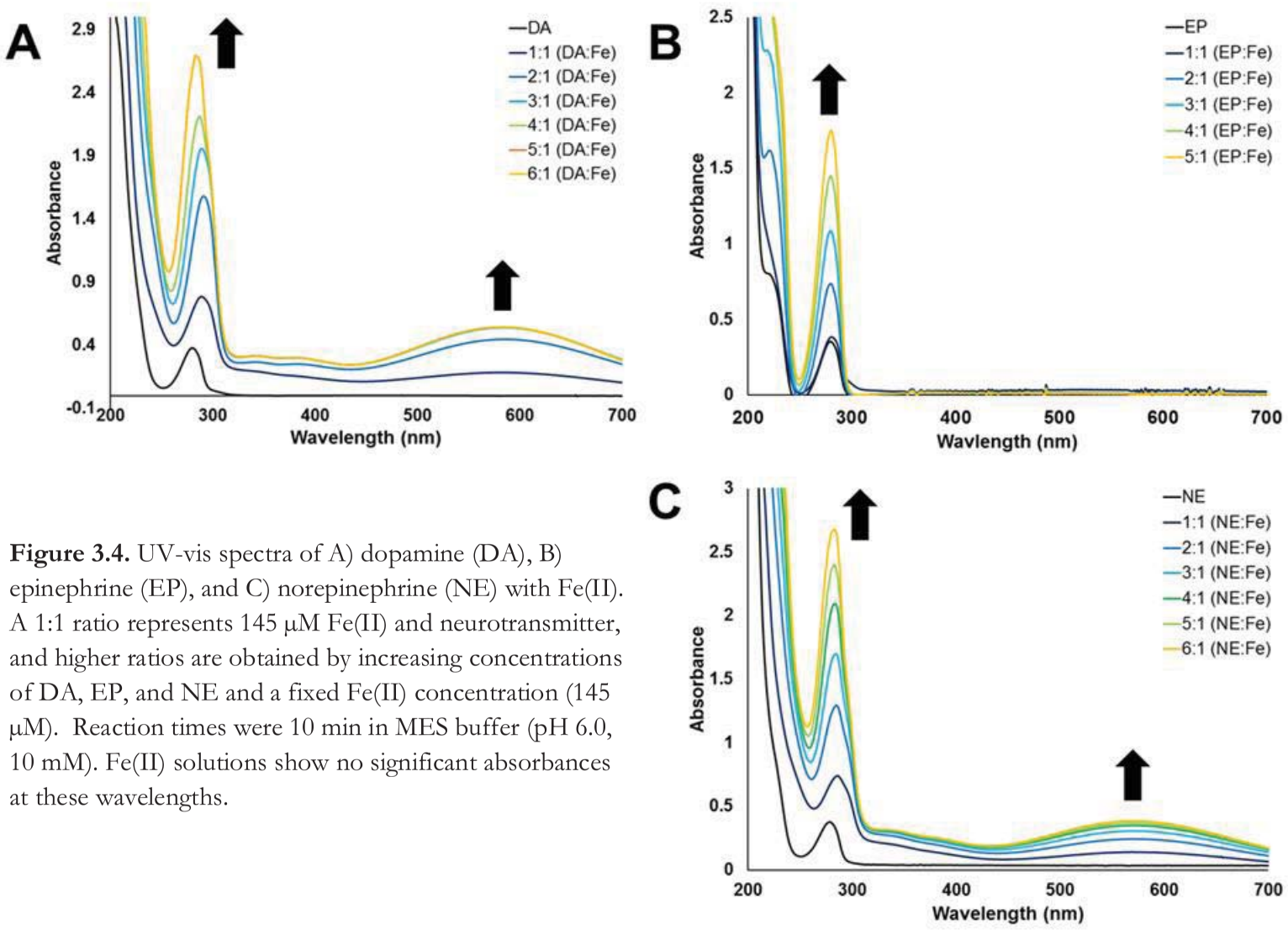

Figure 3.4. UV-vis spectra of A) dopamine (DA), B) epinephrine (EP), and C) norepinephrine (NE) with Fe(II). A 1:1 ratio represents 145 μM Fe(II) and neurotransmitter, and higher ratios are obtained by increasing concentrations of DA, EP, and NE and a fixed Fe(II) concentration (145 μM). Reaction times were 10 min in MES buffer (pH 6.0, 10 mM). Fe(II) solutions show no significant absorbances at these wavelengths.

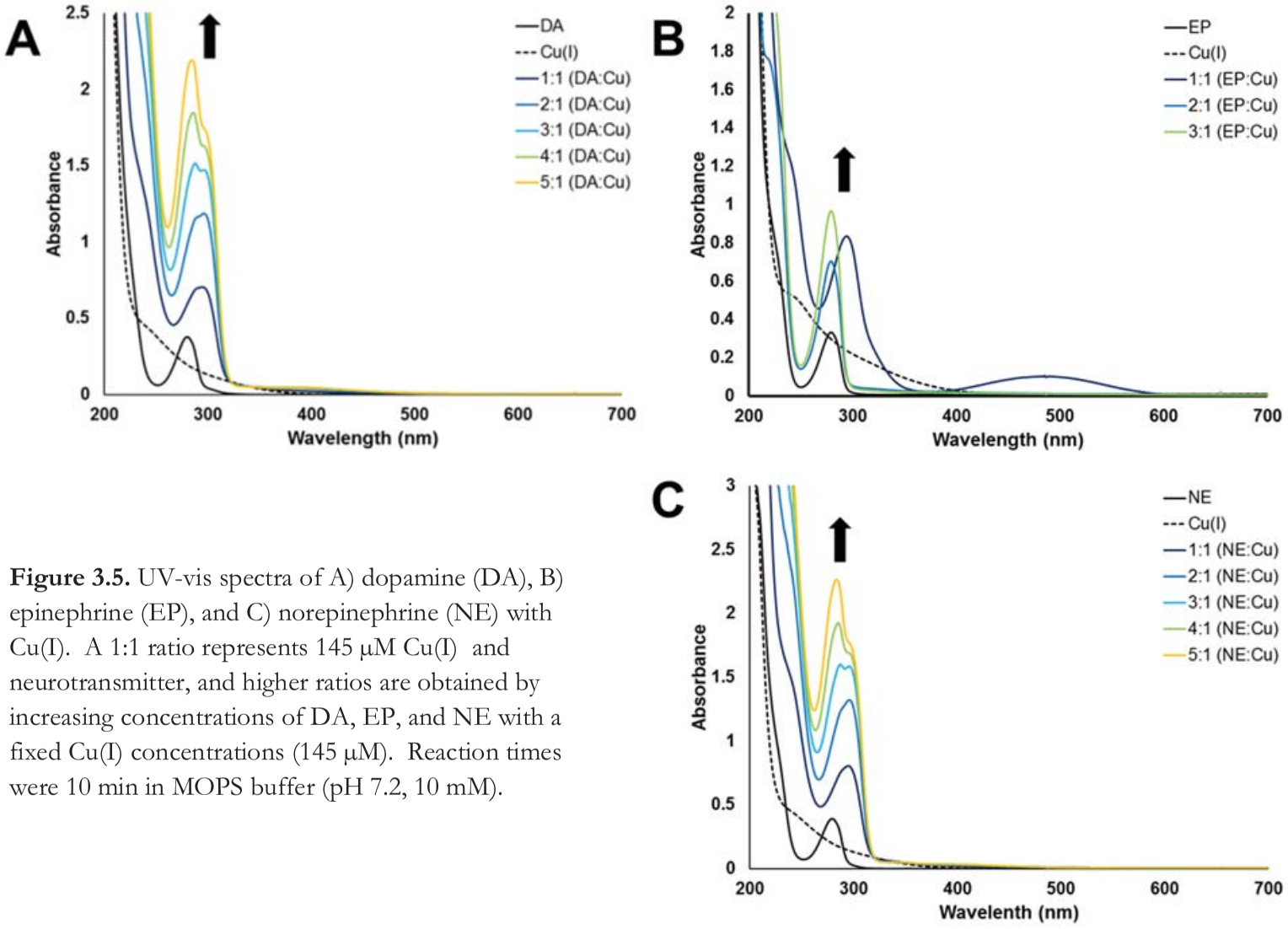

Figure 3.5. UV-vis spectra of A) dopamine (DA), B) epinephrine (EP), and C) norepinephrine (NE) with Cu(I). A 1:1 ratio represents 145 μM Cu(I) and neurotransmitter, and higher ratios are obtained by increasing concentrations of DA, EP, and NE with a fixed Cu(I) concentrations (145 μM). Reaction times were 10 min in MOPS buffer (pH 7.2, 10 mM).

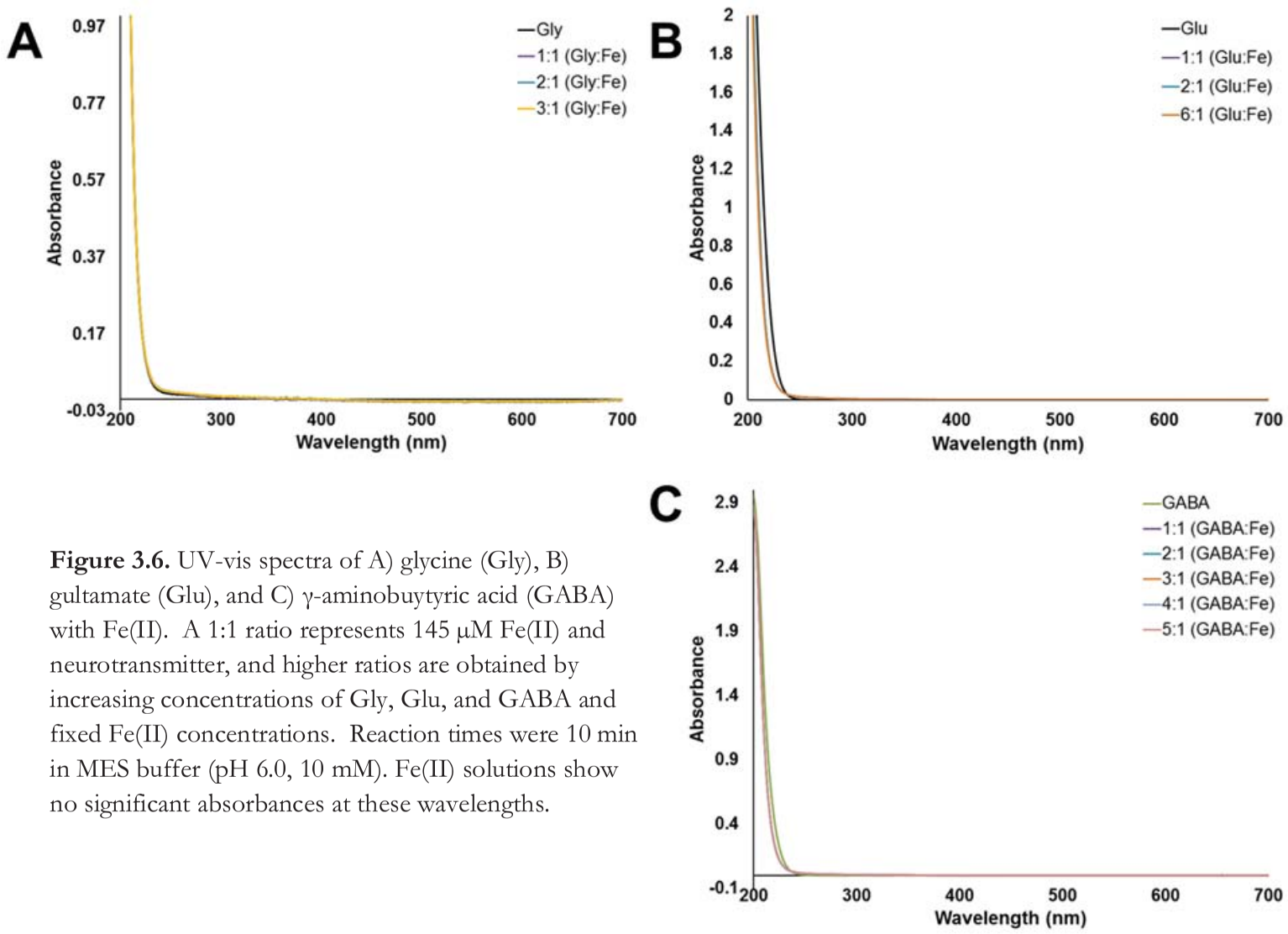

Figure 3.6. UV-vis spectra of A) glycine (Gly), B) gultamate (Glu), and C) γ-aminobuytyric acid (GABA) with Fe(II). A 1:1 ratio represents 145 μM Fe(II) and neurotransmitter, and higher ratios are obtained by increasing concentrations of Gly, Glu, and GABA and fixed Fe(II) concentrations. Reaction times were 10 min in MES buffer (pH 6.0, 10 mM). Fe(II) solutions show no significant absorbances at these wavelengths.

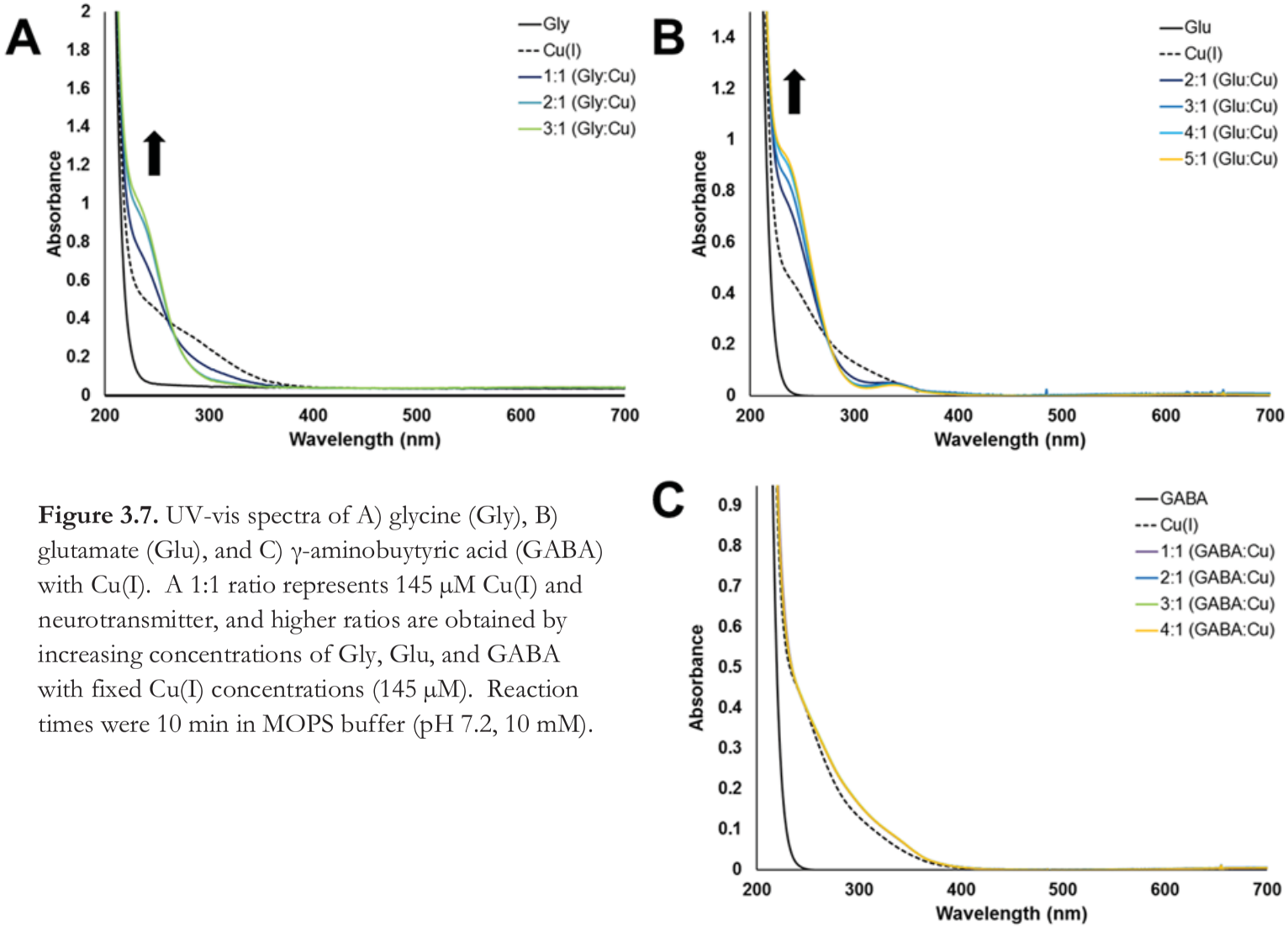

Figure 3.7. UV-vis spectra of A) glycine (Gly), B) glutamate (Glu), and C) γ-aminobuytyric acid (GABA) with Cu(I). A 1:1 ratio represents 145 μM Cu(I) and neurotransmitter, and higher ratios are obtained by increasing concentrations of Gly, Glu, and GABA with fixed Cu(I) concentrations (145 μM). Reaction times were 10 min in MOPS buffer (pH 7.2, 10 mM).

neurotransmitters, DA, EP and EP showed evidence of iron binding and oxidation as determined from the UV-vis spectra. The absorbance bands around 285 nm that increase upon catecholamine addition (Figure 3.4) result from a π-π* transition of the polyphenols [43, 44]. The lower-energy bands around 580 nm observed in the spectra for DA and NE upon iron addition are indicative of an Fe(III)-phenolate bond [45, 46] (Figure 3.4, Table 3.2) similar to curcumin (Chapter 2). These lower-energy bands are consistent with an array of polyphenols that exhibit similar ligand-to-metal charge transfer (LMCT) bands within the same range [47]. The observed absorbance Fe(III) bands in these UV-vis spectra indicate that within the 10 min reaction time, DA and NE not only bind iron, but also promote Fe(II) oxidation to Fe(III). The very small lower-energy Fe(III) LMCT band for EP indicates that EP might have significantly slower oxidation kinetics compared to DA and NE or that EP solubility may be an issue in these experiments at high EP concentrations. Similar iron binding and oxidation behavior has previously been reported for other catechol-containing polyphenol compounds [36].

UV-vis spectra for DA, EP, and NE with Cu(I) show bands around 290 nm (Figure 3.5, Table 3.2), again due to the catechol π-π* aromatic ring transition [43, 44]; the same band is observed in the iron UV-vis spectra. Upon copper addition, EP is the only compound to display any additional band at a lower intensity (at 485 nm) and this band is due to the phenolate-Cu(II) LMCT [48, 49]. As observed with Fe(II), interactions of Cu(I) with these catecholamines can promote Cu(I) oxidation to Cu(II).

In contrast to the catecholamines, UV-vis spectra for the amino acid neurotransmitters Gly, Glu, and GABA show no significant absorbance changes upon Fe(II) addition (Figure 3.6), so iron binding and oxidation cannot be determined using UV-vis

spectroscopy. The UV-vis spectra for Gly and Glu with copper show a band increase at λ_{max} 231 and 234 nm (Figure 3.7), possibly representing σ(O-carboxylate) → Cu(II) LMCT bands [50, 51]. GABA shows no significant absorbances upon copper addition. Although GABA also contains carboxylic acid functional groups, no similar LMCT bands were observed possibly due to slower kinetics of copper oxidation. With Gly and Glu, as well as the catecholamines, Cu(I) is oxidized to Cu(II) upon binding.

Results of the DNA damage assays and UV-vis spectroscopy studies suggest that, not only do catecholamines bind iron, but this iron binding correlates with DNA damage prevention. Because EP is slow to oxidize, Fe(II)-binding, rather than oxidation to Fe(III), may be responsible for the observed DNA damage inhibition. In contrast, the three monoamine carboxylic acids showed no iron binding by UV-vis spectroscopy, and had little or no antioxidant ability to inhibit iron-mediated DNA damage. Two of the amino acid neurotransmitters (Gly and Glu) also bind and oxidize copper. Oxidation of Fe(II) and Cu(I) when bound to neurotransmitters is observed for all complexes with detectable UV-vis bands. These UV-vis spectroscopy studies suggest that iron-binding is essential in preventing DNA damage, since the catecholamines bind and oxidize iron and also prevent iron-mediated DNA damage, whereas the amino acid neurotransmitters provide little or no protection against iron-mediated DNA damage, and no evidence of iron binding and oxidation.

Electrochemical Properties of Neurotransmitters with and without Iron

Because the generation of hydroxyl radical can occur only in a limited electrochemical window (-0.324 V to 0.460 V [52] vs. NHE), stabilization of Fe(III) by

neurotransmittter binding may prevent iron redox cycling and subsequent DNA damage. Cyclic voltammetry was performed to determine the effects of pH and iron interactions on neurotransmitter electrochemical potentials. The monoamine carboxylic acids Gly, Glu, and GABA were all electrochemically inactive at both pH 6.0 and 7.2 within a range of ± 1 V (Figure 3.8). This inability of Gly, Glu, and GABA to participate in redox reactions is consistent with the lack of either prooxidant or antioxidant activity observed in the iron-mediated DNA damage assays.

Catecholamines, however, are known to be electrochemically active under these conditions. Biological redox cycling for catecholamines is proposed to occur by two subsequent electron redox reactions: first, a two-electron oxidation of the catecholamine to the *o*-quinone, then a 1-electron reduction to the radical *o*-semiquinone in the presence of cellular reductants (such as NADPH) [53, 54] (Figure 3.9). The semiquinone can then cycle back to the oxidized quinone form in the presence of oxidants (such as molecular oxygen), creating a perpetual cycle of radical production and resulting in neurotoxicity [53, 54]. At pH 3.0, oxidation potentials for DA, EP, and NE were 0.703 V, 0.772 V, and 0.741 V vs. NHE, respectively, corresponding to oxidation of the catecholamines to the corresponding *o*-quinones [55]. Under the same conditions, these *o*-quinones reduce at 0.338 V, 0.447 V, and 0.338 V vs. NHE, respectively, presumably back to the parent catecholamine compounds [55].

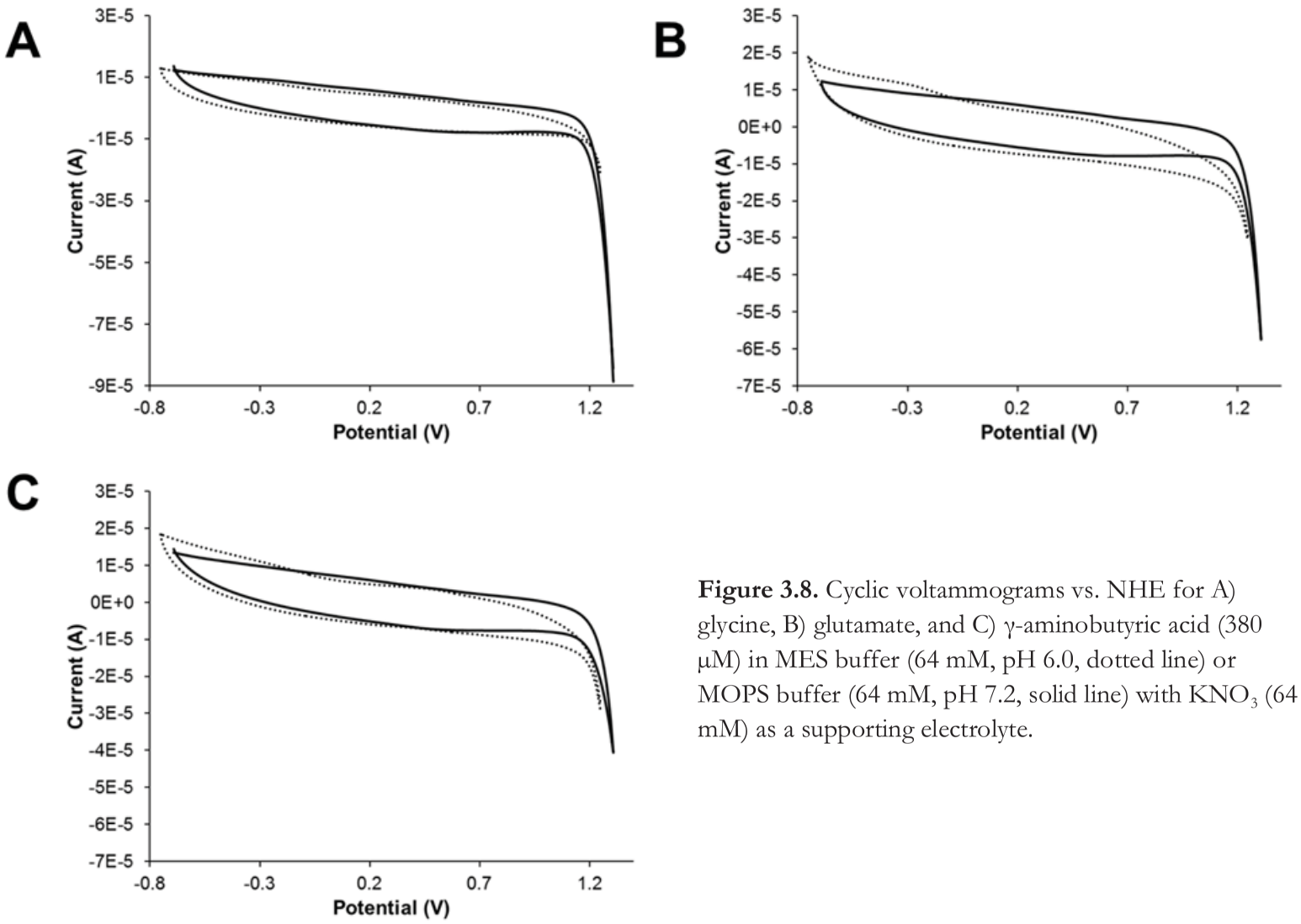

Figure 3.8. Cyclic voltammograms vs. NHE for A) glycine, B) glutamate, and C) γ-aminobutyric acid (380 μM) in MES buffer (64 mM, pH 6.0, dotted line) or MOPS buffer (64 mM, pH 7.2, solid line) with KNO_3 (64 mM) as a supporting electrolyte.

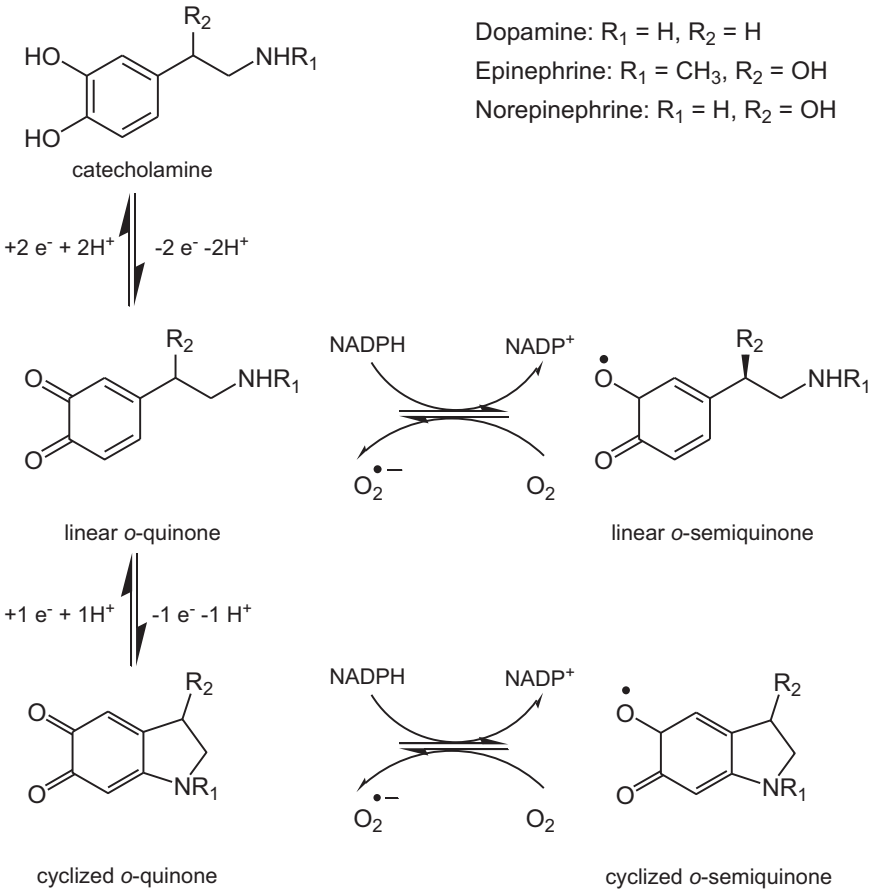

Figure 3.9. Catecholamine oxidation to the cyclized and linear *o*-quinones and biological redox cycling between respective quinones and semiquinones.

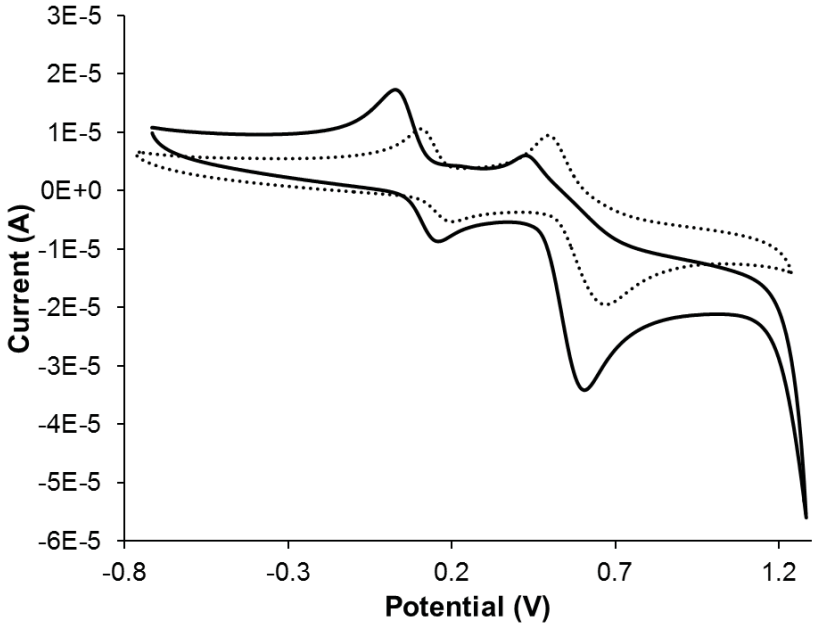

Figure 3.10. Cyclic voltammogram vs. NHE of dopamine (380 μM) in MES buffer (64 mM, pH 6.0, dotted line) or MOPS buffer (64 mM, pH 7.2, solid line) with KNO_3 (64 mM) as the supporting electrolyte.

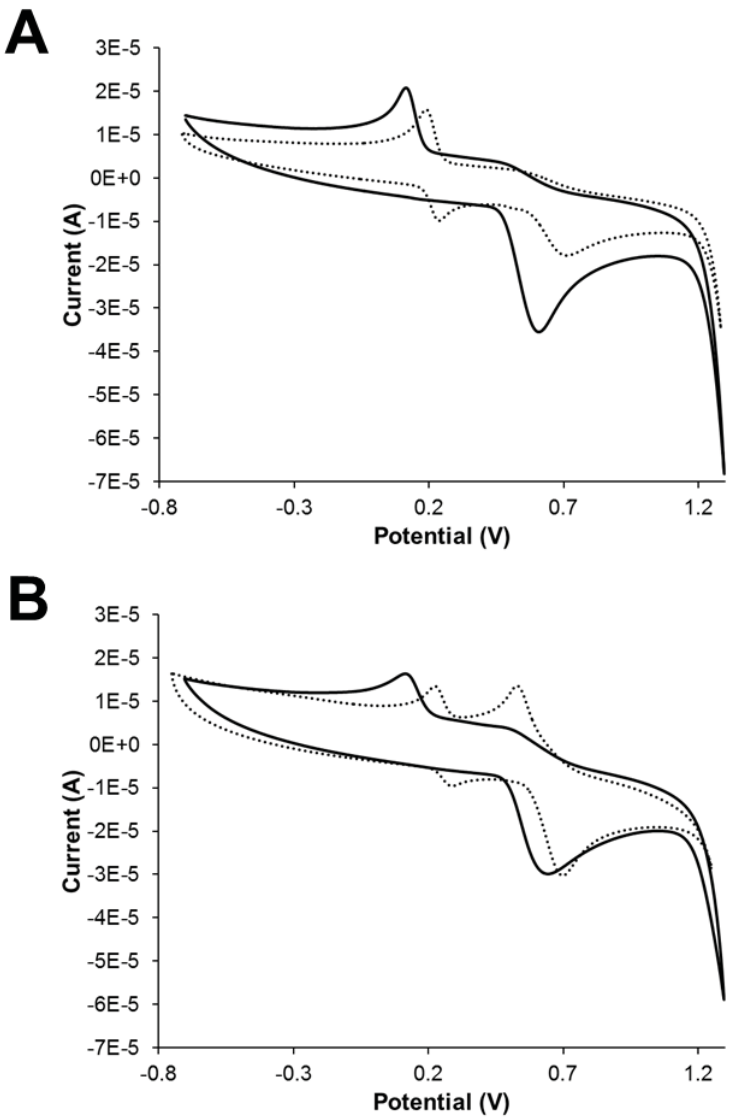

Figure 3.11. Cyclic voltammograms vs. NHE of A) epinephrine and B) norepinephrine. Compounds (380 μM) in MES buffer (64 mM, pH 6.0, dotted line) or MOPS buffer (64 mM, pH 7.2, solid line) with KNO_3 (64 mM) as a supporting electrolyte.

Table 3.2. Electrochemical data vs. NHE for neurotransmitters with and without the addition of 1 equivalent Fe(II).[a]

Compound and pH	Ep_a (V)	Ep_c (V)	ΔE (V)	$E_{1/2}$ (V)
DA (pH 6.0)	0.200, 0.667	0.106, 0.494	0.094, 0.173	0.153, 0.582
DA (pH 7.2)	0.158, 0.605	0.027, 0.425	0.131, 0.180	0.092, 0.515
DA + Fe(II) (pH 6.0)	0.090	0.747	0.657	0.418
NE (pH 6.0)	0.287, 0.696	0.227, 0.527	0.060, 0.169	0.257, 0.612
NE (pH 7.2)	0.642	0.114	0.528	0.378
NE + Fe(II) (pH 6.0)	0.166	0.758	0.592	0.462
EP (pH 6.0)	0.237, 0.711	0.189	0.522[b]	0.045[b]
EP (pH 7.2)	0.606	0.114	0.492	0.360
EP + Fe(II) (pH 6.0)	0.180	0.856	0.676	0.518
$FeSO_4$ (pH 6.0)	0.112	0.5 - 0.65[c]	–	–

[a]Gly, Glu, and GABA showed no electrochemical activity under these conditions. [b]ΔE and $E_{1/2}$ of EP was calculated using 0.711 V for oxidation to coordinate with the *o*-quinone potentials for pH 7.2 for all compounds [55]. [c]Broad wave.

At pH 6.0, the oxidation wave (Ep_a) for DA that occurs at 0.667 results from a 2 electron catecholamine *o*-quinone product (Figure 3.10, Table 3.2), and the reduction wave (Ep_c) observed at the most positive voltage (0.494 V) is likely due to a 2-electron reduction back to the parent compound [54-56]. The second redox couple at pH 6.0 for DA at lower potentials (0.153 V) can be assigned to a reversible, two-electron oxidation of the cyclized catecholamine to the cyclized *o*-quinone (Figure 3.10) [56-58], similar to that described for norepinephrine by Bian, *et al.* The formation of the semiquinones is not observed in these CV studies. It is well-documented that the redox potentials of catecholamines are pH

dependent: as the pH of the solution increases, both the potential of the oxidation and reduction values shift toward a more negative potential voltage [56, 57, 59]. Dopamine exhibits this behavior (Figure 3.7, Table 3.2) in aqueous solution at pH 6.0 and 7.2, with each redox wave shifting about -0.050 V from pH 6.0 to 7.2.

The cyclized *o*-quinone reduction is observed at pH 6.0 for both EP and NE but is not observed to reduce for either EP or NE at pH 7.2. In comparing the voltammograms of the three catecholamine compounds, dopamine is the only compound that has two clear reduction and oxidation potentials at both pH 6.0 and pH 7.2 (Figures 3.10 and 3.11). At these pH values, EP does not show reduction of the linear *o*-quinone. However, NE shows both redox potentials for the linear *o*-quinone. Bian, *et al.* identified two redox couple sets for norepinephrine at 400 μM using a modified glassy carbon electrode; when a unmodified glassy carbon electrode was used, only one redox couple and one oxidation were observed [57]. Thus, both redox couples for EP and NE may be detectable in these experiments if the concentration were increased.

Dopamine toxicity attributed to its autooxidative properties has been well-established [60], leading to death of dopaminergic neurons and causing decreased motor function and, ultimately, Parkinson's disease [61]. Although dopamine and epinephrine both autooxidize, ultimately causing DNA damage *in vitro*, DA caused two times the oxidative DNA damage as epinephrine [26]. Interestingly, DA at low concentrations promotes oxidative DNA damage in the presence of Cu(I) [25]. These CV and DNA damage results indicate that DA can participate in copper redox cycling, perhaps explaining why DA is cytotoxic in systems rich in copper [62]. Similar CV experiments to investigate the effect of Cu(I) on neurotransmitter redox potentials could not be conducted due to precipitation of

the neurotransmitter in the presence of copper. These *in vitro* studies may help to explain why bound copper ions in human serum show no correlation to motor function, whereas labile copper levels have a strong inverse relationship to motor function [20].

Cyclic voltammetry experiments were also conducted with the catecholamines in the presence of 1 equiv Fe(II) at pH 6.0 after a reaction time of 10 min. Under these conditions, the CV of Fe(II)$SO_4 \cdot 7H_2O$ alone shows one sharp oxidation wave and one broad reduction wave around 0.50 – 0.65 V (Figure 3.12A). Differential pulse voltammetry (DPV) experiments resolved this broad reduction wave into two partially overlapping waves (Figure 3.12A, insert). At pH 4.0, Nemtoi and coworkers reported that $FeSO_4 \cdot 7H_2O$ has two reduction waves due to Fe(III) to Fe(II) reduction and Fe electrodeposition, respectively [63]. At pH 6.0, the iron oxidation wave is at 0.112 V, and the two reduction waves are at 0.41 and 0.58 V, respectively. The Fe(II)/Fe(III) redox couple can be attributed to the single anodic wave and the more positive cathodic wave [64].

The cyclic voltammograms for iron in the presence of DA, EP, and NE are all similar in both shape and redox potentials to $FeSO_4 \cdot 7H_2O$, suggesting that the observed waves are from Fe(II)/Fe(III)-based redox reactions. Upon adding 1 equiv neurotransmitter to Fe(II) at pH 6.0 and waiting 10 min, oxidation potentials are observed for DA-Fe, NE-Fe, and EP-Fe at 0.090 V, 0.166 V, and 0.180 V, respectively (Table 3.3). These oxidation potentials are shifted from those of iron alone by -0.022, +0.054, and +0.068 V for DA-, NE-, and EP-Fe, respectively. Only DA-Fe showed an oxidation potential at a lower voltage than Fe(II) alone, suggesting that Fe(II) oxidation to Fe(III) is less spontaneous when iron is bound to dopamine. EP and NE addition yielded higher Fe(II)/Fe(III) oxidation potentials when bound to iron. All the neurotransmitter-Fe anodic potentials are well within the

biological range of the Fenton reaction (-0.324 V to 0.460 V at pH 7 [65]), yet the cathodic waves detected were outside the biologically relevant range, occurring at potentials around 0.7 V - 0.9 V (Table 3.3). The additional waves seen for EP-Fe(II) can be detected by negative DPV and have values of -0.165 and 0.781 V that can be attributed to unbound EP (Figure 3.12). Presence of unbound epinephrine may be due to solubility issues, since a neutral form of the compound was used, unlike NE and DA that were used in salt form. The strong antioxidant potential may lie, then, in the effect on the redox value EP has on iron when EP binds.

The $E_{1/2}$ potentials for the catecholamines suggest that EP-Fe interactions shift the iron redox potentials farthest the range of biological reduction of H_2O_2 ($E_{1/2\ \text{EP-Fe}}$ = 0.518 V), consistent with epinephrine's ability to prevent iron-mediated DNA damage. Iron bound to NE has a redox potential of 0.462 V, just outside of the biologically favorable range. This may explain why, in the presence of iron, NE still prevents damage but not as efficiently as EP. Dopamine-bound iron has the least positive potential (0.418 V) that falls well-into the range for Fe(II) reduction of H_2O_2, explaining its lower antioxidant activity relative to the other catecholamines. These iron-bound potentials correlate with the antioxidant activities of the catecholamine neurotransmitters in the presence of iron, showing agreement between the gel DNA damage assay studies and the iron-neurotransmitter electrochemistry.

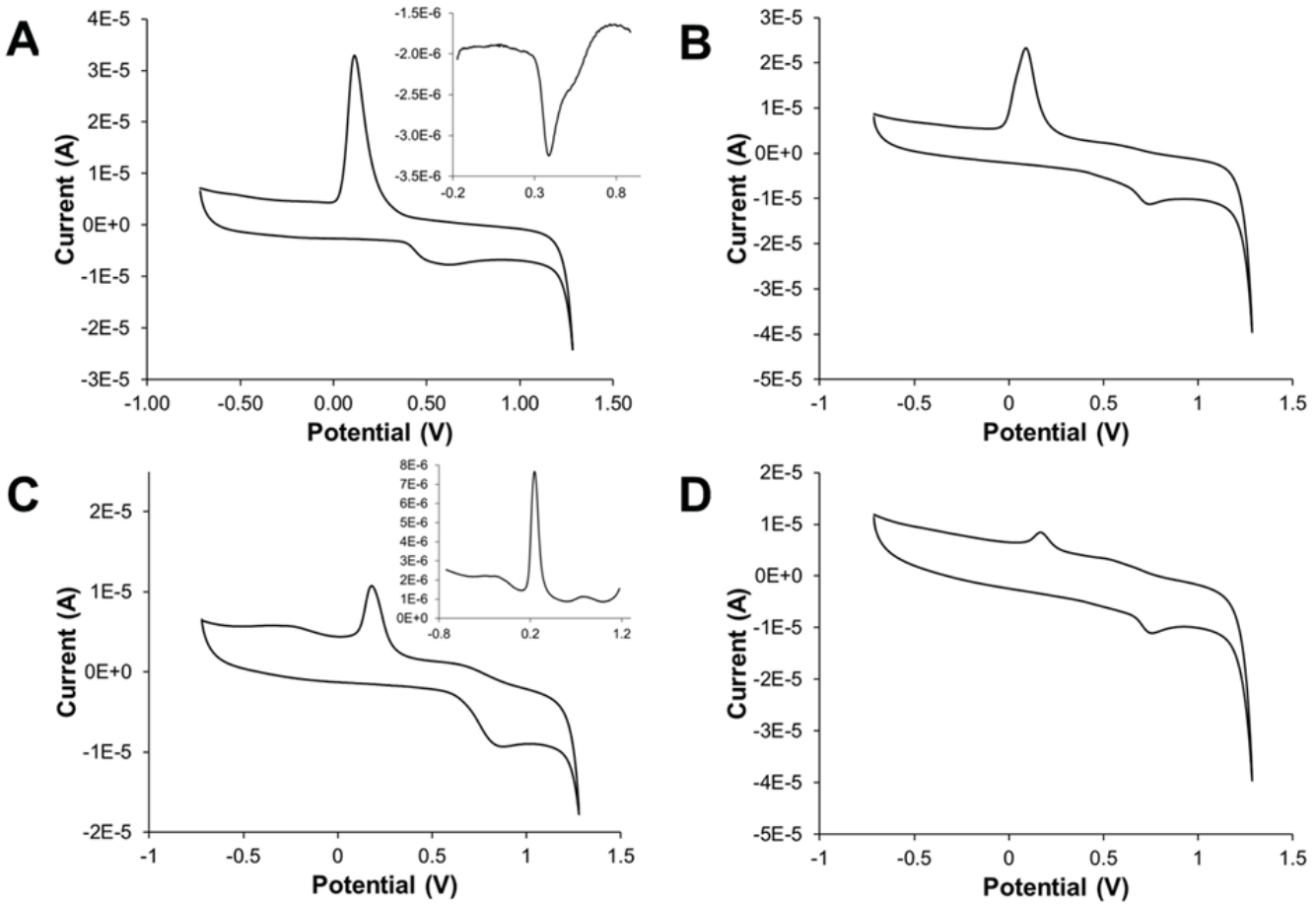

Figure 3.12. Cyclic voltammograms vs. NHE at pH 6.0 (64 mM MES buffer with 64 mM KNO_3 supporting electrolyte) for A) $FeSO_4$ (290 μM; insert is positive DPV with axes of the same units) and neurotransmitter with $FeSO_4$ (145 μM each): B) dopamine, C) epinephrine (insert is negative DPV with axes of the same units), and D) norepinephrine.

Conclusions

Catecholamines and monoamine carboxylic acid neurotransmitters behave quite differently as antioxidants. Three different methods (iron-mediated DNA damage gel electrophoresis, Fe(II)- and Cu(I)-binding UV-vis spectroscopy, and CV both with and without Fe(II) addition) were used to determine antioxidant potential of these neurotransmitters, all of which point to metal binding as a primary factor in the observed antioxidant activity. In the iron-mediated DNA damage assays, the catecholamines DA, EP, and NE were the only compounds to prevent Fe(II) mediated DNA damage. The monoamine carboxylic acids Gly, Glu, and GABA prevented little or no DNA damage under the same conditions. When Fe(II) is chelated prior to adding the catecholamine neurotransmitters, they prevented only a fraction of the DNA damage observed with Fe(II), indicating that iron binding is required for maximal antioxidant efficacy.

UV-vis spectroscopy studies show that the three catecholamines bind Fe(II) and promote oxidation to Fe(III), whereas the three amino acid neurotransmitters showed no evidence of iron binding. The catecholamines also showed much stronger interactions with copper by UV-vis spectroscopy than the amino acids, accelerating Cu(I) oxidation to Cu(II). Cyclic voltammetry provided insight into the behavior of these neurotransmitters both in the presence and absence of iron. The monoamine carboxylic acids were inactive within the accessible aqueous potential window at both pH 6.0 and pH 7.2, which correlates with their inactivity in preventing oxidative DNA damage. In contrast, all three catecholamines show electrochemical evidence of *o*-quinone formation, with DA as the only catecholamine that shows both linear and cyclic quinone formation for both tested pHs. Cyclic voltammetry of the catecholamines in the presence of iron show a trend between higher iron oxidation

potentials and improved antioxidant activity. All of these findings emphasize the importance of iron binding in preventing oxidative DNA damage, suggesting that this antioxidant mechanism should be further investigated when developing treatments for Alzheimer's, Parkinson's, and other diseases with increase labile metal ion concentrations.

Experimental Section

General. Water was purified using a Barnstead NANOpure DIamond Life Science (UV/UF) water deionization system (Barnstead International). Dopamine hydrochloride, 98.5% (Alfa Aesar), L-adrenaline (TCI America), L-noradrenaline bitartrate (TCI America), glycine (J.T. Baker), DL-glutamic acid (TCI Tokyo Kasei), 4-amino-*n*-butyric acid (TCI America), 2-(N-morpholino)ethanesulfonic acid (MES; Calibiochem), 3-(N-morpholino)propanesulfonic acid (MOPS; Alfa Aesar), KNO_3, fine crystal (Mallinckrodt Chemicals), $FeSO_4 \cdot 7H_2O$ (Acros Organics), $CuSO_4 \cdot 5H_2O$ (Fisher), and L-(+)-ascorbic acid, ACS, 99+% (Alfa Aesar), sodium bitartrate (Electron Microscopy Sciences), Chelex 100 resin (Sigma-Aldrich), and disodium dihydrogen ethylenediaminetetraacetate dehydrate (TCI America) were all used as received.

To dissolve L-adrenaline in buffered solutions, 1 M HCl was added as needed (up to 50 μL / 50 mL for a 400 μM solution) until dissolved while maintaining a final pH of 6.0 or 7.2. To prevent oxidation of epinephrine in solution, samples were prepared daily and stored in the dark on ice prior to use. All experiments with norepinephrine bitartrate were also carried out with sodium tartrate as a control. To avoid metal contamination, all microcentrifuge tubes were rinsed in 1 M HCl, triply rinsed in deionized H_2O, and dried

prior to use. Buffered solutions were treated with Chelex resin (2 g / 80 mL buffer) and mixed for 24 h prior to use.

Transfection, amplification, and purification of plasmid DNA. Plasmid DNA (pBSSK) was purified from *E. coli* strain DH1 using a PerfectPrep Spin kit (Fisher). The plasmid DNA was dialyzed at 4 °C against EDTA (1 mM) and NaCl (50 mM) for 24 h and then against NaCl (130 mM) for 24 h to remove metal ions from the DNA. For all experiments, DNA absorbance ratios $A_{250}/A_{260} \leq 0.95$ and $A_{260}/A_{280} \geq 1.8$ were ensured after dialysis.

Gel electrophoresis experiments with Fe(II)/H_2O_2. For each reaction, reagents were added in the following order to achieve the given final concentrations in a final volume of 10 μL: deionized H_2O, MES buffer (10 mM, pH 6.0; to ensure Fe(II) solubility), NaCl (130 mM), 100% ethanol (10 mM), the desired concentration of neurotransmitter (0.01-1500 μM), and Fe(II) (2 μM). Iron solutions were immediately prepared from solid $FeSO_4 \cdot 7H_2O$ prior to each experiment. This mixture was allowed to stand at room temperature for 5 min, followed by addition of plasmid DNA (0.1 pmol in 130 mM NaCl). After 5 min, H_2O_2 (50 μM) was added to initiate DNA damage. After 30 min, EDTA (50 μM) was used to stop the reaction, and loading dye (2 μL) was added to achieve a final volume of 12 μL. Gel electrophoresis was run on a 1% agarose gel in TAE buffer for 30 min at 140 V to separate the nicked and supercoiled forms of the plasmid DNA. Gels were then stained for 5 min using ethidium bromide and washed for an additional 10 min in deionized H_2O before imaging under UV light. The intensities of the damaged and undamaged DNA gel bands

were quantified using UVIproMW software (Jencons Scientific Inc., 2003). Ethidium stains supercoiled DNA less efficiently than nicked DNA, so supercoiled DNA band intensities were multiplied by 1.24 prior to comparison [66, 67]. Intensities of the nicked and supercoiled bands were normalized for each lane so that % nicked + % supercoiled = 100 %. Sodium tartrate prevented only 11.4% of DNA damage at 200 μM (Figure3.20, Table 3.3), the highest concentration of norepinephrine tested, so norepinephrine DNA damage prevention percentages are uncorrected.

Gel electrophoresis experiments with $Fe(EDTA)^{2-}/H_2O_2$. To determine the role of iron binding in neurotransmitter prevention of DNA damage, $Fe(EDTA)^{2-}$ (400 μM) was used as the iron source and experiments were performed as described for the $Fe(II)/H_2O_2$ studies.

Iron and copper binding by UV-vis spectroscopy. All cuvettes were washed in 6 M HCl for at least 30 min, thoroughly rinsed 3 times with deionized water, and dried to avoid metal contamination. Samples were prepared using fresh $FeSO_4 \cdot 7H_2O$ or $CuSO_4 \cdot 5H_2O$ + 1.25 equiv ascorbate in buffered solutions (MES at 10 mM, pH 6.0 for Fe(II) studies and MOPS at 10 mM, pH 7.2 for Cu(I) studies) with neurotransmitter (145 μM) and added to a final concentration of 145 μM and a neurotransmitter to metal ratio of 1:1. For higher neurotransmitter to metal ratios, the neurotransmitter concentration was increased accordingly, keeping the metal concentration at 145 μM. Samples were allowed to stand for 10 min prior to data collection with a Shimadzu UV-3101PC spectrophotometer. Upon Fe(II) addition, sodium tartrate showed only a slight absorbance (0.05 AU) increase at 320 -

330 nm in the UV-vis spectra, making the contribution of tartrate to noradrenaline UV-vis spectra negligible (Figure 3.22A). No absorbances were observed in the UV-vis spectra of Cu(I) + tartrate (Figure 3.22B).

Electrochemical studies. Cyclic voltammetry and differential pulse voltammetry measurements for neurotransmitters alone (380 μM) and neurotransmitters with 1 equiv Fe(II) (145 μM each, final concentration) were measured using a CH Electrochemical Analyzer (CH Instruments, Inc.) in MES buffer (64 mM, pH 6.0) or MOPS buffer (64 mM, pH 7.2) with KNO_3 as a supporting electrolyte (64 mM). Upon Fe(II) addition, samples were allowed to stand for 10 min prior to data collection. Prior to analysis, all solutions were deoxygenated by bubbling with argon for 45 min; during analysis, the sample was blanketed with N_2 to prevent oxidation. For cyclic voltammetry, the samples were cycled between -1.0 V and 1.0 V vs. Ag/AgCl/3 M KCl (+199 mV vs. NHE [68, 69]) using a glassy carbon working electrode and a platinum counter-electrode at a scan rate of 100 mV/s. Each sample was allowed to complete one full ± 1 V cycle prior to data collection. Differential pulse voltammetry was performed from -1.0 V to 1.0 V in increments of 0.004 V at an amplitude 0.05 V, a pulse width of 0.05 s, a sample width 0.0167 s, and a pulse period 0.2 s; the sensitivity ranged from 1×10^{-5} to 1×10^{-6} A/V. Tartrate showed no electrochemical activity in this range at pH 6.0 or 7.2 (Figure 3.23), so norepinephrine CV data are uncorrected.

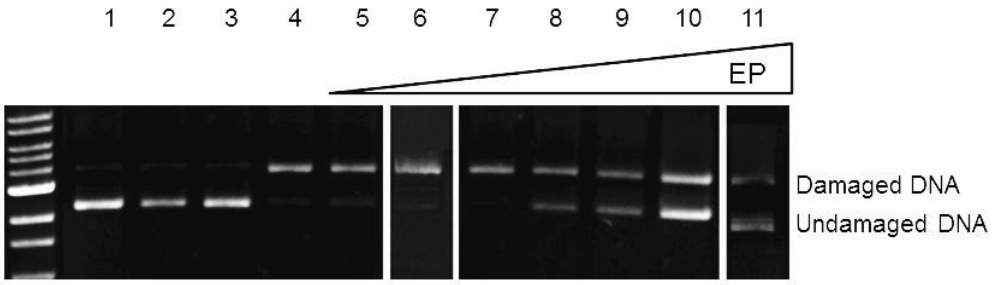

Figure 3.13. Gel electrophoresis image of epinephrine prevention of DNA damage by Fe(II) (2 μM) and H_2O_2 (50 μM). Lanes: MW = 1 kb ladder; 1 = plasmid DNA (p); 2 = p + H_2O_2; 3 = p + 50 μM epinephrine + H_2O_2; 4 = p + $Fe(EDTA)^{2-}$ + H_2O_2; and lanes 5-11: p + $Fe(EDTA)^{2-}$ + H_2O_2 + 1, 5, 10, 15, 25, 30, and 50 μM epinephrine, respectively.

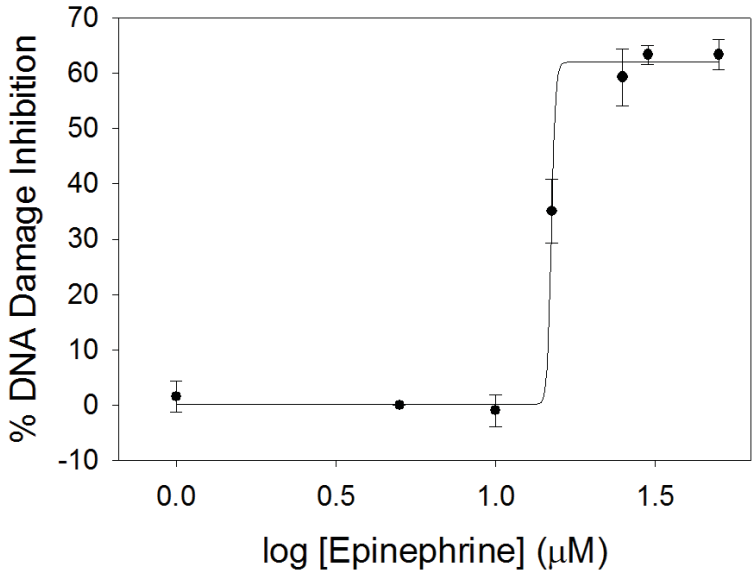

Figure 3.14. Dose-response curve for epinephrine inhibition of iron-mediated DNA damage. Data are reported as the average of three trials with calculated standard deviations.

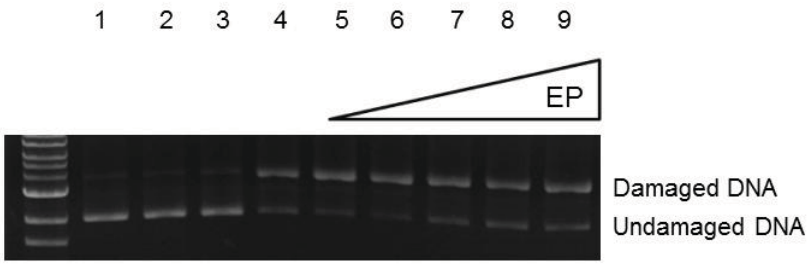

Figure 3.15. Gel electrophoresis image of epinephrine prevention of DNA damage with $Fe(EDTA)^{2-}$ (400 μM) and H_2O_2 (50 μM). Lanes: MW = 1 kb ladder; 1 = plasmid DNA (p); 2 = p + H_2O_2; 3 = p + 50 μM epinephrine + H_2O_2; and 4 = p + $Fe(EDTA)^{2-}$ + H_2O_2; lanes 5-9: p + $Fe(EDTA)^{2-}$ + H_2O_2 + 1, 5, 15, 25, and 50 μM epinephrine, respectively.

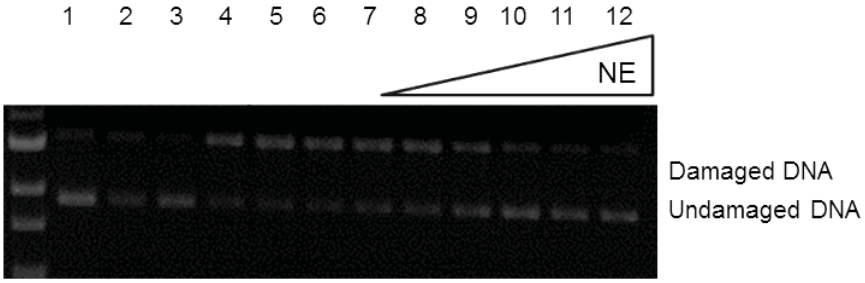

Figure 3.16. Gel electrophoresis image of norepinephrine prevention of DNA damage Fe(II) (2 μM) and H_2O_2 (50 μM). Lanes: MW = 1 kb ladder; 1 = plasmid DNA (p); 2 = p + H_2O_2; 3 = p + 200 μM norepinephrine + H_2O_2; and 4 = p + Fe(II) + H_2O_2; lanes 5-12: p + Fe(II) + H_2O_2 + 2, 5, 10, 25, 50, 100, 150, and 200 μM norepinephrine, respectively.

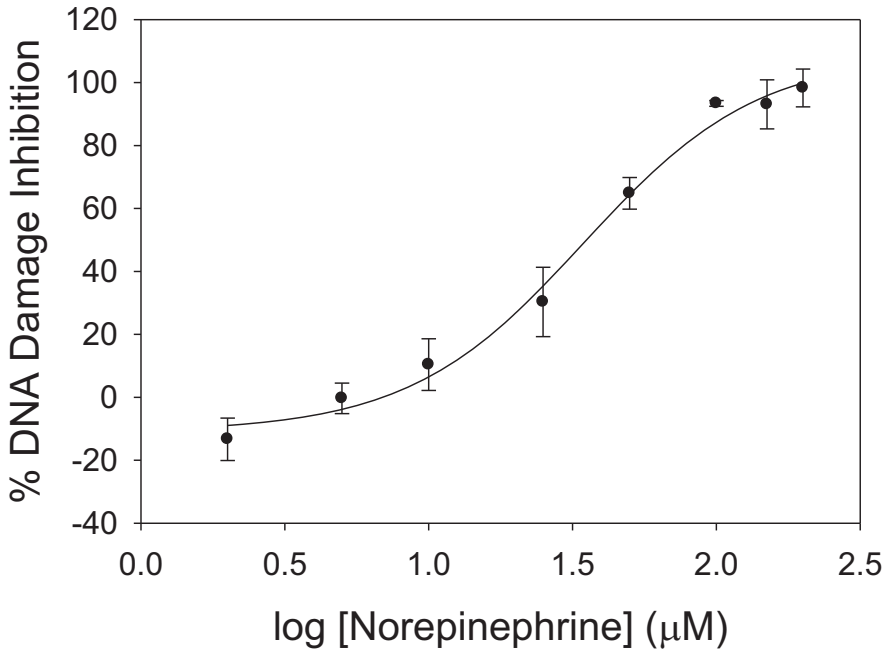

Figure 3.17. Dose-response curve for norepinephrine inhibition of iron-mediated DNA damage. Data are reported as the average of three trials with calculated standard deviations.

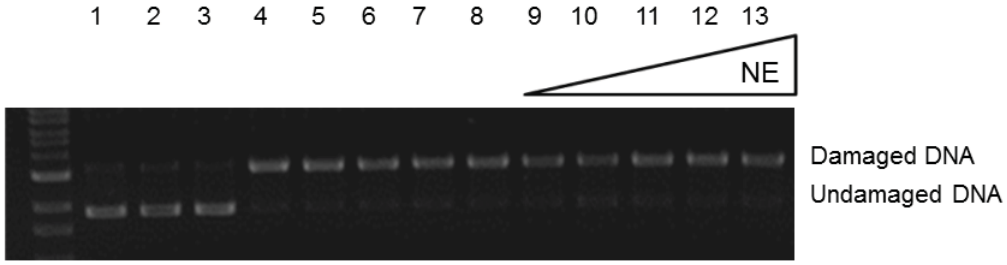

Figure 3.18. Gel electrophoresis image of norepinephrine prevention of DNA damage with $Fe(EDTA)^{2-}$ (400 μM) and H_2O_2 (50 μM). Lanes: MW = 1 kb ladder; 1 = plasmid DNA (p); 2 = p + H_2O_2; 3 = p + 200 μM norepinephrine + H_2O_2; and 4 = p + $Fe(EDTA)^{2-}$ + H_2O_2; lanes 5-9: p + $Fe(EDTA)^{2-}$ + H_2O_2 + 1, 2, 5, 10, 25, 50, 100, 150, and 200 μM norepinephrine, respectively.

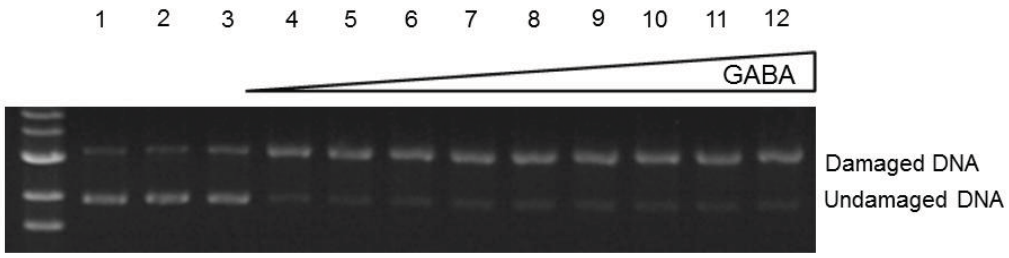

Figure 3.19. Gel electrophoresis image of GABA prevention of DNA damage with Fe(II) (2 μM) and H_2O_2 (50 μM). Lanes: MW = 1 kb ladder; 1 = plasmid DNA (p); 2 = p + H_2O_2; 3 = p + 300 μM GABA + H_2O_2; and 4 = p + Fe(II) + H_2O_2; lanes 5-12: p + Fe(II) + H_2O_2 + 1, 5, 50, 75, 100, 150, 200, and 300 μM GABA, respectively.

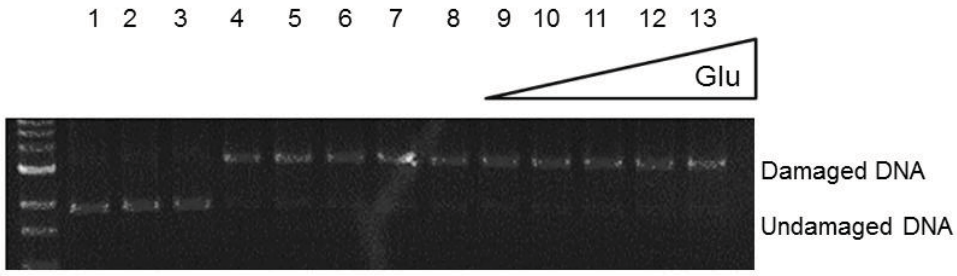

Figure 3.20. Gel electrophoresis image of glutamate prevention of DNA damage by Fe(II) (2 μM) and H_2O_2 (50 μM). Lanes: MW = 1 kb ladder; 1 = plasmid DNA (p); 2 = p + H_2O_2; 3 = p + 200 μM Glu + H_2O_2; and 4 = p + $Fe(EDTA)^{2-}$ + H_2O_2; lanes 5-13: p + Fe(II) + H_2O_2 + 1, 2, 5, 10, 25, 50, 100, 150, and 200 μM Glu, respectively.

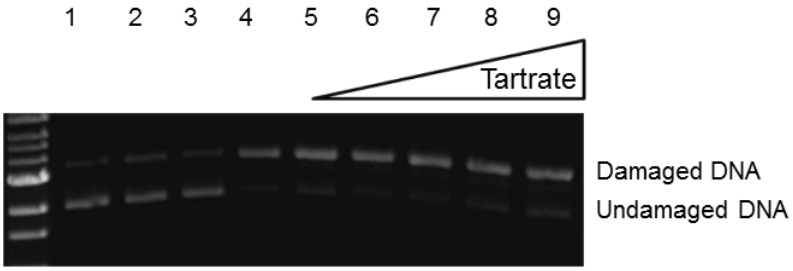

Figure 3.21. Gel electrophoresis image of tartrate prevention of DNA damage with Fe(II) (2 μM) and H_2O_2 (50 μM). Lanes: MW = 1 kb ladder; 1 = plasmid DNA (p); 2 = p + H_2O_2; 3 = p + 400 μM tartrate + H_2O_2; and 4 = p + Fe(II) + H_2O_2. Lanes 5-9: p + Fe(II) + H_2O_2. + 1, 25, 75, 200, and 400 μM tartrate, respectively.

Table 3.3. Tabulation of gel electrophoresis results for tartrate DNA damage assays with 2 μM Fe(II) and 50 μM H_2O_2.

Gel lane	Tartrate, μM	% Supercoiled	% Nicked	% Damage Inhib.	*p* Values
1: plasmid (p)	–	94.25 ± 3.87	5.75 ± 3.87	–	–
2: p + H_2O_2	–	96.47 ± 2.49	3.53 ± 2.49	–	–
3: p + H_2O_2 + Tart	400	96.40 ± 1.97	3.60 ± 1.97	–	–
4: Fe(II)+ H_2O_2	0	13.21 ± 7.87	86.79 ± 7.87	0	–
5	1	18.73 ± 7.86	81.27 ± 7.86	7.07 ± 0.91	5.47×10^{-3}
6	25	16.77 ± 7.55	83.23 ± 7.55	4.33 ± 2.46	9.28×10^{-2}
7	75	19.10 ± 9.50	80.90 ± 9.50	7.57 ± 3.64	6.92×10^{-2}
8	200	21.93 ± 8.71	78.07 ± 8.71	11.43 ± 3.50	2.98×10^{-2}
9	400	27.11 ± 5.85	72.89 ± 5.85	18.04 ± 1.89	3.63×10^{-3}

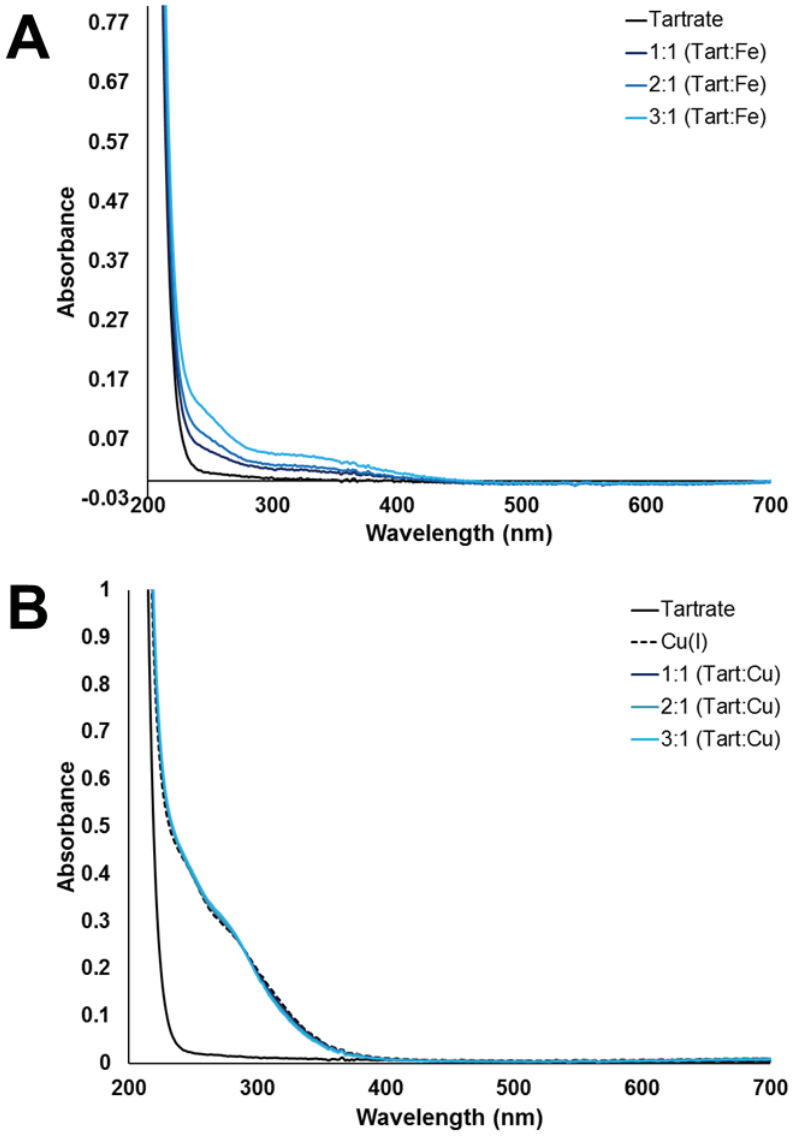

Figure 3.22. UV-vis spectra of tartrate (145 μM) with iron and copper in A) MES buffer (pH 6.0, 10 mM) with Fe(II) and B) MOPS buffer (pH 7.2, 10 mM) with Cu(I). A 1:1 ratio represents 145 μM neurotransmitter to 145 μM Fe(II) or Cu(I), respectively, and higher concentration ratios are obtained by increasing tartrate concentrations with fixed Fe(II) and Cu(I) concentrations (145 μM). Fe(II) solutions show no significant absorbances at these wavelengths.

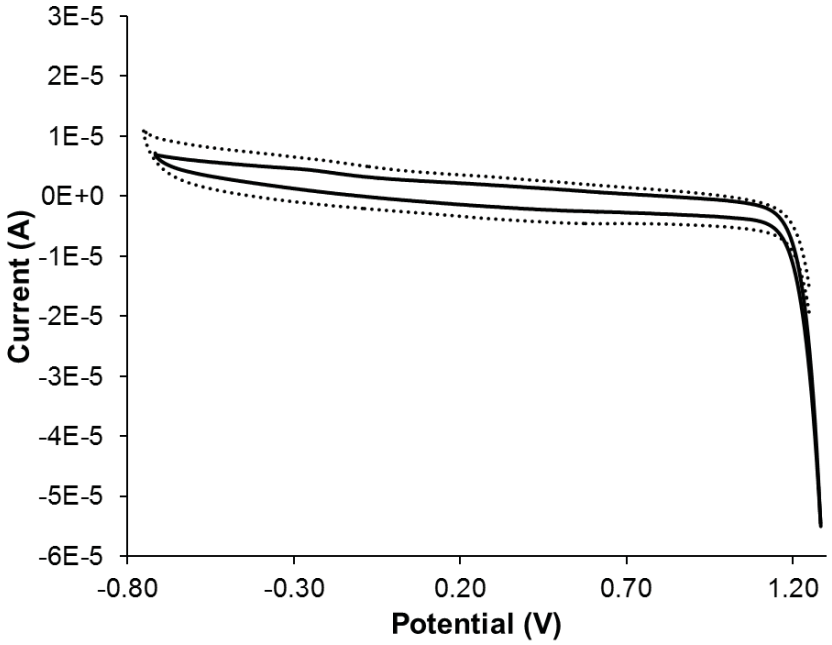

Figure 3.23. Cyclic voltammograms of tartrate in MES buffer (64 mM, pH 6.0, dotted line) or MOPS buffer (64 mM, pH 7.2, solid line) with 64 mM KNO_3 as a supporting electrolyte.

Table 3.4. Tabulation of gel electrophoresis results for dopamine DNA damage assays with 2 μM Fe(II) and 50 μM H_2O_2.

Gel lane	DA, μM	% Supercoiled	% Nicked	% Damage Inhib.	*p* Values
1: plasmid (p)	–	94.16 ± 2.64	5.84 ± 2.64	–	–
2: p + H_2O_2	–	93.29 ± 2.20	6.71 ± 2.20	–	–
3: p + H_2O_2 + DA	1600	95.85 ± 2.10	4.15 ± 2.10	–	–
4: Fe(II) + H_2O_2	0	8.49 ± 2.0	91.51 ± 2.0	0	–
5	1	3.92 ± 7.20	96.08 ± 7.20	-1.04 ± 1.78	0.418
6	10	3.87 ± 4.76	96.13 ± 4.76	-2.93 ± 1.79	0.105
7	30	8.01 ± 5.69	91.99 ± 5.69	2.55 ± 3.74	0.359
8	50	21.75 ± 6.33	78.25 ± 6.33	12.06 ± 3.71	3.01×10^{-2}
9	80	30.60 ± 9.42	69.40 ± 9.42	25.05 ± 5.11	1.36×10^{-2}
10	100	47.72 ± 7.38	52.28 ± 7.38	40.54 ± 4.19	3.54×10^{-3}
11	150	68.60 ± 4.02	31.40 ± 4.02	65.53 ± 5.70	2.51×10^{-3}
12	200	76.28 ± 1.81	23.72 ± 1.81	75.11 ± 2.83	4.73×10^{-4}
13	400	79.26 ± 1.15	20.74 ± 1.15	81.92 ± 1.32	8.65×10^{-5}
14	600	86.08 ± 3.82	13.92 ± 3.82	89.07 ± 3.83	6.16×10^{-4}
15	1000	88.97 ± 4.26	11.03 ± 4.26	94.39 ± 3.86	5.57×10^{-4}
16	1200	90.53 ± 2.26	9.47 ± 2.26	97.06 ± 1.36	6.54×10^{-5}
17	1600	92.23 ± 2.09	7.78 ± 2.09	98.19 ± 1.14	4.49×10^{-5}

Table 3.5. Tabulation of gel electrophoresis results for dopamine DNA damage assays with 400 μM $Fe(EDTA)^{2-}$ and 50 μM H_2O_2.

Gel lane	DA, μM	% Supercoiled	% Nicked	% Damage Inhib.	*p* Values
1: plasmid (p)	–	93.93 ± 1.86	6.07 ± 1.86	–	–
2: p + H_2O_2	–	92.35 ± 1.81	8.82 ± 1.81	–	–
3: p + H_2O_2 + DA	1200	94.61 ± 1.17	5.39 ± 1.17	–	–
4: $Fe(EDTA)^{2-}$ + H_2O_2	0	2.22 ± 1.09	97.78 ± 1.09	0	–
5	10	5.16 ± 4.78	94.84 ± 4.78	3.26 ± 2.91	0.192
6	80	9.07 ± 4.98	90.93 ± 4.98	7.17 ± 3.18	5.98×10^{-2}
7	150	15.44 ± 3.27	84.56 ± 3.27	14.79 ± 1.83	5.06×10^{-3}
8	600	21.34 ± 2.58	78.66 ± 2.58	21.50 ± 1.44	1.49×10^{-3}
9	1200	22.30 ± 0.25	77.70 ± 0.25	21.66 ± 1.08	8.23×10^{-3}

Table 3.6. Tabulation of gel electrophoresis results for epinephrine DNA damage assays with 2 μM Fe(II) and 50 μM H_2O_2.

Gel lane	EP, μM	% Supercoiled	% Nicked	% Damage Inhib.	*p* Values
1: plasmid (p)	–	96.71 ± 3.08	3.29 ± 3.08	–	–
2: p + H_2O_2	–	93.30 ± 5.23	6.70 ± 5.23	–	–
3: p + H_2O_2 + EP	50	95.92 ± 5.71	4.08 ± 5.71	–	–
4: Fe(II) + H_2O_2	0	9.56 ± 7.03	90.44 ± 7.03	0	–
5	1	10.81 ± 8.23	89.19 ± 8.23	1.48 ± 2.79	0.455
6	5	0.76 ± 0.11	99.24 ± 0.11	0.0016 ± 0.0013	0.167
7	10	12.85 ± 10.70	87.15 ± 10.70	3.81 ± 6.81	0.435
8	15	39.98 ± 7.71	60.02 ± 7.71	35.08 ± 5.77	8.90×10^{-3}
9	25	61.18 ± 1.37	38.82 ± 1.37	59.29 ± 5.13	2.48×10^{-3}
10	30	64.59 ± 4.64	35.41 ± 4.64	63.35 ± 1.75	2.56×10^{-4}
11	50	65.67 ± 3.23	34.33 ± 3.23	63.34 ± 2.76	6.32×10^{-4}

Table 3.7. Tabulation of gel electrophoresis results for epinephrine DNA damage assays with 400 μM $Fe(EDTA)^{2-}$ and 50 μM H_2O_2.

Gel lane	EP, μM	% Supercoiled	% Nicked	% Damage Inhib.	*p* Values
1: plasmid (p)	–	96.90 ± 2.86	3.10 ± 2.86	–	–
2: p + H_2O_2	–	93.96 ± 5.27	6.04 ± 5.27	–	–
3: p + H_2O_2 + EP	50	96.45 ± 3.39	3.55 ± 3.39	–	–
4: $Fe(EDTA)^{2-}$ + H_2O_2	0	12.84 ± 8.59	87.16 ± 8.59	0	–
5	1	22.81 ± 9.14	77.19 ± 9.14	11.98 ± 3.56	2.82×10^{-2}
6	5	28.44 ± 9.10	71.56 ± 9.10	18.69 ± 5.46	2.73×10^{-2}
7	15	31.08 ± 0.90	68.92 ± 0.90	21.02 ± 6.60	3.13×10^{-3}
8	25	43.06 ± 2.18	56.94 ± 2.18	35.16 ± 6.62	1.16×10^{-3}
9	50	36.56 ± 3.49	63.44 ± 3.49	27.72 ± 6.40	1.74×10^{-3}

Table 3.8. Tabulation of gel electrophoresis results for norepinephrine DNA damage assays with 2 μM Fe(II) and 50 μM H_2O_2.

Gel lane	NE, μM	% Supercoiled	% Nicked	% Damage Inhib.	*p* Values
1: plasmid (p)	–	94.82 ± 1.82	5.18 ± 1.84	–	–
2: p + H_2O_2	–	94.15 ± 3.25	5.85 ± 3.25	–	–
3: p + H_2O_2 + NE	200	97.19 ± 3.15	2.81 ± 3.15	–	–
4: Fe(II) + H_2O_2	0	23.99 ± 8.42	76.01 ± 8.42	0	–
5	2	14.88 ± 8.30	85.12 ± 8.30	-13.34 ± 6.76	7.60×10^{-2}
6	5	23.70 ± 12.12	76.30 ± 12.12	-0.33 ± 4.86	0.917
7	10	21.18 ± 11.02	75.82 ± 11.02	10.37 ± 8.21	0.160
8	25	40.24 ± 13.62	59.76 ± 13.62	30.28 ± 11.00	4.13×10^{-2}
9	50	67.56 ± 2.35	32.44 ± 2.35	64.79 ± 5.04	1.73×10^{-3}
10	100	84.41 ± 6.15	15.59 ± 6.15	93.37 ± 0.91	3.17×10^{-5}
11	150	89.44 ± 5.06	10.56 ± 5.06	93.06 ± 7.80	2.33×10^{-3}
12	200	87.81 ± 9.75	12.19 ± 9.75	98.29 ± 5.99	1.24×10^{-3}

Table 3.9. Tabulation of gel electrophoresis results for norepinephrine DNA damage assays with 400 μM $Fe(EDTA)^{2-}$ and 50 μM H_2O_2.

Gel lane	NE, μM	% Supercoiled	% Nicked	% Damage Inhib.	*p* Values
1: plasmid (p)	–	96.53 ± 4.19	3.47 ± 4.19	–	–
2: p + H_2O_2	–	90.91 ± 6.28	9.09 ± 6.28	–	–
3: p + H_2O_2 + NE	200	95.40 ± 3.49	4.60 ± 3.49	–	–
4: $Fe(EDTA)^{2-}$ + H_2O_2	0	4.50 ± 0.05	95.50 ± 0.05	0	–
5	1	10.60 ± 0.53	89.40 ± 0.53	6.70 ± 0.28	5.82×10^{-4}
6	2	8.72 ± 2.60	91.28 ± 2.60	4.66 ± 2.94	0.111
7	5	7.91 ± 3.04	92.09 ± 3.04	3.80 ± 3.43	0.195
8	10	8.26 ± 0.94	91.74 ± 0.94	4.12 ± 0.95	1.73×10^{-2}
9	25	6.13 ± 0.22	93.87 ± 0.22	1.79 ± 0.27	7.50×10^{-3}
10	50	4.51 ± 0.16	95.49 ± 0.16	0.01 ± 0.13	0.906
11	100	3.18 ± 3.97	96.82 ± 3.97	-1.42 ± 4.39	0.632
12	150	3.37 ± 5.27	96.63 ± 5.27	-1.19 ± 5.83	0.757
13	200	2.70 ± 2.72	97.30 ± 2.72	-1.96 ± 2.99	0.374

Table 3.10. Tabulation of gel electrophoresis results for γ-aminobutyric acid DNA damage assays with 2 μM Fe(II) and 50 μM H_2O_2.

Gel lane	GABA, μM	% Supercoiled	% Nicked	% Damage Inhib.	*p* Values
1: plasmid (p)	–	97.22 ± 2.71	2.78 ± 2.71	–	–
2: p + H_2O_2	–	94.77 ± 4.93	5.23 ± 4.93	–	–
3: p + H_2O_2 + GABA	300	85.49 ± 2.00	14.51 ± 2.00	–	–
4: Fe(II) + H_2O_2	0	15.05 ± 12.69	84.95 ± 12.69	0	–
5	1	11.74 ± 10.06	84.95 ± 10.06	-4.78 ± 5.44	0.267
6	5	11.57 ± 9.74	88.43 ± 9.74	-5.07 ± 5.08	0.226
7	50	13.78 ± 12.52	86.22 ± 12.52	-1.75 ± 1.07	0.105
8	75	16.69 ± 16.69	83.31 ± 16.69	2.56 ± 8.10	0.639
9	100	13.92 ± 12.61	86.08 ± 12.61	-1.55 ± 1.10	0.135
10	150	11.13 ± 9.41	88.87 ± 9.41	-5.74 ± 5.07	0.189
11	200	12.68 ± 5.59	87.32 ± 5.59	-4.39 ± 9.29	0.499
12	300	12.46 ± 5.06	87.54 ± 5.06	-4.73 ± 9.81	0.492

Table 3.11. Tabulation of gel electrophoresis results for glutamate with 2 μM Fe(II) and 50 μM H_2O_2.

Gel lane	Glu, μM	% Supercoiled	% Nicked	% Damage Inhib.	*p* Values
1: plasmid (p)	–	97.79 ± 3.01	2.21 ± 3.01	–	–
2: p + H_2O_2	–	97.30 ± 2.71	2.70 ± 2.71	–	–
3: p + H_2O_2 + Glu	200	98.13 ± 3.12	1.87 ± 3.12	–	–
4:Fe(II) + H_2O_2	0	12.52 ± 21.68	87.48 ± 21.68	0	–
5	1	11.12 ± 19.27	88.88 ± 19.27	-2.24 ± 3.87	0.422
6	2	11.96 ± 16.39	88.04 ± 16.39	-1.96 ± 8.34	0.724
7	5	18.20 ± 15.76	81.80 ± 15.76	3.54 ± 22.55	0.811
8	10	11.66 ± 20.20	88.34 ± 20.20	-1.37 ± 2.38	0.423
9	25	11.53 ± 18.39	88.47 ± 18.39	-1.93 ± 5.12	0.581
10	50	11.19 ± 19.39	88.81 ± 19.39	-2.13 ± 3.69	0.423
11	100	13.17 ± 22.58	86.83 ± 22.58	0.99 ± 1.49	0.367
12	150	15.54 ± 26.22	84.46 ± 26.22	4.69 ± 7.43	0.389
13	200	19.19 ± 31.05	80.81 ± 31.05	10.19 ± 15.49	0.375

References

[1] M. Joshua, A. Adler, H. Bergman, Curr. Opin. Neurobiol. 19 (2009) 615-620.

[2] N.T. Bello, A. Hajnal, Pharmacol. Biochem. Behavior 97 (2010) 25-33.

[3] B.W. Dunlop, C.B. Nemeroff, Arch. Gen. Psychiatry 64 (2007) 327-337.

[4] J. Wortsman, Endocrinol. Metab. Clin. North Amer. 31 (2002) 79-106.

[5] I.S. Morozov, G.S. Pukhova, E.R. Ivanov, Fiziol. Chel. 9 (1983) 812-818.

[6] A.W. Goddard, S.G. Ball, J. Martinez, M.J. Robinson, C.R. Yang, J.M. Russell, A. Shekhar, Depress. Anx. 27 (2010) 339-350.

[7] T.S. Naka, M. Yaguchi, N. Okado, Brain Res. 924 (2002) 124-126.

[8] F. Musshoff, D.W. Lachenmeier, P. Schmidt, R. Dettmeyer, B. Madea, Alcohol. Clin. Exp. Res. 29 (2005) 46-52.

[9] R. Ramakrishnan, A. Namasivayam, Neurosci. Lett. 186 (1995) 200-202.

[10] B. Rasch, C. Dodt, M. Molle, J. Born, Psychoneuroendochrinology 32 (2007) 884-891.

[11] P.L. Brooks, J.H. Peever, J. Neurosci. 31 (2011) 7111-7121.

[12] J. Jaeken, J. Child Neurol. 17 (2002) 3S84-83S88.

[13] C. Yuksel, D. Ongur, Biol. Psychiat. 68 (2010) 785-794.

[14] D. Nitz, J.M. Siegel, Neuroscience 78 (1997) 795-801.

[15] J.L. Wu, Y. Lin, Z.W. Shen, Y.W. Miao, R.H. Wu, L.Z. J., BMEI 2 (2008) 348-352.

[16] C. Ballini, L.D. Corte, M. Pazzagli, M.A. Colivicchi, G. Pepeu, K.F. Tipton, M.G. Giovannini, J. Neurochem. 106 (2008) 1035-1043.

[17] Y.Z. Feng, T. Zhang, R.W. Rockhold, I.K. Ho, Neurochem. Res. 20 (1995) 745-751.

[18] D. Strzelecki, J. Rabe-Jablonska, Eur. Neuropsychoparmacol. 20 (2010) S470-S471.

[19] C.N. Epperson, K. Haga, G.F. Mason, E. Sellars, R. Gueorguieva, W. Zhang, E. Weiss, D.L. Rothman, J.H. Krystal, Arch. Gen. Psychiatry 59 (2002) 851-858.

[20] C. Salustri, G. Barbati, R. Ghidoni, L. Quintiliani, S. Ciappina, G. Binetti, R. Squitti, Clin. Neurophys. 121 (2010) 502-507.

[21] R. Squitti, C.C. Quattrocchi, G.D. Forno, P. Antuono, D.R. Wekstein, C.R. Capo, C. Salustri, P.M. Rossini, Biomarker Insights 1 (2006) 205-213.

[22] M.B.H. Youdim, G. Stephenson, D.B. Shachar, Ann. N. Y. Acad. Sci. 1012 (2004) 306-325.

[23] T. Shimizu, Y. Nakanishi, M. Nakahara, N. Wada, Y. Moro-oka, T. Hirano, T. Konishi, S. Matsugo, J. Clin. Biochem. Nutr. 47 (2010) 181-190.

[24] Y. Nishino, M. Ando, R. Makino, K. Ueda, Y. Okamoto, N. Kojima, Neurotox. Res. 20 (2011) 84-92.

[25] M. Ando, K. Ueda, Y. Okamoto, N. Kojima, J. Health Sci. 57 (2011) 204-209.

[26] W.A. Spencer, J. Jeyabalan, S. Kichambre, R.C. Gupta, Free Radic. Biol. Med. 50 (2011) 139-147.

[27] Y.Z. Fang, S. Yang, G. Wu, Nutrition 8 (2002) 872-879.

[28] J. Feng, W.Q. Ma, Z.R. Xu, J. He, X., Y.Z. Wang, J.X. Liu, Animal Feed Sci. Tech. 150 (2009) 106-113.

[29] R. Sivakumar, P.V.A. Babu, C.S. Shyamaladevi, Exp. Toxicol. Pathol. 63 (2011) 137-142.

[30] H.F. Wang, S.M. Chuang, C.C. Hsiao, S.H. Cherng, Food Chem. Toxicol. 49 (2011) 955-962.

[31] P. Mao, P.H. Reddy, Biochim. Biophys. Acta 1812 (2011) 1359-1370.

[32] F.C. Luft, J. Mol. Med. 83 (2005) 241-243.

[33] S. Maynard, S.H. Schurman, C. Harboe, N.C. Souza-Pinto, V.A. Bohr, Carcinogenesis 30 (2009) 2-10.

[34] D. Plesca, S. Mazumder, A. Almasan, Methods Enzymol. 446 (2008) 107-122.

[35] W.P. Roos, B. Kaina, Trends Molec. Med. 12 (2006) 440-450.

[36] N.R. Perron, J.N. Hodges, M. Jenkins, J.L. Brumaghim, Inorg. Chem. 47 (2008) 6153-6161.

[37] R.R. Ramoutar, J.L. Brumaghim, Main Group Chem. 6 (2007) 143-153.

[38] E.E. Battin, J.L. Brumaghim, J. Inorg. Biochem. 102 (2008) 2036-2042.

[39] E.E. Battin, The role of metal coordination in the inhibition of iron(II)- and copper(I)-mediated DNA damage by organoselenium and organosulfur compounds., Clemson University, Clemson, SC, 2008, 117-156.

[40] N.R. Perron, J.N. Hodges, M. Jenkins, J.L. Brumaghim, Inorg. Chem. 47 (2008) 6153-6161.

[41] N.R. Perron, Effects of Polyphenol Compounds on Iron- and Copper-Mediated DNA Damage: Mechanisms and Predictive Models., Clemson University, Clemson, 2008, 63-140.

[42] E.E. Battin, N.R. Perron, J.L. Brumaghim, Inorg. Chem. 45 (2006) 499-501.

[43] L. Li, D.M. Lubman, Anal. Chem. 59 (1987) 2538-2541.

[44] P.K. Jha, G.P. Halada, Chem. Central J. 5 (2011) 1-7.

[45] M. Velusamy, M. Palaniandavar, Inorg. Chem. 42 (2003) 8283-8293.

[46] C.H. Wang, J.W. Lu, H.H. Wei, M. Takeda, Inorg. Chim. Acta 360 (2007) 2944-2952.

[47] N.R. Perron, J.L. Brumaghim, Cell Biochem. Biophys. 53 (2009) 75-100.

[48] A. Granata, E. Monzani, L. Casella, J. Biol. Inorg. Chem. 9 (2004) 903-913.

[49] B.A. Jazdzewski, P.L. Holland, M. Pink, V.G. Young, D.J.E. Spencer, W.B. Tolman, Inorg. Chem. 40 (2001) 6097-6107.

[50] T.G. Fawcett, E.E. Bernaducci, K. Krogh-Jesperen, H.J. Schugar, J. Am. Chem. Soc. 102 (1980) 2598-2604.

[51] R.C. Holz, J.M. Brink, F.T. Gobena, C.J. O'Connor, Inorg. Chem. 33 (1994) 6086-6092.

[52] J.L. Pierre, M. Fontecave, BioMetals 12 (1999) 195-199.

[53] S. Baez, J.S. Aguilar, M. Widersten, A.N. Johansson, B. Mannervik, Biochem. J. 324 (1997) 25-28.

[54] B. Wolfrum, M. Zevenbergen, S. Lemay, Anal. Chem. 80 (2008) 972-977.

[55] A. Kumar, J.P. Hart, D.V. McCalley, J. Chromatog. A 1218 (2011) 3854-3861.

[56] S.M. Chen, K.T. Peng, J. Electroanal. Chem. 547 (2003) 179-189.

[57] C. Bian, Q. Zeng, H. Xiong, X. Zhang, S. Wang, Bioelectrochemistry 79 (2010) 1-5.

[58] M.D. Hawley, S.V. Tatawawadi, S. Piekarski, R.N. Adams, J. Am. Chem. Soc. 89 (1967) 447-450.

[59] M.T. Shreenivas, B.E.K. Swamy, U. Chandra, B.S. Sherigara, Internat. J. Electrochem. 2011 (2011) 1-5.

[60] I. Miyazaki, M. Asanuma, Neurochem. Res. 34 (2009) 698-706.

[61] R.L. Miller, M.J. Kracke, G.Y. Sun, A.Y. Sun, Neurochem. Res. 34 (2009) 55-65.

[62] A.G. Siraki, P.J. O'Brien, Toxicology 177 (2002) 81-90.

[63] G. Nemtoi, H. Chiriac, O. Dragos, M.O. Apostu, D. Lutic, Acta Chim. IASI 17 (2009) 151-168.

[64] H.M.N. Akhtar, A.A. Shaikh, M.Q. Ehsan, Elektrokhimiya 14 (2008) 1504-1509.

[65] J.L. Pierre, M. Fontecave, R.R. Crichton, BioMetals 15 (2002) 341-346.

[66] P. Ryan, M.J. Hynes, J. Coord. Chem. 61 (2008) 3711-3726.

[67] R.T. Borchardt, J.A. Huber, J. Med. Chem. 18 (1975) 120-122.

[68] E.P. Friis, J.E.T. Andersen, L.L. Madsen, N. Bonander, P. Moller, J. Ulstrup, Electrochim. Acta 43 (1998) 1114-1122.

[69] D.T. Sawyer, A. Sobkowiak, J.L. Roberts Electrochemistry for Chemists, Wiley-Interscience, New York, 1995, 184-204.

CHAPTER FOUR

CONCLUSIONS

Indications of Copper Redox Cycling in the Presence of Polyphenol Compounds

Electron paramagnetic resonance spectroscopy has been successfully used to investigate polyphenol radical formation with and without addition of Cu(I) and H_2O_2. The results indicate that hydroxyl radical formation occurs in the presence of methyl 3,4,5-trihydroxybenzoate (MEGA), methyl 3,4-dihydroxybenzoate (MEPCA), (-)-epicatechin (EC), and (-)-epigallocatechin-3-gallate (EGCG) upon Cu(I) and H_2O_2 addition, with MEPCA suppressing hydroxyl radical formation more than the other polyphenols and that hydrogen radical formation also occurs for a prooxidant compound, epicatechin (EC). These results correlate with Cu(I)/H_2O_2 DNA damage gel assays that determined EC was a prooxidant and MEPCA was the most potent antioxidant under these conditions. Semiquinone radical formation was also detected for all compounds without Cu(I) or H_2O_2 addition, with the exception of MEPCA. The formation of semiquinone radical species independent of either Cu(I) or ascorbate presence is indicative of polyphenol redox cycling, and could explain the cellular toxicity observed for these compounds.

The Role of Iron Binding in Neurotransmitter and Polyphenol Prevention of DNA Damage

Neurotransmitter and polyphenol compounds capable of binding iron behave as antioxidants to prevent iron-mediated DNA damage. 5-Hydroxychromone, epinephrine, norepinephrine, dopamine, and curcumin all show evidence of iron oxidation upon binding to iron, and all effectively inhibit iron-mediated DNA damage (IC_{50} values ranging from 15 μM – 416 μM). Upon chelating the iron with EDTA prior to conducting DNA damage assays, these compounds exhibited less than half their antioxidant potential compared to DNA damage assays with unchelated

Fe(II), indicating that iron binding must occur for maximal antioxidant behavior. Compounds that prevent little or no iron-mediated DNA damage show no iron binding by ultraviolet-visible spectroscopy, including glycine, glutamate, and γ-aminobutyric acid. Thus, iron binding is a primary mechanism for the antioxidant neurotransmitter and polyphenol compounds.

Electrochemical Potentials of Neurotransmitters and Polyphenols Affect Antioxidant Potential

The ability of a neurotransmitter or polyphenol compound to prevent iron-mediated DNA damage correlates directly with its redox activity in an aqueous solution. The tested catecholamines (dopamine (DA), epinephrine (EP) and norepinephrine (NE)) and curcumin are all effective antioxidants and are electrochemically active within a ± 1 V range at physiological pH. Electrochemically inactive compounds, including glycine, glutamate, γ-aminobutyric acid, and 5-hydroxychromone, are either inactive or very ineffective at inhibiting iron-mediated DNA damage. Upon binding to iron, catecholamines shift the Fe(III)/Fe(II) redox potential; these shifts correlate to the efficacy of the individual catecholamines to prevent DNA damage by in a Fe(II)/H_2O_2.

Future Work

To further analyze the importance of metal-binding on neurotransmitter antioxidant activity, copper DNA damage experiments can be carried out to investigate the ability of neurotransmitters to inhibit copper-mediated DNA damage. To determine whether copper coordination is required for the observed activity, DNA damage assays with completely chelated $[Cu(bipy)_2]^+$ instead of aqueous Cu(I) could be conducted. The Cu(I)/H_2O_2 results could then be compared to the collected Cu(I) UV-vis data to determine if copper binding correlates with prevention of copper-mediated DNA damage. Establishing neurotransmitter behavior in a copper-rich environment

would be valuable in mimicking a biological environment, particularly due to the mis-regulation and accumulation of copper found in patients with neurodegenerative diseases.

APPENDIX A

ELSEVIER LICENSE
TERMS AND CONDITIONS

Jun 13, 2011

This is a License Agreement between Carla R Garcia ("You") and Elsevier ("Elsevier") provided by Copyright Clearance Center ("CCC"). The license consists of your order details, the terms and conditions provided by Elsevier, and the payment terms and conditions.

All payments must be made in full to CCC. For payment instructions, please see information listed at the bottom of this form.

Supplier	Elsevier Limited The Boulevard,Langford Lane Kidlington,Oxford,OX5 1GB,UK
Registered Company Number	1982084
Customer name	Carla R Garcia
Customer address	117C Heritage Riverwood Drive Central, SC 29630
License number	2687190757880
License date	Jun 13, 2011
Licensed content publisher	Elsevier
Licensed content publication	Journal of Inorganic Biochemistry
Licensed content title	Antioxidant and prooxidant effects of polyphenol compounds on copper-mediated DNA damage
Licensed content author	Nathan R. Perron, Carla R. García, Julio R. Pinzón, Manuel N. Chaur, Julia L. Brumaghim
Licensed content date	May 2011
Licensed content volume number	105
Licensed content issue number	5
Number of pages	9
Start Page	745
End Page	753
Type of Use	reuse in a thesis/dissertation
Portion	full article
Format	both print and electronic
Are you the author of this Elsevier article?	Yes
Will you be translating?	No
Order reference number	

Title of your thesis/dissertation	Antioxidant and Prooxidant Activities of Selected Compounds and Neurotransmitters in the Presence of Iron and Copper
Expected completion date	Aug 2011
Estimated size (number of pages)	80
Elsevier VAT number	GB 494 6272 12
Permissions price	0.00 USD
VAT/Local Sales Tax	0.0 USD / 0.0 GBP
Total	0.00 USD
Terms and Conditions	

INTRODUCTION

1. The publisher for this copyrighted material is Elsevier. By clicking "accept" in connection with completing this licensing transaction, you agree that the following terms and conditions apply to this transaction (along with the Billing and Payment terms and conditions established by Copyright Clearance Center, Inc. ("CCC"), at the time that you opened your Rightslink account and that are available at any time at http://myaccount.copyright.com).

GENERAL TERMS

2. Elsevier hereby grants you permission to reproduce the aforementioned material subject to the terms and conditions indicated.

3. Acknowledgement: If any part of the material to be used (for example, figures) has appeared in our publication with credit or acknowledgement to another source, permission must also be sought from that source. If such permission is not obtained then that material may not be included in your publication/copies. Suitable acknowledgement to the source must be made, either as a footnote or in a reference list at the end of your publication, as follows:

"Reprinted from Publication title, Vol /edition number, Author(s), Title of article / title of chapter, Pages No., Copyright (Year), with permission from Elsevier [OR APPLICABLE SOCIETY COPYRIGHT OWNER]." Also Lancet special credit - "Reprinted from The Lancet, Vol. number, Author(s), Title of article, Pages No., Copyright (Year), with permission from Elsevier."

4. Reproduction of this material is confined to the purpose and/or media for which permission is hereby given.

5. Altering/Modifying Material: Not Permitted. However figures and illustrations may be altered/adapted minimally to serve your work. Any other abbreviations, additions, deletions and/or any other alterations shall be made only with prior written authorization of Elsevier Ltd. (Please contact Elsevier at permissions@elsevier.com)

6. If the permission fee for the requested use of our material is waived in this instance, please be advised that your future requests for Elsevier materials may attract a fee.

7. Reservation of Rights: Publisher reserves all rights not specifically granted in the

combination of (i) the license details provided by you and accepted in the course of this licensing transaction, (ii) these terms and conditions and (iii) CCC's Billing and Payment terms and conditions.

8. License Contingent Upon Payment: While you may exercise the rights licensed immediately upon issuance of the license at the end of the licensing process for the transaction, provided that you have disclosed complete and accurate details of your proposed use, no license is finally effective unless and until full payment is received from you (either by publisher or by CCC) as provided in CCC's Billing and Payment terms and conditions. If full payment is not received on a timely basis, then any license preliminarily granted shall be deemed automatically revoked and shall be void as if never granted. Further, in the event that you breach any of these terms and conditions or any of CCC's Billing and Payment terms and conditions, the license is automatically revoked and shall be void as if never granted. Use of materials as described in a revoked license, as well as any use of the materials beyond the scope of an unrevoked license, may constitute copyright infringement and publisher reserves the right to take any and all action to protect its copyright in the materials.

9. Warranties: Publisher makes no representations or warranties with respect to the licensed material.

10. Indemnity: You hereby indemnify and agree to hold harmless publisher and CCC, and their respective officers, directors, employees and agents, from and against any and all claims arising out of your use of the licensed material other than as specifically authorized pursuant to this license.

11. No Transfer of License: This license is personal to you and may not be sublicensed, assigned, or transferred by you to any other person without publisher's written permission.

12. No Amendment Except in Writing: This license may not be amended except in a writing signed by both parties (or, in the case of publisher, by CCC on publisher's behalf).

13. Objection to Contrary Terms: Publisher hereby objects to any terms contained in any purchase order, acknowledgment, check endorsement or other writing prepared by you, which terms are inconsistent with these terms and conditions or CCC's Billing and Payment terms and conditions. These terms and conditions, together with CCC's Billing and Payment terms and conditions (which are incorporated herein), comprise the entire agreement between you and publisher (and CCC) concerning this licensing transaction. In the event of any conflict between your obligations established by these terms and conditions and those established by CCC's Billing and Payment terms and conditions, these terms and conditions shall control.

14. Revocation: Elsevier or Copyright Clearance Center may deny the permissions described in this License at their sole discretion, for any reason or no reason, with a full refund payable to you. Notice of such denial will be made using the contact information provided by you. Failure to receive such notice will not alter or invalidate the denial. In no event will Elsevier or Copyright Clearance Center be responsible or liable for any costs, expenses or damage incurred by you as a result of a denial of your permission request, other than a refund of the amount(s) paid by you to Elsevier and/or Copyright Clearance Center for denied permissions.

LIMITED LICENSE

The following terms and conditions apply only to specific license types:

15. **Translation**: This permission is granted for non-exclusive world **English** rights only unless your license was granted for translation rights. If you licensed translation rights you may only translate this content into the languages you requested. A professional translator must perform all translations and reproduce the content word for word preserving the integrity of the article. If this license is to re-use 1 or 2 figures then permission is granted for non-exclusive world rights in all languages.

16. **Website**: The following terms and conditions apply to electronic reserve and author websites:
Electronic reserve: If licensed material is to be posted to website, the web site is to be password-protected and made available only to bona fide students registered on a relevant course if:
This license was made in connection with a course,
This permission is granted for 1 year only. You may obtain a license for future website posting,
All content posted to the web site must maintain the copyright information line on the bottom of each image,
A hyper-text must be included to the Homepage of the journal from which you are licensing at http://www.sciencedirect.com/science/journal/xxxxx or the Elsevier homepage for books at http://www.elsevier.com , and
Central Storage: This license does not include permission for a scanned version of the material to be stored in a central repository such as that provided by Heron/XanEdu.

17. **Author website** for journals with the following additional clauses:

All content posted to the web site must maintain the copyright information line on the bottom of each image, and
he permission granted is limited to the personal version of your paper. You are not allowed to download and post the published electronic version of your article (whether PDF or HTML, proof or final version), nor may you scan the printed edition to create an electronic version,
A hyper-text must be included to the Homepage of the journal from which you are licensing at http://www.sciencedirect.com/science/journal/xxxxx , As part of our normal production process, you will receive an e-mail notice when your article appears on Elsevier's online service ScienceDirect (www.sciencedirect.com). That e-mail will include the article's Digital Object Identifier (DOI). This number provides the electronic link to the published article and should be included in the posting of your personal version. We ask that you wait until you receive this e-mail and have the DOI to do any posting.
Central Storage: This license does not include permission for a scanned version of the material to be stored in a central repository such as that provided by Heron/XanEdu.

18. **Author website** for books with the following additional clauses:
Authors are permitted to place a brief summary of their work online only.
A hyper-text must be included to the Elsevier homepage at http://www.elsevier.com

All content posted to the web site must maintain the copyright information line on the bottom of each image

You are not allowed to download and post the published electronic version of your chapter, nor may you scan the printed edition to create an electronic version.

Central Storage: This license does not include permission for a scanned version of the material to be stored in a central repository such as that provided by Heron/XanEdu.

19. **Website** (regular and for author): A hyper-text must be included to the Homepage of the journal from which you are licensing at http://www.sciencedirect.com/science/journal/xxxxx. or for books to the Elsevier homepage at http://www.elsevier.com

20. **Thesis/Dissertation**: If your license is for use in a thesis/dissertation your thesis may be submitted to your institution in either print or electronic form. Should your thesis be published commercially, please reapply for permission. These requirements include permission for the Library and Archives of Canada to supply single copies, on demand, of the complete thesis and include permission for UMI to supply single copies, on demand, of the complete thesis. Should your thesis be published commercially, please reapply for permission.

21. **Other Conditions**:

v1.6

Gratis licenses (referencing $0 in the Total field) are free. Please retain this printable license for your reference. No payment is required.

If you would like to pay for this license now, please remit this license along with your payment made payable to "COPYRIGHT CLEARANCE CENTER" otherwise you will be invoiced within 48 hours of the license date. Payment should be in the form of a check or money order referencing your account number and this invoice number RLNK11002480.
Once you receive your invoice for this order, you may pay your invoice by credit card. Please follow instructions provided at that time.

Make Payment To:
Copyright Clearance Center
Dept 001
P.O. Box 843006
Boston, MA 02284-3006

For suggestions or comments regarding this order, contact Rightslink Customer Support: customercare@copyright.com or +1-877-622-5543 (toll free in the US) or +1-978-646-2777.

ELSEVIER LICENSE
TERMS AND CONDITIONS

Oct 11, 2011

This is a License Agreement between Carla R Garcia ("You") and Elsevier ("Elsevier") provided by Copyright Clearance Center ("CCC"). The license consists of your order details, the terms and conditions provided by Elsevier, and the payment terms and conditions.

All payments must be made in full to CCC. For payment instructions, please see information listed at the bottom of this form.

Supplier	Elsevier Limited The Boulevard,Langford Lane Kidlington,Oxford,OX5 1GB,UK
Registered Company Number	1982084
Customer name	Carla R Garcia
Customer address	117C Heritage Riverwood Drive Central, SC 29630
License number	2765700014096
License date	Oct 10, 2011
Licensed content publisher	Elsevier
Licensed content publication	Journal of Inorganic Biochemistry
Licensed content title	Iron binding of 3-hydroxychromone, 5-hydroxychromone, and sulfonated morin: Implications for the antioxidant activity of flavonols with competing metal binding sites
Licensed content author	Andrea M. Verdan,Hsiao C. Wang,Carla R. García,William P. Henry,Julia L. Brumaghim
Licensed content date	October 2011
Licensed content volume number	105
Licensed content issue number	10
Number of pages	9
Start Page	1314
End Page	1322
Type of Use	reuse in a thesis/dissertation
Portion	full article
Format	both print and electronic
Are you the author of this Elsevier article?	Yes
Will you be translating?	No
Order reference number	
Title of your thesis/dissertation	Antioxidant and Prooxidant Activities of Selected Compounds and Neurotransmitters in the Presence of Iron and Copper
Expected completion date	Nov 2011
Estimated size (number of pages)	80
Elsevier VAT number	GB 494 6272 12

Permissions price	0.00 USD
VAT/Local Sales Tax	0.0 USD / 0.0 GBP
Total	**0.00 USD**

Terms and Conditions

INTRODUCTION

1. The publisher for this copyrighted material is Elsevier. By clicking "accept" in connection with completing this licensing transaction, you agree that the following terms and conditions apply to this transaction (along with the Billing and Payment terms and conditions established by Copyright Clearance Center, Inc. ("CCC"), at the time that you opened your Rightslink account and that are available at any time at http://myaccount.copyright.com).

GENERAL TERMS

2. Elsevier hereby grants you permission to reproduce the aforementioned material subject to the terms and conditions indicated.
3. Acknowledgement: If any part of the material to be used (for example, figures) has appeared in our publication with credit or acknowledgement to another source, permission must also be sought from that source. If such permission is not obtained then that material may not be included in your publication/copies. Suitable acknowledgement to the source must be made, either as a footnote or in a reference list at the end of your publication, as follows:
"Reprinted from Publication title, Vol /edition number, Author(s), Title of article / title of chapter, Pages No., Copyright (Year), with permission from Elsevier [OR APPLICABLE SOCIETY COPYRIGHT OWNER]." Also Lancet special credit - "Reprinted from The Lancet, Vol. number, Author(s), Title of article, Pages No., Copyright (Year), with permission from Elsevier."
4. Reproduction of this material is confined to the purpose and/or media for which permission is hereby given.
5. Altering/Modifying Material: Not Permitted. However figures and illustrations may be altered/adapted minimally to serve your work. Any other abbreviations, additions, deletions and/or any other alterations shall be made only with prior written authorization of Elsevier Ltd. (Please contact Elsevier at permissions@elsevier.com)
6. If the permission fee for the requested use of our material is waived in this instance, please be advised that your future requests for Elsevier materials may attract a fee.
7. Reservation of Rights: Publisher reserves all rights not specifically granted in the combination of (i) the license details provided by you and accepted in the course of this licensing transaction, (ii) these terms and conditions and (iii) CCC's Billing and Payment terms and conditions.
8. License Contingent Upon Payment: While you may exercise the rights licensed immediately upon issuance of the license at the end of the licensing process for the transaction, provided that you have disclosed complete and accurate details of your proposed use, no license is finally effective unless and until full payment is received from you (either by publisher or by CCC) as provided in CCC's Billing and Payment terms and conditions. If full payment is not received on a timely basis, then any license preliminarily granted shall be deemed automatically revoked and shall be void as if never granted. Further, in the event that you breach any of these terms and conditions or any of CCC's Billing and Payment terms and conditions, the license is automatically revoked and shall be void as if never granted. Use of materials as described in a revoked license, as well as any use of the materials beyond the scope of an unrevoked license, may constitute copyright infringement and publisher reserves the right to take any and all action to protect its copyright in the materials.
9. Warranties: Publisher makes no representations or warranties with respect to the licensed material.
10. Indemnity: You hereby indemnify and agree to hold harmless publisher and CCC, and their respective officers, directors, employees and agents, from and against any and all claims arising out of your use of the licensed material other than as specifically authorized pursuant to this license.
11. No Transfer of License: This license is personal to you and may not be sublicensed, assigned, or transferred by you to any other person without publisher's written permission.
12. No Amendment Except in Writing: This license may not be amended except in a writing signed by both parties (or, in the case of publisher, by CCC on publisher's behalf).
13. Objection to Contrary Terms: Publisher hereby objects to any terms contained in any purchase order, acknowledgment, check endorsement or other writing prepared by you, which terms are inconsistent with these terms and conditions or CCC's Billing and Payment terms and conditions. These terms and conditions, together with CCC's Billing and Payment terms and conditions (which are incorporated herein), comprise the entire agreement between you and publisher (and CCC) concerning this licensing transaction. In the event of any conflict between your obligations established by these terms and conditions and those established by CCC's Billing and Payment terms and conditions, these terms and conditions shall control.
14. Revocation: Elsevier or Copyright Clearance Center may deny the permissions described in this License at their sole discretion, for any reason or no reason, with a full refund payable to you. Notice of such denial will be made using the contact information provided by you. Failure to receive such notice will not alter or invalidate the denial. In no event will Elsevier or Copyright Clearance Center be responsible or liable for any costs, expenses or damage incurred by you as a result of a denial of your permission request, other than a refund of the amount(s) paid by you to Elsevier and/or Copyright Clearance Center for denied permissions.

LIMITED LICENSE

The following terms and conditions apply only to specific license types:
15. **Translation**: This permission is granted for non-exclusive world **English** rights only unless your license was granted for translation rights. If you licensed translation rights you may only translate this content into the languages you requested. A professional translator must perform all translations and reproduce the content word for word preserving the integrity of the article.
If this license is to re-use 1 or 2 figures then permission is granted for non-exclusive world rights in all languages.
16. **Website**: The following terms and conditions apply to electronic reserve and author websites:
Electronic reserve: If licensed material is to be posted to website, the web site is to be password-protected and made available only to bona fide students registered on a relevant course if:
This license was made in connection with a course,
This permission is granted for 1 year only. You may obtain a license for future website posting,
All content posted to the web site must maintain the copyright information line on the bottom of each image,
A hyper-text must be included to the Homepage of the journal from which you are licensing at http://www.sciencedirect.com /science/journal/xxxxx or the Elsevier homepage for books at http://www.elsevier.com , and
Central Storage: This license does not include permission for a scanned version of the material to be stored in a central repository such as that provided by Heron/XanEdu.
17. **Author website** for journals with the following additional clauses:
All content posted to the web site must maintain the copyright information line on the bottom of each image, and
he permission granted is limited to the personal version of your paper. You are not allowed to download and post the published electronic version of your article (whether PDF or HTML, proof or final version), nor may you scan the printed edition to create an electronic version,
A hyper-text must be included to the Homepage of the journal from which you are licensing at http://www.sciencedirect.com /science/journal/xxxxx , As part of our normal production process, you will receive an e-mail notice when your article appears on Elsevier's online service ScienceDirect (www.sciencedirect.com). That e-mail will include the article's Digital Object Identifier (DOI). This number provides the electronic link to the published article and should be included in the posting of your personal version. We ask that you wait until you receive this e-mail and have the DOI to do any posting.
Central Storage: This license does not include permission for a scanned version of the material to be stored in a central repository such as that provided by Heron/XanEdu.
18. **Author website** for books with the following additional clauses:
Authors are permitted to place a brief summary of their work online only.
A hyper-text must be included to the Elsevier homepage at http://www.elsevier.com
All content posted to the web site must maintain the copyright information line on the bottom of each image
You are not allowed to download and post the published electronic version of your chapter, nor may you scan the printed edition to create an electronic version.
Central Storage: This license does not include permission for a scanned version of the material to be stored in a central repository such as that provided by Heron/XanEdu.

19. **Website** (regular and for author): A hyper-text must be included to the Homepage of the journal from which you are licensing at http://www.sciencedirect.com/science/journal/xxxxx. or for books to the Elsevier homepage at http://www.elsevier.com
20. **Thesis/Dissertation**: If your license is for use in a thesis/dissertation your thesis may be submitted to your institution in either print or electronic form. Should your thesis be published commercially, please reapply for permission. These requirements include permission for the Library and Archives of Canada to supply single copies, on demand, of the complete thesis and include permission for UMI to supply single copies, on demand, of the complete thesis. Should your thesis be published commercially, please reapply for permission.
21. **Other Conditions**:

v1.6

If you would like to pay for this license now, please remit this license along with your payment made payable to "COPYRIGHT CLEARANCE CENTER" otherwise you will be invoiced within 48 hours of the license date. Payment should be in the form of a check or money order referencing your account number and this invoice number RLNK0.
Once you receive your invoice for this order, you may pay your invoice by credit card. Please follow instructions provided at that time.

Make Payment To:
Copyright Clearance Center
Dept 001
P.O. Box 843006
Boston, MA 02284-3006

For suggestions or comments regarding this order, contact RightsLink Customer Support: customercare@copyright.com or +1-877-622-5543 (toll free in the US) or +1-978-646-2777.

Gratis licenses (referencing $0 in the Total field) are free. Please retain this printable license for your reference. No payment is required.
